

Development and Application of Two-Stage Friction Damper

by

Alexander W. Olson

A Report Submitted to the Faculty of the
Milwaukee School of Engineering
in Partial Fulfillment of the
Requirements for the Degree of
Master of Science in Architectural Engineering

Milwaukee, Wisconsin

September 2021

Abstract

Within the course of structure engineering, several mechanisms have been used to limit the force applied to structures during high seismic events. These mechanisms, known as dampers, dissipate the seismic energy and hence reduce the actual loads in lateral load resisting elements of the system and allow for a more efficient and economical design. This leads to design and fabrication of different types of energy dissipating systems within the industry for various applications. This research focuses on one type of damping system known as the friction damper. Applied to a standard braced frame lateral system, the friction damper is made up of a friction pad placed between two plates. These plates are attached by means of a series of bolts within predetermined length slotted holes. By post tensioning the bolts, a specific friction force (i.e., slip force) between the plates and friction pads can be achieved and seismic energy can be dissipated at the interface of the friction pads and the plates. This process dissipates the seismic energy and reduces the force resisted by the braced frame.

Currently, friction dampers come in a single stage, allowing structural engineers to design for a specific slip force and limit state (service or strength limit state). This research focuses on the development and applications of a two-stage friction dampers that can be designed and tuned to dissipate seismic energy at both the service and strength limit states. This device, functioning at each stage like a one-stage friction damper, will consist of two plate and friction pad mechanisms with separate bolts and slotted holes. The first stage, slipping at a service level loading, will be activated at a low intensity and more frequent earthquake events. The second stage, will be activated at a seismic event with higher intensity (DBE or MCE). This system will allow the structural engineers to take advantage of the two-stage friction dampers at low and high intensity seismic events and meet both the serviceability and strength criteria defined.

The finite element simulations and numerical analyses in this study, conducted using CSI's structural building analysis and design software ETABS®, consisted of a series of preliminary analyses to validate the behavior of the system and accuracy of the model. Using a series of nonlinear links, a four-story, four-bay building was modeled with two-stage friction dampers. This structure was designed to meet predetermined inter-story drift limits and then subjected to a suite of 44 ground motions. The ground motions were scaled to both the service level earthquake (SLE) and maximum considered earthquake (MCE) spectrum for San Diego, California. The story shear and inter-story drift ratios were recorded and compared to those of a system without friction dampers (i.e. elastic system) to check the effectiveness of the two-stage friction dampers.

The results showed that the structure with the dampers produced an average base shear of 160 kips versus nearly 1000 kips in the elastic system and 50 kips versus nearly 250 kips subjected to MCE and SLE ground motions, respectively. This reduction factors of 6.25 for MCE level and 5.0 for SLE level proved the effectiveness and damping capabilities of the two-stage friction dampers to control the performance of the structure.

The study was limited to a preliminary analysis and development of the two-stage friction damper. Future research and studies can be conducted on this topic to further develop this type of damping system in terms of fabrication, design, optimization, and efficiency in building applications.

Acknowledgments

Thanks are in order to many people that made this research possible. Without the involvement, sacrifice, or assistance of these people, the study would never have been at the level it is. I would like to first thank the Milwaukee School of Engineering for providing me with a platform, supportive community, and the technology to conduct the trials needed.

The work would not have been possible without the guidance and support of my advisor, Pouria Bahmani, PhD. Without him, many questions would have been left unanswered and the quality of the research would have been significantly diminished. I would also like to extend gratitude to my committee of Chris Raebel, PhD, and Todd Davis, PhD. Having the feedback from them allowed me to explore items that would not have been touched otherwise and format the study in a manner that was much more sufficient and applicable to true applications.

Finally, I am ever so grateful to my friends and family. I want to thank my parents for setting me up with success and always supporting my work, no matter the outcome. To the rest of my family, thank you for allowing me to spend time on the study and focus on my schoolwork in the process. To my friends, thank you for supporting me, asking questions, and allowing me to miss out on events to complete this research. I look forward to being able to celebrate and make up for lost time with all of you.

Table of Contents

| | |
|---|----|
| List of Figures | 7 |
| List of Tables | 9 |
| Nomenclature | 10 |
| Glossary | 12 |
| Chapter 1: Introduction | 13 |
| Chapter 2: Literature Review | 16 |
| 2.1 Damping Characteristics of Friction Damped Braced Frame and its Effectiveness in the Mega-Sub Controlled Structure System by Yeda and Cherry..... | 16 |
| 2.2 Testing of Passive Energy Dissipation Systems by Aiken <i>et al.</i> | 17 |
| 2.3 Simplified Seismic Code Design Procedure for Friction-Damped Steel Frames by Fu and Cherry..... | 19 |
| 2.4 Earthquake Response of Mid-Rise to High-Rise Buildings with Friction Dampers by Kaur, Matsagar, and Nagpal..... | 21 |
| 2.5 Seismic Performance of Friction Dampers Using Flexure of RC Shear Wall by Chung <i>et al.</i> | 23 |
| 2.6 Friction Dampers for Seismic Upgrade of St Vincent Hospital, Ottawa by Malhotra <i>et al.</i> | 23 |

| | | |
|--|---|----|
| 2.7 | Dynamic Response of Structure with Tuned Mass Friction Damper by Pisal and Jangid..... | 24 |
| Chapter 3: Analytic Work and Numerical Modeling..... | | 26 |
| 3.1 | Introduction..... | 26 |
| 3.2 | Link Modeling | 26 |
| 3.2.1 | Wen Links | 27 |
| 3.2.2 | Gap Links..... | 28 |
| 3.2.3 | Hook Links..... | 30 |
| 3.2.4 | Combination of Links | 31 |
| 3.2.5 | Defining Link Parameters | 33 |
| 3.3 | Pushover Analysis..... | 39 |
| 3.4 | Cyclic Loading Trials | 41 |
| 3.5 | Single Bay Seismic Analysis | 43 |
| 3.5.1 | Application of Loads..... | 43 |
| 3.5.2 | Building Geometry and Effective Weight | 45 |
| 3.6 | 4-Bay Seismic Analysis | 46 |
| 3.6.1 | Scaling Ground Motions | 46 |
| 3.6.2 | Scaled Analysis | 48 |
| 3.7 | 4-Story Analysis Setup | 52 |
| Chapter 4: Analytical and Numerical Results..... | | 57 |

| | | |
|--|---|-----------|
| 4.1 | Initial Final Trials | 57 |
| 4.2 | Adjusted SLE Values | 59 |
| 4.3 | Final Trial Displacement..... | 61 |
| 4.4 | Final Trial Base Shear..... | 63 |
| Chapter 5: Discussion and Conclusion | | 70 |
| 5.1 | Conclusions..... | 70 |
| 5.1.1 | Modeling within ETABS© | 70 |
| 5.1.2 | Reduction Ratios | 71 |
| 5.2 | Future Work | 72 |
| 5.2.1 | Energy Dissipation..... | 72 |
| 5.2.2 | Design and Fabrication | 74 |
| 5.2.3 | Optimization and Expansion..... | 76 |
| References..... | | 79 |
| Appendices..... | | 81 |
| Appendix A | Cyclic Loading Trials | 81 |
| Appendix B | 1-Story, 1-Bay Unscaled Ground Motion Trials..... | 83 |
| Appendix C | 1-Story, 4-Bay Initial Scaled Ground Motion Trials | 88 |
| Appendix D | 4-Story, 4-Bay Initial Final Trial | 121 |
| Appendix E | 4-Story, 4-Bay Updated Final Trial | 124 |
| Appendix F | 4-Story, 4-Bay Elastic Trials (No Friction Damper Applied)..... | 133 |

List of Figures

| | |
|--|----|
| Figure 1.1-1: Energy Dissipation via Hysteresis Curve..... | 14 |
| Figure 2.2-1: Testing Setup for Viscoelastic Dampers (left) and Friction Dampers (right)..... | 18 |
| Figure 2.3-1: Basic Hysteresis Loop for Single-Stage Friction Damper..... | 20 |
| Figure 2.4-1: Breakdown of Friction Damper Hysteresis Loop and Comparison to Typical Braced Frame System..... | 22 |
| Figure 2.7-1: SDOF Modeling Procedure of Tuned Mass Friction Damper..... | 25 |
| Figure 3.2-1: Wen Link Modeling Diagram as Friction Damper..... | 27 |
| Figure 3.2-2: ETABS© Wen Link Input Parameters..... | 28 |
| Figure 3.2-3: Gap Link Modeling Diagram as Compression Slip Distance..... | 29 |
| Figure 3.2-4: ETABS© Gap Link Input Parameters..... | 30 |
| Figure 3.2-5: Hook Link Modeling Diagram as Tension Slip Distance..... | 30 |
| Figure 3.2-6: ETABS© Hook Link Input Parameters..... | 31 |
| Figure 3.2-7: ETABS© Modeled Braced Frame with Two-Stage Friction Damper..... | 32 |
| Figure 3.2-8: Combined Diagram of Link Behaviors..... | 33 |
| Figure 3.2-9: Two-Stage Friction Damper Parameter Graphic..... | 35 |
| Figure 3.3-1: Pushover Analysis - Single Bay, Single Story Model..... | 40 |
| Figure 3.3-2: Pushover Analysis Results..... | 41 |
| Figure 3.4.1: Cyclic Loading Trial Hysteresis Diagram..... | 42 |
| Figure 3.5-1: ATC 63 Ground Motions..... | 44 |
| Figure 3.5-2: Effective Weight Loading Applied within ETABS©..... | 45 |

| | |
|---|----|
| Figure 3.5-3: Hysteresis Plot under Randomly Selected Ground Motion, Scaled to 1.0g..... | 46 |
| Figure 3.6-1: 4-Bay ETABS© Model with Two Two-Stage Friction Dampers..... | 48 |
| Figure 3.6-2: MCE 1.0 Scaled Outputs..... | 49 |
| Figure 3.6-3: MCE 0.8 Scaled Outputs..... | 51 |
| Figure 3.6-4: MCE 0.6 Scaled Outputs..... | 51 |
| Figure 3.6-5: MCE 0.4 Scaled Outputs..... | 52 |
| Figure 3.7-1: 4-Story, 4-Bay Friction Damper Model Building Elevation..... | 53 |
| Figure 3.7-2: 4-Story, 4-Bay Friction Damper Model Plan View..... | 54 |
| Figure 4.1-1: MCE Initial Final Trial Inter-Story Drift Ratios – 0.4 Scaled..... | 58 |
| Figure 4.2-1: Adjusted SLE Response Spectrum (0.35*DBE) for San Diego, CA..... | 61 |
| Figure 4.3-1: Updated SLE Inter-Story Drift Ratio Plots..... | 62 |
| Figure 4.4-1: Final Trials MCE with Two-Stage Friction Damper Base Shear Plots..... | 65 |
| Figure 4.4-2: Final Trials SLE with Two-Stage Friction Damper Base Shear Plots | 66 |
| Figure 4.4-3: Final Elastic SLE Trials without Friction Damper Base Shear Plots | 67 |
| Figure 4.4-4: Final Elastic MCE Trials without Friction Damper Base Shear Plots..... | 69 |
| Figure 5.2-1: Bracing Member with Friction Damper Spring Properties..... | 74 |
| Figure 5.2-2: Two-Stage Friction Damper Preliminary Construction..... | 76 |
| Figure 5.2-3: Optimized Two-Stage Friction Damper Building Diagram..... | 77 |

List of Tables

Table 3.6-1: Link Input Values for 1.0 Scaled Two-Stage Friction Damper.....49

Table 3.6-2: Link Input Values for 0.8 Scaled Two-Stage Friction Damper50

Nomenclature

Symbols

l - length of bracing member

a - area of bracing member

d_1 - elastic deformation of bracing member under axial load, f_1

d_2 - elastic deformation of bracing member under axial load, f_2

D_1 - stage 1 slip distance

D_2 - stage 2 slip distance

E - modulus of elasticity for frame material

f_1 - Stage 1 axial force on bracing members

f_2 - Stage 2 axial force on bracing member

H - frame height

L - frame length

P_1 - Stage 1 lateral load

P_2 - Stage 2 lateral load

δ_1 - total brace deformation after stage 1

δ_2 - total brace deformation after stage 2

Δ_1 - total story drift at stage one

Δ_2 - total story drift at stage two

θ - angle of bracing member with respect to the horizontal line

' – feet

“ – inches

Abbreviations

ADAS – added damping and stiffness

ft – feet

FD – friction damper

in – inches

lbs or lb – pounds

LFRS – lateral force resisting system

k – kips

MCE – maximum considered event

MRF – moment resisting frame

SLE – service level expectation

typ – typical

Glossary

hysteresis - the phenomenon in which the value of a physical property lags behind changes in the effect causing it, as for instance when magnetic induction lags behind the magnetizing force.

kip – 1000 lbs

Chapter 1: Introduction

Lateral force resisting systems (LFRS) within building and structural engineering have been undergoing a great deal of renaissance within the last 100 years. With the addition of mid- to high-rise building being on the rise, the addition of advancements and the desire to build in even the highest seismic zones on the globe have made it a key point in the advancement of structural systems. More recently, the addition of energy dissipating systems to traditional LFRS has allowed great steps to be taken to build more efficiently, maintain easier, and most importantly, build safer.

Dampers, which can come in many forms, began to take shape around the early 1900's. Beginning with the tuned mass damper, the ideology of the dampers was to dissipate some of the lateral energy generated within the building's structural system, thus reducing the load on structural members which leads to lower deflections and base shear for the entire structure. Friction dampers, a more recent form of these damping systems, allow for this energy dissipation to happen through the process of mechanical friction. The attachment to the simple braced frame system allows for minimal excess construction or maintenance. Using two friction surfaces attached with a bolt in a slotted hole, the system slides at a predetermined friction force; the work done by the friction force is equal to the energy dissipated by the friction damper. This can be seen graphically applied as the area under the curve to the hysteresis curve output by the damper in Figure 1.1-1.

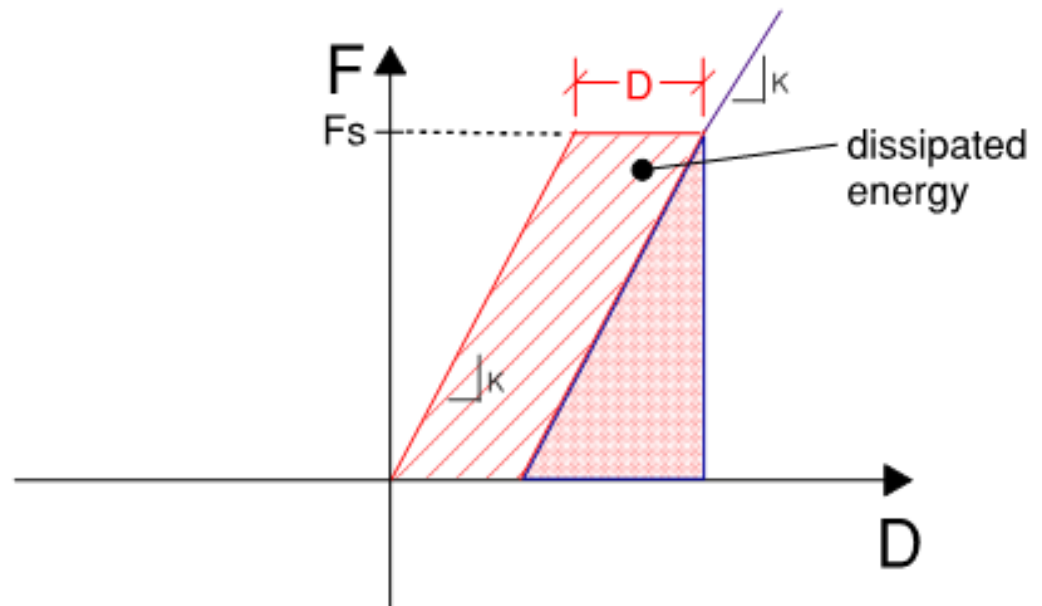


Figure 1.1-1: Energy Dissipation via Hysteresis Curve.

Currently, friction dampers allow for this slip and damper engagement to happen at a single predetermined force. This force is usually found to be at the ultimate design load for the building being designed. In current practice, buildings are designed to meet both the service and strength limit states criteria; and hence, friction dampers can be designed to meet the design requirements of each limit states. Using this approach, the friction damper should be designed to allow for a two-stage energy dissipation system. This two-stage aspect creates a slip stage at two predetermined forces, rather than one. Slipping at the first stage, the friction damper can dissipate energy and control the deflection of the building for the service level conditions. In the same way, the second stage of the damper can slip at the ultimate lateral force, limiting the forces of the structural system at the strength limit states. The two-stage friction damper can dissipate

energy at both limit states, and thus leads to more efficient design of lateral force resisting system of the structure.

The purpose of this research is to develop a two-stage friction damper system and to investigate its effectiveness in enhancing the performance of buildings subjected to lateral loads. The behavior of the two-stage friction dampers were investigated analytically and numerically using extensive nonlinear dynamic analyses. The results are compared to the same building without the dampers (i.e., elastic model) to show the effectiveness of using friction dampers in reducing the story shear demand at both the service and strength limit states.

Chapter 2: Literature Review

Extensive research to encapsulate both the design and modeling approach to dampers in general, and more specifically, a single-stage friction damper allows for ease of analysis for the research found within this study. The review creates a process in which the modeling of the damper is common to that already in practice for items pertaining the dampers and energy dissipation within structural engineering. To the best of the author's knowledge, no research has been conducted to investigate the design and application of two-stage friction dampers; therefore, much of the analysis in this study is created as a first in the industry.

2.1. Damping Characteristics of Friction Damped Braced Frame and its Effectiveness in the Mega-Sub Controlled Structure System by Yeda and Cherry

Going into the theory and understanding of the dampening systems and processes in the friction damper application, the Yeda and Cherry [1] offer a great background for the research. The equations for the main action, the slipping time and displacement that allows the friction damper to be activated are outlined in their article and imperative to the applications used within the modeling and development of the two-stage damper. The concepts of the hysteresis loops and energy dissipation due to friction dampers were introduced and studied within this research. These loops were the basis of the testing and preliminary modeling of the two-stage damper to ensure accuracy.

The article offers input on how the dampers can be implemented and save the need for a mega beam/column system or additional columns by just simply being

integrated into a tall building's existing frame system. While offering a large amount of theory and design applications behind the friction dampers, the writing also offers the efficiency of dampers versus other systems. In fact, the authors state that the displacement response was nearly a tenth of that of the traditional system and a quarter of the acceleration response. This allows these systems to be an excellent alternative to the traditional systems in terms of material savings, maintenance, and overall simplicity in new construction, as well as rehabilitation and reconstruction.

2.2. Testing of Passive Energy Dissipation Systems by Aiken *et al.*

Observing the analysis of several different passive energy dissipation systems at the Pacific Earthquake Engineering Research Center at UC-Berkeley, Aiken *et al.* [2] created a comparison and effective assessment of each system. The systems studied were as followed: Sumitomo friction dampers, 3M viscoelastic dampers (viscoelastic damper), Pall friction device, Added Damping and Stiffness (ADAS) elements, steel moment resisting frames (MRF) with friction slip devices, Fluor-Daniel energy dissipating restraint, and NiTi shape-memory alloy dampers. The testing and data analysis were conducted in two phases, a large-scale earthquake and Phase II, a small-scale study. The steel moment resisting frame (MRF) and the Fluor-Daniel energy dissipating restraint were tested in Phase II of this research program. Figure 2.2.1 shows the testing setup used.

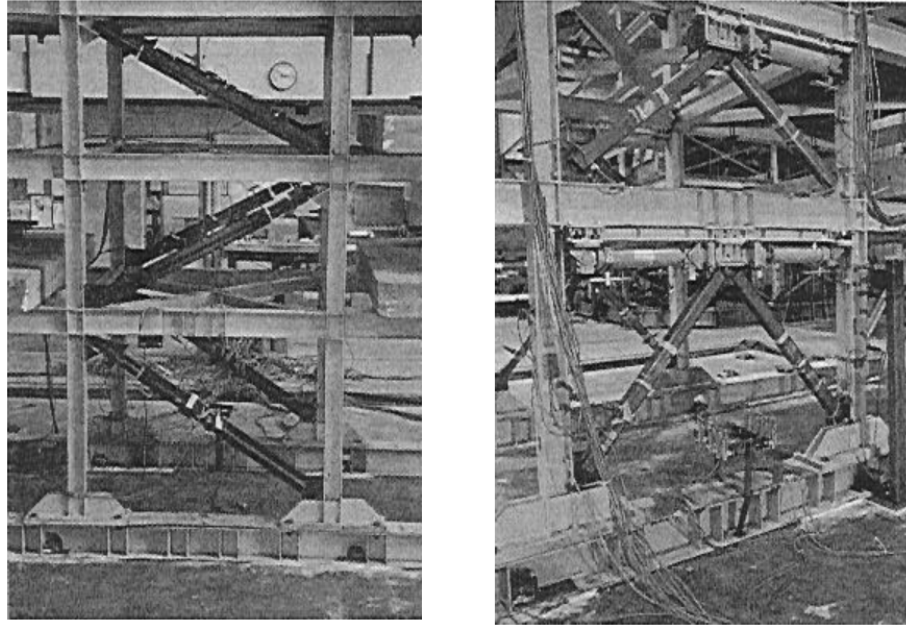


Figure 2.2-1: Testing Setup for Viscoelastic Dampers (left) and Friction Dampers (right) [2].

In the first test, the Sumitomo friction damper and the 3M viscoelastic dampers were both tested on the same 9-story structure. The test structures were subjected to a suite of 14 ground motions. It was found that the two structures both showed hysteresis behaviors in response to the motions but were found to exhibit two largely different results. This was attributed to the fact that the friction damper requires a force at or greater than the slip force to dissipate the energy unlike the VE damper which can dissipate energy for all earthquake excitations. It was found that in general the acceleration and displacement responses were quite similar between the VE and the friction dampers, including peak base shears. As well, they were both found to be equal or less than the base shears found in the undamped MRF structure and the drifts were reduced to half of that of the MRF. The results show the effectiveness of a damper within

a simple braced frame system to reduce base shear and overall deflection of the structures drifts without having the design and detail a full MRF structure.

2.3. Simplified Seismic Code Design Procedure for Friction-Damped Steel

Frames by Fu and Cherry

Further explaining the ideology of the hysteresis of the friction damper and its behavior, an article by Fu and Cherry [3] delved into the changes of the codes as it pertained to the design of structures exposed to seismic loading. The journal entry summarizes the basic process of how to design using a friction damper. Fu and Cherry show the modeling aspects of using a single degree of freedom (SDOF) model or a multiple degree of freedom (MDOF) model, including the benefits and applications for both scenarios. They discuss the introduction of the R factor, or the force modification factor, introduced to the code in 1990. This factor allowed for modifications that allowed the assignment of systems such as passive energy dissipation systems. The friction damper was the system continued to be discussed within the rest of the study, providing a great introduction to the idea of the hysteresis of the system.

The introduction of the hysteresis from the article was key in the research outlined within this essay. By having a backbone for the behavior of the single stage damper, the two-stage preliminary modeling and trials were able to be justified as accurate. The hysteresis, simply, is the behavior of the building's LFRS as the force is applied to the structure over time. The behavior shown in Figure 2.3-1, is the plot of the force versus displacement of the structure. The structure displacement is seen to linearly increase as the force applied increases, showing the typical elastic deformation seen in a braced

frame system. Once reached the slip force is reached, the respective stage of the damper becomes activated, causing a horizontal portion of the graph. At this point, the bolt has slipped within the slotted hole, activating the friction pads of the damper. The system then goes through the unloading process before slipping back to the neutral positive and repeating the process for the negative loading. This figure is one that will be seen repeatedly throughout the research and as stated, is the basis for the preliminary testing of the two-stage friction damper modeling.

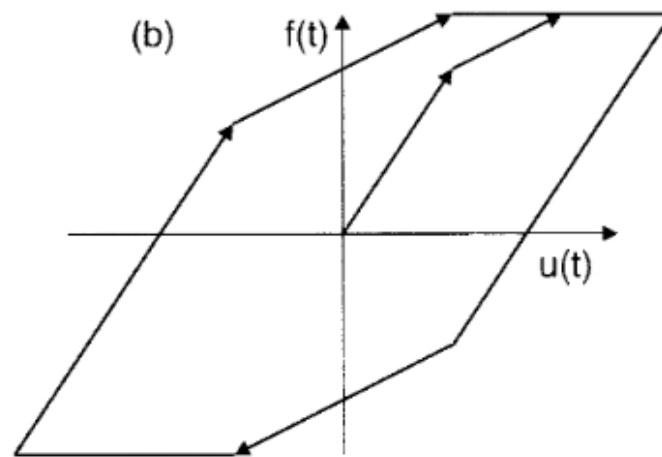


Figure 2.3-1: Basic Hysteresis Loop for Single-Stage Friction Damper [3].

The application of the R factor, explained as the ratio of the elastic base shear over the design base shear is covered extensively in the excerpt. In addition, insight on the distribution of stiffness within the system is addressed in analysis. Other items are addressed to give a full overview on the friction damper design process. Included is member sizing and deflection checks. A great aspect the article addresses comes near the end, touching upon the damage statuses that need to be taken in to account after an earthquake, including the sliding on the friction damper or the buckling/yielding of the

brace members themselves. The addressing of the latter is one that needs to be taken to account with the further application and selection of friction damper applications, whether single or dual stages in building LFRS.

The application of friction dampers and their effect on several parameters are assessed in this journal entry. Steel buildings of varying heights are compared using real earthquake ground motions. Buildings of five to twenty stories are modeled using braced frame (BF), moment-resisting frame (MRF), and friction damper frame (FDF). Items such as top floor acceleration and displacement, story shear, and base shear are recorded. Energy plots were also created in order to observe the energy dissipation of each system type.

2.4. Earthquake Response of Mid-Rise to High-Rise Buildings with Friction Dampers by Kaur, Matsagar, and Nagpal

Within a numerical study by Kaur, Matsagar, and Nagpal [4], the elasto-plastic behavior of the damper was analyzed. Using the hysteresis loop of the damper and the elastic brace behavior, figures of the combined behavior showed the result of the damper within the system. Shown in Figure 2.4-1, the article breaks down each aspect of the hysteresis loop into further detail.

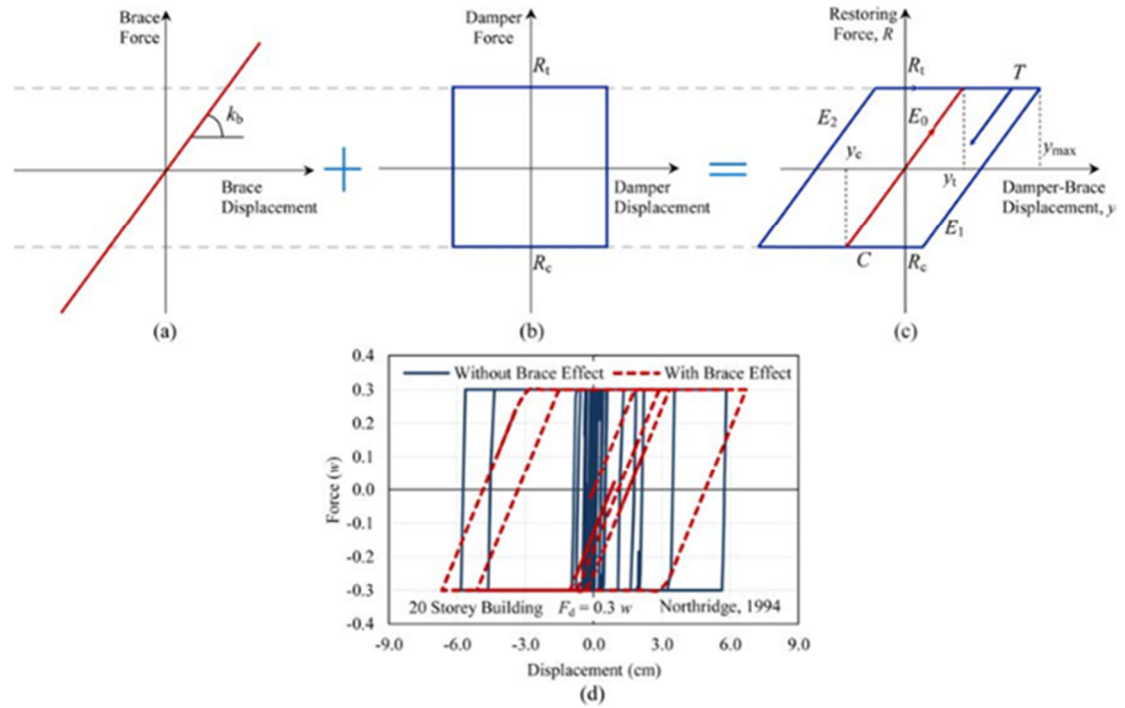


Figure 2.4-1: Breakdown of Friction Damper Hysteresis Loop and Comparison to Typical Braced Frame System [4].

These were then compared to the behavior of the brace frame system without a damper. Through almost every test of the systems, it was found that the FDF outperformed the other systems. Values of floor displacement and acceleration consistently decreased in value with the FDF system over the other two. When looking at energy dissipation, it was found that nearly half of the energy in most cases, if not more, was dissipated by the dampers. A key takeaway was that the FDF system found a maximum response reduction of nearly 50% from the MRF in base shear.

2.5. Seismic Performance of Friction Dampers Using Flexure of RC Shear Wall by Chung *et al.*

In this report by Chung *et al.* [5], the retrofitting of a concrete reinforced shear wall system, specifically in a residential high rise is analyzed. The report looks at changing the retrofit process from the traditional stiffness retrofit to utilizing a friction damper. This system allows for a braced frame with the dampers to be input to the frame. This method, rather than trying to retrofit a beam that will be exposed to flexural and torsional forces allows for easier maintenance and inspection.

The study was done through computer modeling with the overall goal to reduce story drift and story forces in the structure to reduce structure damage due to lateral forces caused by earthquakes. The studies used different friction dampers and models. Ultimately it was found that compared to the rigid structure, the damper could reduce the story rotation by nearly half and the dissipated energy could be nearly triple. The study also emphasized the location and placement of the dampers, showing that spacing them out rather than grouping in the middle, top, or bottom floors reduced the overall displacement of the structure.

2.6. Friction Dampers for Seismic Upgrade of St Vincent Hospital, Ottawa by Malhotra *et al.*

Another approach to the use of a friction damper in building applications is applying the system to existing structures in the form of a lateral system retrofit. In this article by Malhotra *et al.* [6], the hospital of St Vincent in downtown Ottawa, Ontario is studied for its rehabilitation of its lateral system in the form of Pall Dynamics Limited's

friction dampers rather than the traditional reinforcement of the current concrete shear walls. This study emphasizes the importance of upgrading these structures easily and efficiently. This upgrade reduces the susceptibility to earthquake damage on the buildings and its occupants.

The building was modeled in ETABS© modeling software and was compared to that of implementing a rigid brace into the project. It was found that the axial forces in the columns of the building with friction dampers were reduced by 70% compared to the structure with rigid bracing members. In addition, the shear in the bracing members, peak displacements, and story drifts were all reduced using this friction dampening system due to the large energy dissipation of the friction dampers.

2.7. Dynamic Response of Structure with Tuned Mass Friction Damper by Pisal and Jangid

Explored in this article by Pisal and Jangid [7] is a different approach to friction dampers, in the form of tuned mass dampers. The short study explains the idea of how combining the ideologies of the tuned mass dampers and a friction damper came to and the modeling aspect of using the systems together in a single degree of freedom analysis, presented in Figure 2.7-1. The conclusions that came from the analysis and study are that there are several controlling and optimal ranges of values that allow a single degree of freedom system to control rather than a multiple degree of freedom system.

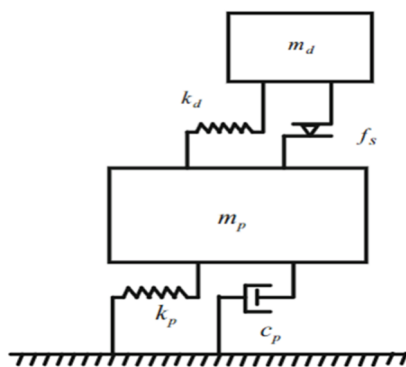


Figure 2.7-1: SDOF Modeling Procedure of Tuned Mass Friction Damper [7].

Chapter 3: Analytical Work and Numerical Modeling

3.1. Introduction

Numerical and nonlinear dynamic analysis was completed entirely in the structural analysis software ETABS©. ETABS© is a structural building analysis and design software created by Computers and Structures, CSI. The program, which allows for linear and nonlinear analyses, allows for an array of analysis and modeling. Catering to mostly multi-story building design, the program offers several facets that were integral for the ease of modeling in the research conducted. In order to model the two-stage damper, ETABS© modeling aspects needed to be combined and modified to achieve the desired behavior of the system. Following the introduction of these components (e.g., link elements), a few test models were run with a single-story system to better understand the behavior of the system. Ground motions were then defined and scaled to appropriate response spectrum in order to run series of nonlinear dynamic analysis. The structural model was expanded to a larger multi-bay system and then expanded to the final building structure design. After each run, the response of the structure was checked to ensure that each level was working as desired and that the results were clearly recorded. This allows all results to be consistent and outliers, if any, to be observed and addressed correctly.

3.2. Link Modeling

To develop the hysteresis plot desired and to allow the ETABS© model to function as a proper friction damper, a series of links were established. A link within ETABS allows a connection between two joints that creates a specific structural

behavior. The links come in different forms to allow for any situation to be modeled and simulated within the software. For the application of the two stage friction dampers, three links were used for each stage of the damper. These links, applied within the local “x” or “u” axis in line with the lateral load applied, allow the bracing member to exhibit all the structural behaviors needed to create the damper effect and to allow for the hysteresis plot to be created. The links used within the two-stage damper model to achieve this plot and behavior consisted of a Wen link, a Gap link, and a Hook link for each of the stages for the damper, totaling six dampers per bracing element.

3.2.1. Wen Links

The first link, known as a Wen link, was applied to the frame. The Wen link offers a uniaxial elastic behavior to be applied. This allows for linear properties to be allowed to the linked member, creating a modified stiffness, yield strength, along with a post yield stiffness ratio. These properties can be modified for each degree of freedom for the joint applied. Figure 3.2-1 present the two Wen Links for modeling stage 1 and stage 2 of the friction damper.

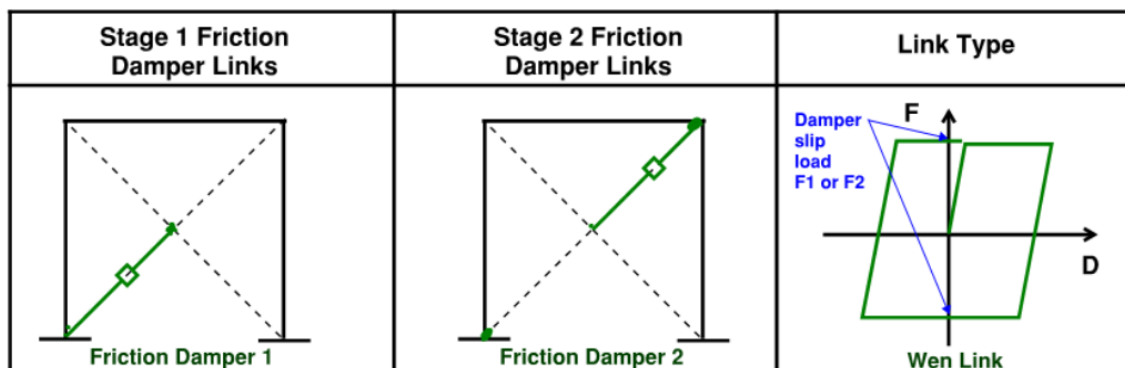


Figure 3.2-1: Wen Link Modeling Diagram as Friction Damper.

The Wen link was used within the two-stage damper application to define the slip forces for each of the stages of the damper. To achieve the slip force desired, the above-mentioned yield strength property was set to the slip force. This allowed the damper to “yield” or slip at this desired force. Each damper was given an individual slip force to allow it to be activated at the different level of lateral loads, both for service level earthquake (SLE) and maximum considered earthquake (MCE) loading. Figure 3.2-2 presents the input parameters for defining a Wen Link in ETABS.

The screenshot shows the 'Link/Support Directional Properties' dialog box in ETABS. The dialog is titled 'Link/Support Directional Properties' and has a close button (X) in the top right corner. It is divided into three main sections: 'Identification', 'Properties Used For Linear Analysis Cases', and 'Properties Used For Nonlinear Analysis Cases'. The 'Identification' section contains four fields: 'Property Name' (Friction_D1), 'Direction' (U1), 'Type' (Plastic (Wen)), and 'NonLinear' (Yes). The 'Properties Used For Linear Analysis Cases' section contains two fields: 'Effective Stiffness' (500000) and 'Effective Damping' (0.). The 'Properties Used For Nonlinear Analysis Cases' section contains four fields: 'Stiffness' (500000), 'Yield Strength' (5000), 'Post Yield Stiffness Ratio' (0.0001), and 'Yielding Exponent' (10). At the bottom of the dialog are 'OK' and 'Cancel' buttons.

| Link/Support Directional Properties | |
|---|---------------|
| Identification | |
| Property Name | Friction_D1 |
| Direction | U1 |
| Type | Plastic (Wen) |
| NonLinear | Yes |
| Properties Used For Linear Analysis Cases | |
| Effective Stiffness | 500000 |
| Effective Damping | 0. |
| Properties Used For Nonlinear Analysis Cases | |
| Stiffness | 500000 |
| Yield Strength | 5000 |
| Post Yield Stiffness Ratio | 0.0001 |
| Yielding Exponent | 10 |
| <input type="button" value="OK"/> <input type="button" value="Cancel"/> | |

Figure 3.2-2: ETABS© Wen Link Input Parameters.

3.2.2. Gap Links

The second link input known as a Gap link allowed for values of compression forces and behavior to be analyzed within the model. The Gap link allows for a

displacement of a specified length to occur in a member, but only within the compression loading. Much like the Wen link, non-linear properties such as stiffness and that displacement, or open, value can be input to define the link and its behavior.

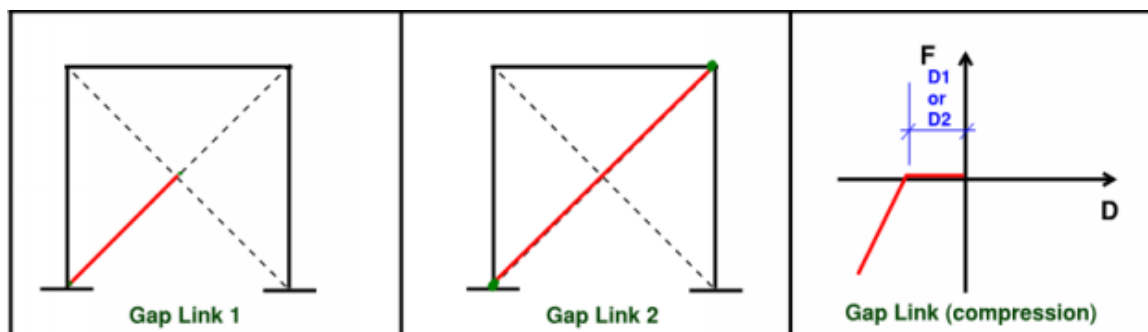
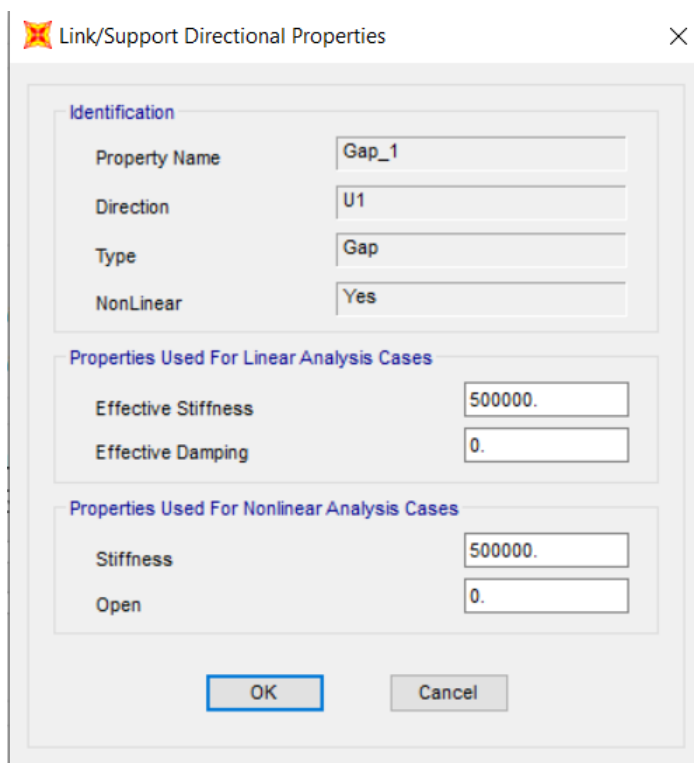


Figure 3.2-3: Gap Link Modeling Diagram as Compression Slip Distance.

In the two-stage application, the Gap links allow the displacement of each damper to be controlled once the slip force has been achieved. This is essentially half of the length of the slotted hole within the damper itself. By inputting a value for each of the dampers, the values of D1 and D2 can be controlled. These values shown in Figure 3.2-3 as D1 and D2 are applied to stage 1 and stage 2 of the friction damper, respectively. Figure 3.2-4 presents the input parameters for defining a Gap Link in ETABS.



Link/Support Directional Properties

Identification

Property Name: Gap_1

Direction: U1

Type: Gap

NonLinear: Yes

Properties Used For Linear Analysis Cases

Effective Stiffness: 500000.

Effective Damping: 0.

Properties Used For Nonlinear Analysis Cases

Stiffness: 500000.

Open: 0.

OK Cancel

Figure 3.2-4: ETABS© Gap Link Input Parameters.

3.2.3. Hook Links

Much like the Gap link, the final applied link to achieve the desired behavior and analysis inputs for the two-stage damper was the Hook link. Behaving nearly exactly the same as a Gap link, the Hook link only differs in the fact that all of the properties defined in the Gap link for compression apply in tension for the Hook link (see Figure 3.2-5).

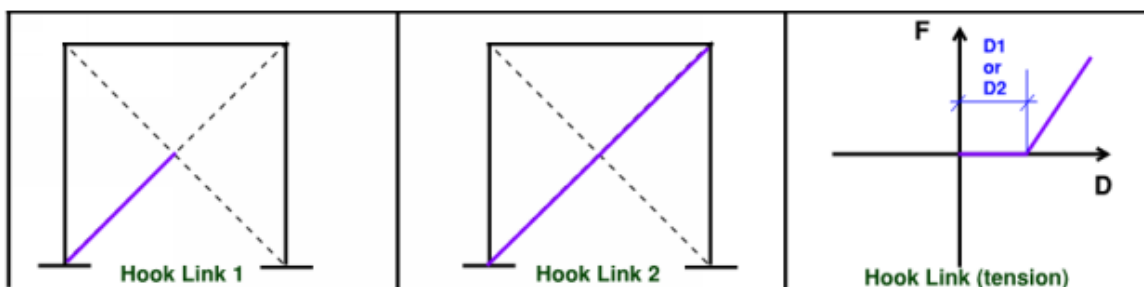


Figure 3.2-5: Hook Link Modeling Diagram as Tension Slip Distance.

Due to the large similarity of the Gap and Hook links as described, their inputs and application to the research vary minimally. The Hook link still created the D1 and D2 values desired but for tension forces within the damper. This completes the hysteresis plot and allows the model to behave as desired for both tension and compression forces. This allows for the complete analysis of the two-stage damper to design all other elements within the system. Figure 3.2-6 presents the input parameters for defining a Hook Link in ETABS.

| Link/Support Directional Properties | |
|---|---------|
| Identification | |
| Property Name | Hook_1 |
| Direction | U1 |
| Type | Hook |
| NonLinear | Yes |
| Properties Used For Linear Analysis Cases | |
| Effective Stiffness | 500000. |
| Effective Damping | 0. |
| Properties Used For Nonlinear Analysis Cases | |
| Stiffness | 500000. |
| Open | 0. |
| <input type="button" value="OK"/> <input type="button" value="Cancel"/> | |

Figure 3.2-6: ETABS© Hook Link Input Parameters.

3.2.4. Combination of Links

With the Wen, Gap, and Hook links in series within the braced frame model, the braced frame will act as a two-stage friction damper. Figure 3.2-7 depicts the combined

links correctly shown within the ETABS© model. In order to limit the outside forces and effects, a bracing member was added to the frame. This member shown at the upper left to the center of the frame, prevents any buckling to occur in the braced frame, allowing for only the desired forces and damper behavior to be captured.

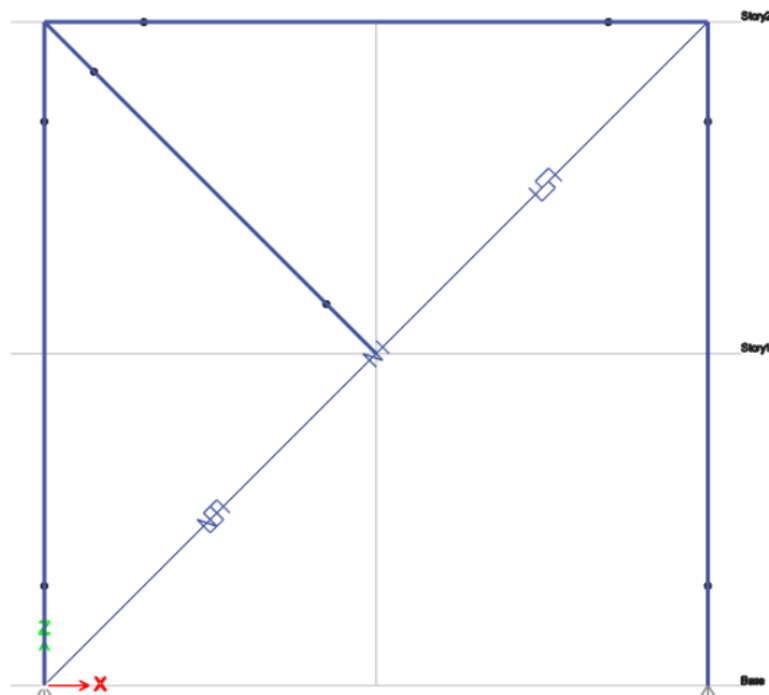


Figure 3.2-7: ETABS© Modeled Braced Frame with Two-Stage Links Input.

With the parameter inputs placed in the correct link properties as discussed above, the braced frame will act as a bracing member of a stiffness with a two-stage friction damper applied. Using the Wen link, the damper will slip at the input forces for the respective stage. The first Wen link, Friction_D1, will slip at the input service load found from the design calculations and will slip, either in compression or tension, to the distance input within the Gap and Hook links parameters described. The same process will take place at the second stage Wen link, Friction_D2, for the ultimate load input and

found based on design calculations. Again, once reaching this desired ultimate force, the model structure would again slip to the distance input within the final Gap and Hook links, Gap_D2 and Hook_D2. The combination of these links allows the structure to behave in the motion of the desired hysteresis. The diagrammatic breakdown of the links individual and combined behaviors to achieve this can be found within Figure 3.2-8.

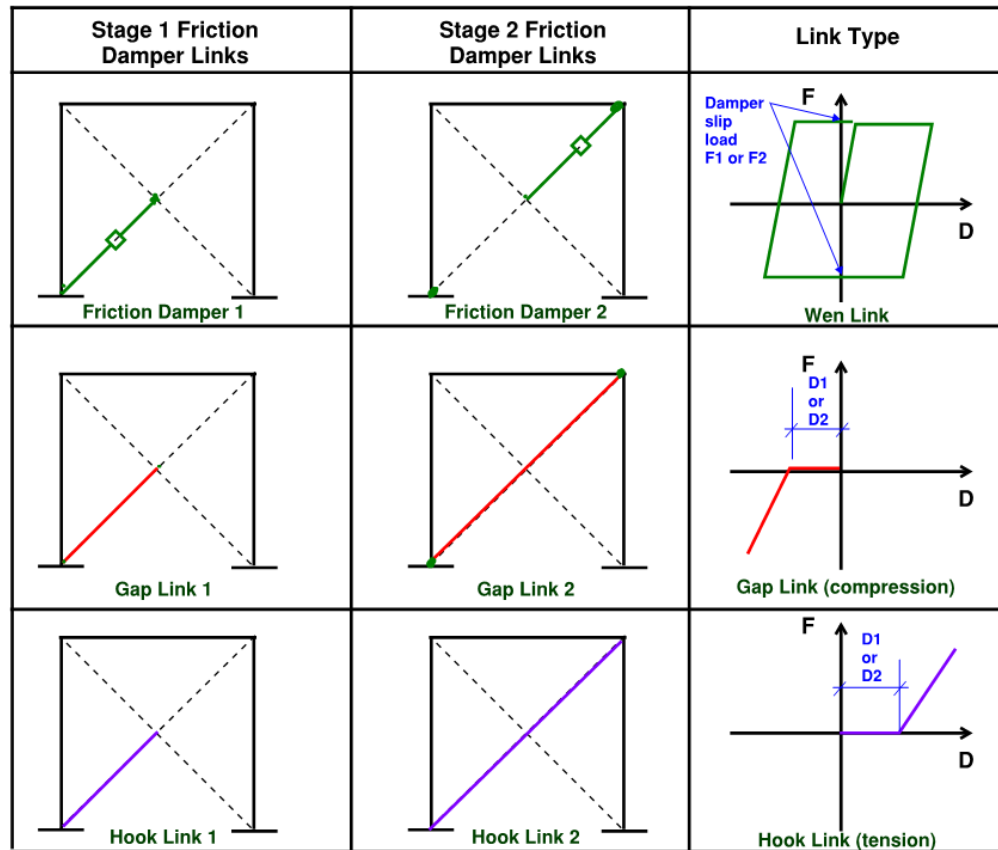


Figure 3.2-8: Combined Diagram of Link Behaviors.

3.2.5. Defining Link Parameters

To achieve the desired inputs for ETABS© analysis of the two-stage friction damper, a series of equations as well as several design parameters were needed. The design parameters were as follows: Stage 1 Lateral Force (P1), Stage 2 Lateral Force

(P2), braced frame height (H), braced frame length (L), Stage 1 slip (D1), Stage 2 slip (D2). These design values for Stage 1 and 2 of the friction damper are determined such that the structure meets the performance criteria defined by building code (e.g. SLE and MCE lateral forces and drift limits for a building subjected to seismic loads). The braced frame height and length are determined based on building geometry for the building. In this study, prototype buildings are used to keep the focus on behavior of the two-stage friction dampers and not the design of the frames themselves. In addition, a member size for the braced frame must be selected to determine the global lateral stiffness and elastic deformation of the building.

For the ETABS© inputs to be obtained, the input parameters should be adjusted using a series of equations to represent the actual stiffness and deformation of the system and braced frame. Local forces and displacements can be transformed to global forces and displacement using the angle (θ) of the bracing member in the braced frame. Figure 3.2-9 presents a generic braced frame with local and global parameters.

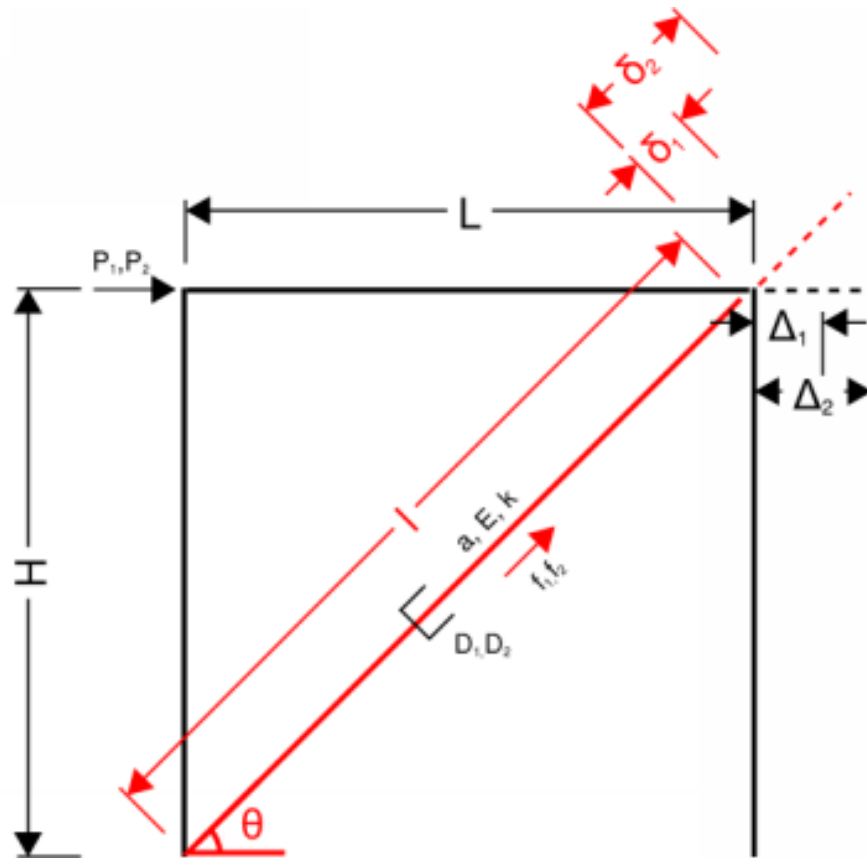


Figure 3.2-9: Two-Stage Friction Damper Parameter Graphic.

The local parameters being used in this transformation are as follows:

l = length of bracing member,

a = area of bracing member,

f_1 = Stage 1 axial force on bracing members,

f_2 = Stage 2 axial force on bracing member,

d_1 = elastic deformation of bracing member under axial load f_1 ,

d_2 = elastic deformation of bracing member under axial load, f_2 ,

D_1 = stage 1 slip distance,

D_2 = stage 2 slip distance,

δ_1 = total brace deformation after stage 1,

δ_2 = total brace deformation after stage 2.

The global parameters being used in this study are as follows:

P_1 = Stage 1 lateral load,

P_2 = Stage 2 lateral load,

θ = angle of bracing member with respect to the horizontal line,

E = modulus of elasticity for frame material,

H = frame height,

L = frame length,

Δ_1 = total story drift at stage one, and

Δ_2 = total story drift at stage two.

Using the parameters defined in this section, the following series of equations was used to model a two-stage friction damper in ETABS. The angle θ of the bracing member can be calculated using Equation (3.2-1):

$$\theta = \tan^{-1}\left(\frac{H}{L}\right). \quad (3.2 - 1)$$

The lateral forces P_1 and P_2 need to be converted to axial forces along the longitudinal axis of the bracing member, f_1 and f_2 , using Equation (3.2-2):

$$f = \frac{P}{\cos \theta}. \quad (3.2 - 2)$$

The axial deformation due to axial force, f , can be calculated using Equation (3.2-3):

$$d = \frac{fL}{aE}. \quad (3.2 - 3)$$

Following the axial deformation, the defined slip distance D_1 and D_2 for each respective stage is used to find the overall deformation of the bracing member, δ , at each stage using Equation (3.2-4):

$$\delta = d + D. \quad (3.2 - 4)$$

Using this, the overall deformation in the local coordinate system of the brace is defined for each stage, and the global lateral displacement of the frame can be calculated using Equation (3.2-5):

$$\Delta = \frac{\delta}{\cos \theta}. \quad (3.2 - 5)$$

ETABS© inputs and parameters can be defined in order to model the two-stage friction dampers inside of a braced frame. Stiffness parameters, defined in local coordinate system of the link, for linear and nonlinear behavior should also be defined. The stiffness values can be determined using the relationship between the axial load in the local coordinate system of the bracing member and its deformation under Equation (3.2-6):

$$k = \frac{f}{d} . \quad (3.2 - 6)$$

The yield strength, F_s , for the link can be determined. This value is the value at which the damper is engaged at each stage and is equal to the axial force, f_1 and f_2 , for stage 1 and stage 2, respectively. These values are used as input for the yield strength for stage 1 (FD1) and stage 2 (FD2).

For the Hook and Gap links, a value of “open” is needed to simulate the slip distance from the friction damper. This value Open1 and Open2, for each stage is found using the total deformation desired of the member. These values, δ_1 and δ_2 , at each stage are input in the respective Hook/Gap link parameters. These values are used to determine the points at which the members stiffness is enacted again, and the slip distance has been achieved.

To use the links to create the two-stage friction damper behavior, the links must be defined in the model correctly. For the hook and gap links, it is essential that the extent of the links is connected to the correct nodes within ETABS. Since these links

control the slip and deformation of the system. Therefore, as shown in Figure 3.2-8, those links for the first stage extend to the middle node of the frame. This allows the system to “slip” or displace at Stage 1 and continue to displace following. By extending the links in Stage 2 to the upper right node of the frame, this limits the system to stop displacing at the end of Stage 2, i.e. maximum displacement can be controlled.

To define the friction damper, the two stage parameters call for the Stage 1 Wen link to have its extents to the middle node of the bracing frame. For the second stage, the link extends from the center node to the upper right node to define the second slip of the damper. The Wen links also define the stiffness of the bracing member which is the result for the linear elastic deformation leading up to the slip force for each stage. Appendix B presents the spreadsheet in Excel developed to calculate the parameters of a two-stage friction damper.

3.3. Pushover Analysis

To ensure the validity of the equations defined above, as well as to check the behavior of the links defined within the software, a series of trials were conducted on a simple SDOF model. Within ETABS©, a one-story, one bay braced frame was created. At a height of 12 feet and a width of 12 feet, the single-story, single-bay frame was outfitted with a two-stage friction damper in the form of the combination of nonlinear links described in the previous sections (Figure 3.3-1).

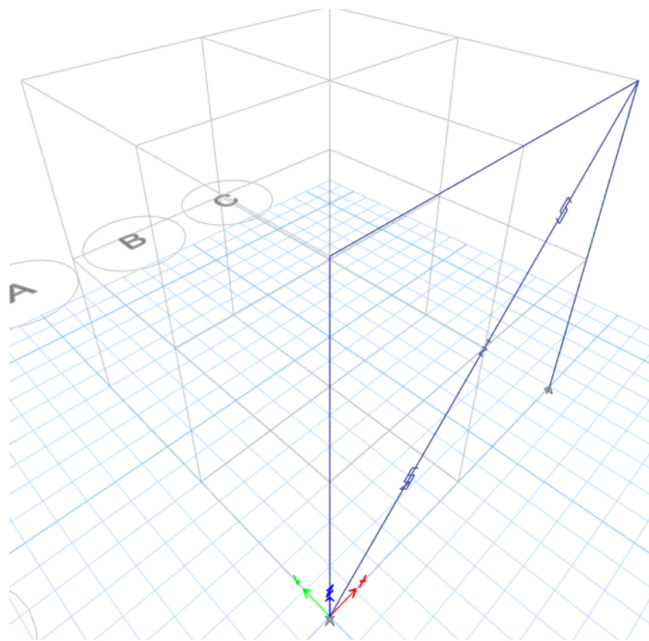


Figure 3.3-1: Pushover Analysis - Single-Bay, Single-Story Model.

The model was then subjected to a displacement-controlled Pushover Analysis. This analysis, defined within ETABS© as a nonlinear static load case, allows a load to be placed at the upper story of the frame. A load case is then applied for this load. The load case is defined as a multiple state, displacement-controlled load application, meaning the structure will be subjected to a load of increasing magnitude until reaching a desired displacement value. By using a multiple state analysis, all results over the course of the loading will be saved. This allows for a hysteresis and time history analysis to be generated following the analysis. Using a displacement-controlled value of 5 inches, a Pushover Analysis was run on the model. The results, shown in Figure 3.3-2, show the desired results, with the friction damper slipping at the defined first-stage force, and again at the desired second-stage force.

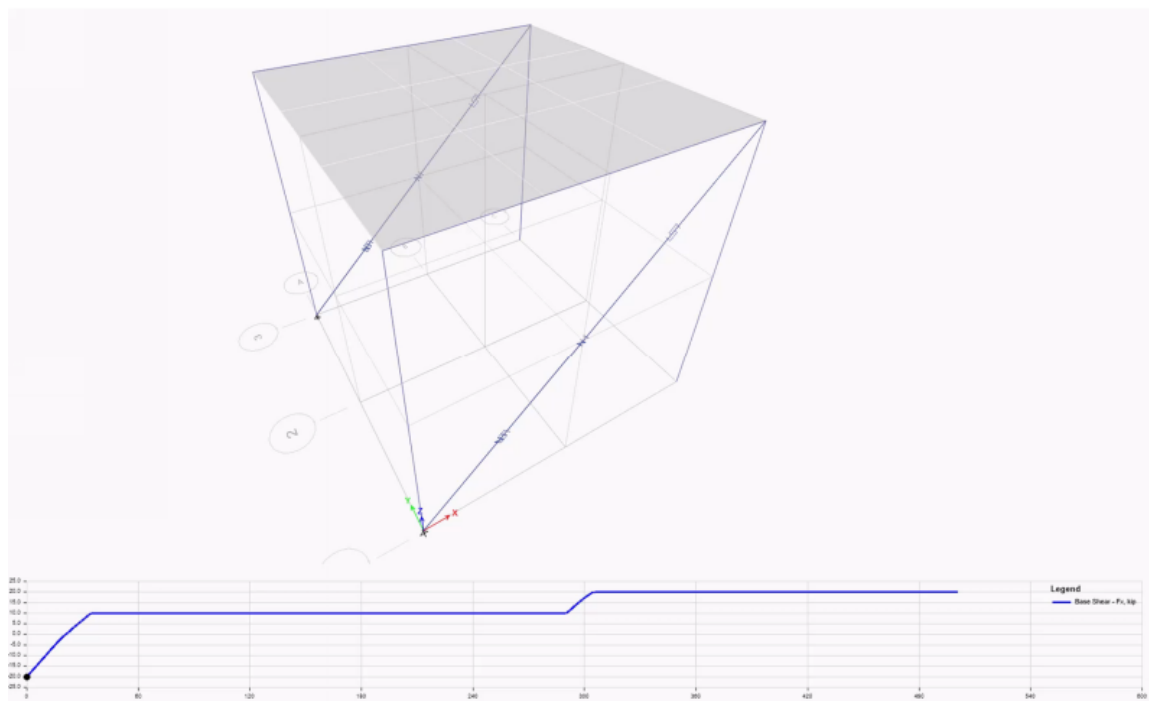


Figure 3.3-2: Pushover Analysis Results.

3.4. Cyclic Loading Trials

Following the successful running of the Pushover Analysis to check the behavior of the links defined within the model, a series of Cyclic Loading Trials was applied to the model. These trials, ran as a series of Pushover Analyses, allow the behavior of the model under loading and unloading in both directions. Using this, the overall hysteresis of the model can be observed to ensure the two-stage friction damper is correctly simulated by the links.

The equations from Section 3.2.5 of this report were used to determine the ETABS© link inputs needed to limit the structure to a displacement value of 3% of the structure's height using a HSS3x3x1/2 bracing member. Arbitrary lateral loading slip values, P1 and P2, of 10 and 20 kips, respectively, were applied to the structure. This

meant that the structure should reach the first stage of the damper, slipping at the force over a distance of D_1 , when the loading reached a value of 10 kips. In the same way, the structure would slip again, at the value of 20 kips over a distance D_2 . Following this value, the model would deform through elastic deformation of the bracing member until reaching the desired displacement limit.

Using four Pushover Analyses to define the positive and negative loading, in the x-direction, and the first and second stages of each, the hysteresis for the trial was able to be determined. This behavior, shown in Figure 3.4-1, shows the accurate representation of the links to model the two-stage friction damper behavior within the software.

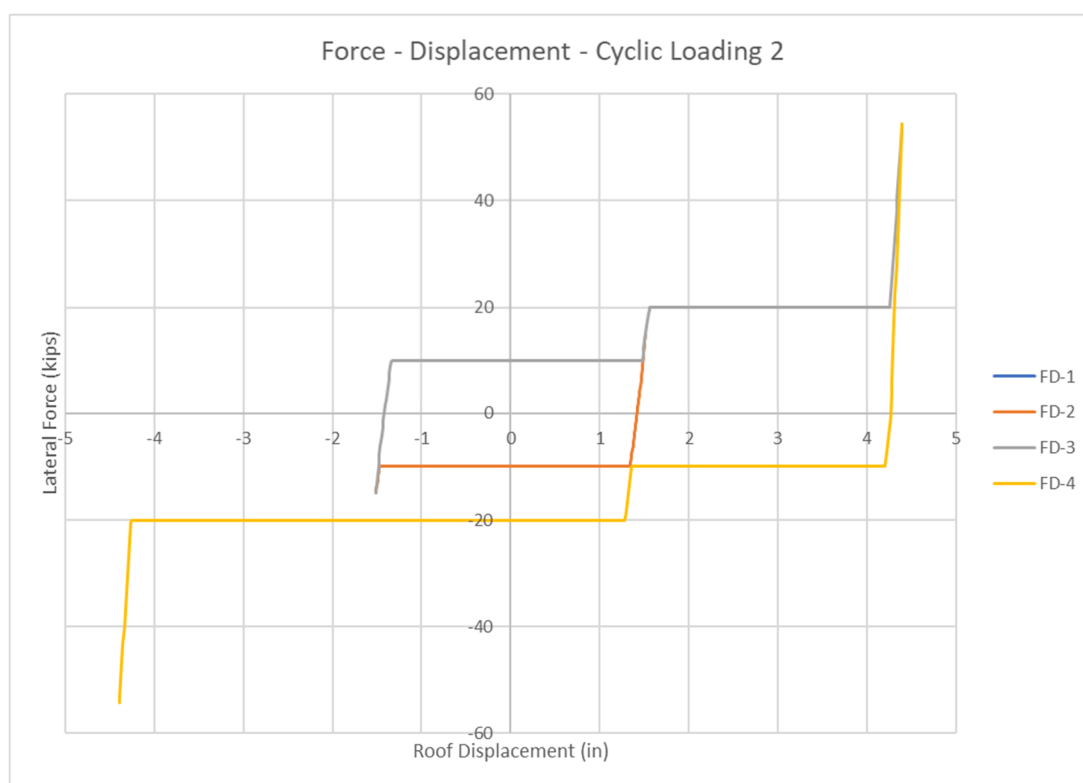


Figure 3.4-1: Cyclic Loading Trial Hysteresis Results.

As shown by the hysteresis achieved from the trials, the damper behavior simulated by the links created the desired results. The first stage, being enacted at the 10-kip loading, allowed the damper to be engaged, slipping the D_1 distance before returning the frame to elastic deformation. Likewise, the second stage, enacted at the 20-kip loading, allowed the damper to slip again a distance D_2 before returning the elastic deformation only. This was repeated in the unloading process, with the damper slipping back, returning the neutral position and the slipping again for the negative loading of the structure. Given the accuracy of the results, the Cyclic Loading Trials confirmed that the damper behavior desired was simulated within the ETABS© model using the combination of links.

3.5. Single Bay Seismic Analysis

3.5.1. Application of Loads

With the verification of the links modeled to show the correct behavior of the two-stage friction damper, a more realistic loading could be applied to the model structure. To achieve this, seismic loading needed to be accurately applied to the building. Using a suite of ground motions is the best approach to determine the application of the two-stage damper in any scenario or location. The Applied Technology Council, or the ATC, completed a study in 2009 for the Federal Emergency Management Agency (FEMA) [8]. This study, labeled ATC-63, reported the data from 14 earthquakes across the world. The study by the ATC identified items such as response factors for performance and design work. For the purpose of the research covered within this study, the ATC data were used to apply the 44 ground motions from the study to the

modeled two-stage damper (see Figure 3.5-1). This application allowed for a major-realistic loading spectrum to be subjected on the frames modeled.

| ID No. | Earthquake | | | Recording Station | |
|--------|------------|------|--------------------|------------------------------|----------|
| | Mag. | Year | Name | Name | Owner |
| 1 | 6.7 | 1994 | Northridge | Beverly Hills - 14145 Mulhol | USC |
| 2 | 6.7 | 1994 | Northridge | Canyon Country-W Lost Cany | USC |
| 3 | 7.1 | 1999 | Duzce, Turkey | Bolu | ERD |
| 4 | 7.1 | 1999 | Hector Mine | Hector | SCSN |
| 5 | 6.5 | 1979 | Imperial Valley | Delta | UNAMUCSD |
| 6 | 6.5 | 1979 | Imperial Valley | El Centro Array #11 | USGS |
| 7 | 6.9 | 1995 | Kobe, Japan | Nishi-Akashi | CUE |
| 8 | 6.9 | 1995 | Kobe, Japan | Shin-Osaka | CUE |
| 9 | 7.5 | 1999 | Kocaeli, Turkey | Duzce | ERD |
| 10 | 7.5 | 1999 | Kocaeli, Turkey | Arcelik | KOERI |
| 11 | 7.3 | 1992 | Landers | Yermo Fire Station | CDMG |
| 12 | 7.3 | 1992 | Landers | Coolwater | SCE |
| 13 | 6.9 | 1989 | Loma Prieta | Capitola | CDMG |
| 14 | 6.9 | 1989 | Loma Prieta | Gilroy Array #3 | CDMG |
| 15 | 7.4 | 1990 | Manjil, Iran | Abbar | BHRC |
| 16 | 6.5 | 1987 | Superstition Hills | El Centro Imp. Co. Cent | CDMG |
| 17 | 6.5 | 1987 | Superstition Hills | Poe Road (temp) | USGS |
| 18 | 7.0 | 1992 | Cape Mendocino | Rio Dell Overpass - FF | CDMG |
| 19 | 7.6 | 1999 | Chi-Chi, Taiwan | CHY101 | CWB |
| 20 | 7.6 | 1999 | Chi-Chi, Taiwan | TCU045 | CWB |
| 21 | 6.6 | 1971 | San Fernando | LA - Hollywood Stor FF | CDMG |
| 22 | 6.5 | 1976 | Friuli, Italy | Tolmezzo | -- |

Far-Field Set (Events)

- 14 Events
- 22 Records

44 Comp's

- Magnitudes:

Avg - M7.0

Max – M7.6

Min – M6.5

ATC-63 Project

Figure 3.5-1: ATC 63 Ground Motions [8].

The ground motions, shown in Figure 3.5-1, came with two components for each quake, totaling 44 ground motions. Importing these ground motions to the ETABS© module, the model was able to be subjected to loading based on realistic ground motions.

3.5.2. Building Geometry and Effective Weight

To apply the ground motions and achieve the true seismic loading applied to the building, a definite building geometry and design criteria needed to be determined. The modeled building was expanded to be a single-story, single-bay system. The spacing, out of plane of the lateral force, of the frames was determined to be 75 feet. Using an effective weight of 75 psf for the floor loading, the total effective loading at the top of each frame's structure was found to be 2.813 kips per foot of length. This was applied within ETABS© as a gravity loading, labeled W_Eff. This loading was assigned, also, as the mass source for all the ground motions imported. This meant that the loading of the seismic lateral load would be realistic applied as desired (see Figure 3.5-2).

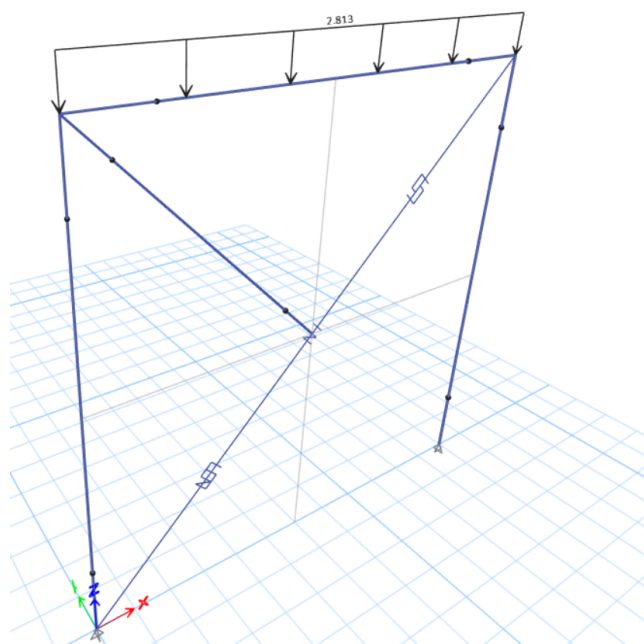


Figure 3.5-2: Effective Weight Loading Applied within ETABS©.

The single bay was analyzed via a random selection of one of the 44 ground motions to ensure the behavior of the frame under the new applied loading. Randomly selecting a few of the ground motions ran allowed confirmation that the model was being ran correctly to simulate the damper behavior. The results, shown in Figure 3.5-3, found the hysteresis to be shown as before, slipping at the predetermined force values. Note that the loading applied was not enough to engage the second stage of the damper.

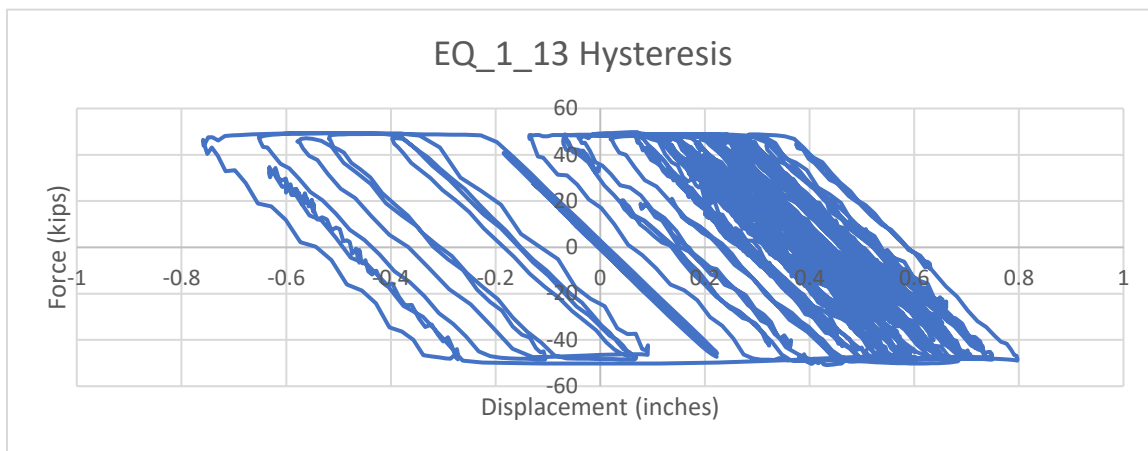


Figure 3.5-3: Hysteresis Plot Under Randomly Selected Ground Motion, Scaled to 1.0g.

3.6. 4-Bay Seismic Analysis

3.6.1. Scaling Ground Motions

Expanding the building and its LFRS to a larger more realistic system, the model was expanded to a four-bay, single story structure (Figure 3.6-1). Placing a bracing member at each of the ends of this frame with a two-stage friction damper, the now increased lateral force generated from the added effective weight would be shared by each frame, considering a rigid diaphragm for the building.

Scaling Ground Motions

With the current ground motions applied within the model, the motions are based off the data provided within the ATC-63 study. While valid, these values are those recorded from each location in which the quake was recorded. To dial in the design of the dampers and model, a specific location was selected. Using the location of San Diego, California, the dampers could be subjected to a much more specific suite of ground motions. To do so, the motions needed to be scaled to a response spectrum for both the service loads, SLE, and the ultimate loads, MCE.

The response spectrum for the San Diego location chosen were retrieved from the online database, ATC Hazards. This site, along with providing wind and snow data, gives design values and parameters for seismic design across the United States. Importing both the S_{DS} and S_{DI} values via the database to ETABS© properties allowed for the software to create the response spectrum. The values from the database, however, were not the correct values needed to scale the spectrum to the SLE and MCE levels. To do this, the values retrieved were scaled. For the SLE loading, the design values from the source were reduced by a factor of 0.70. The SLE factor of 0.7 was a conservative value used for the preliminary analysis of the damper and would be refined if needed. In the same way, the design values were increased by a factor of $3/2$ (or 1.5) to achieve the ultimate loading spectrum of MCE levels.

All 44 ground motions were scaled to the two spectrums (i.e., SLE and MCE). Using the spectrum matching function within ETABS©, the ground motions were scaled to the correct levels for analysis.

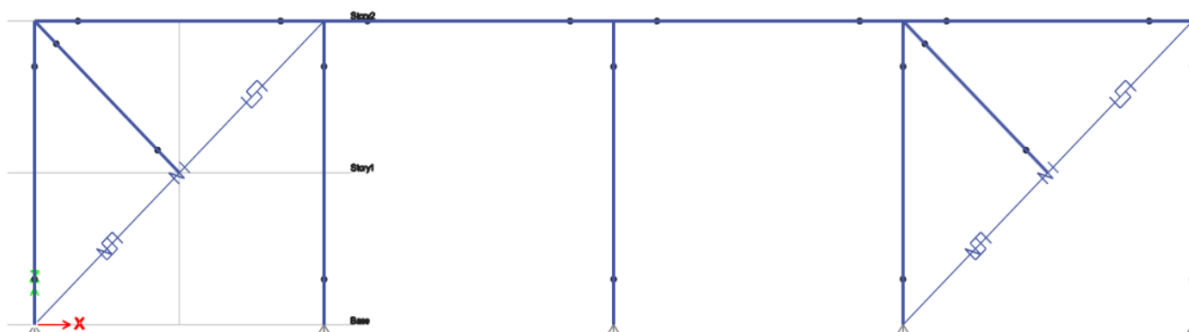


Figure 3.6-1: 4-Bay ETABS© Model with Two Two-Stage Friction Dampers.

3.6.2. Scaled Analysis

Applying the scaling to the ground motions allows for a service level and ultimate level analysis to be conducted. Running the equations from Section 3.2.5, the values of the inputs could be determined. For the MCE level loading at each brace, the effective weight of 2.813 kips per foot was applied over half of the LFRS length, 48 feet, resulting in a value of 67.5 kips. This value, applied laterally, was used at the second stage slip force, P_2 , applied. Scaling down by a factor of 0.7, the SLE slip force was found to be 47.25 kips, used as the first stage slip force, P_1 . These values were used to find the inputs for the ETABS© link properties. The values used in this analysis are presented in Table 3.6-1.

Table 3.6-1: Link Input Values for 1.0 Scaled Two-Stage Friction Damper.

| ETABs Input Values | | | | |
|--------------------|---------------|------------------|----------------|-------|
| | Lin Stiffness | Nonlin Stiffness | Yield Strength | Open |
| | lb/in | lb/in | lb | in |
| FD1 | 915654.18 | 915654.18 | 66822 | --- |
| FD2 | 915654.18 | 915654.18 | 96167 | --- |
| Hook1 | 915654.18 | 915654.18 | --- | 0.503 |
| Hook2 | 915654.18 | 915654.18 | --- | 2.58 |
| Gap1 | 915654.18 | 915654.18 | --- | 0.503 |
| Gap2 | 915654.18 | 915654.18 | --- | 2.58 |

The model was run using these inputs, generating a hysteresis for each of the 44 ground motions for both the SLE and MCE levels, totaling 88 plots. Looking at the plots, the values of MCE forces under the scaled ground motions never reached the second stage force of 135 kips (67.5 kips per bay) in several of the trials. This can be shown from the sample plots from the 44 MCE trials in Figure 3.6-2.

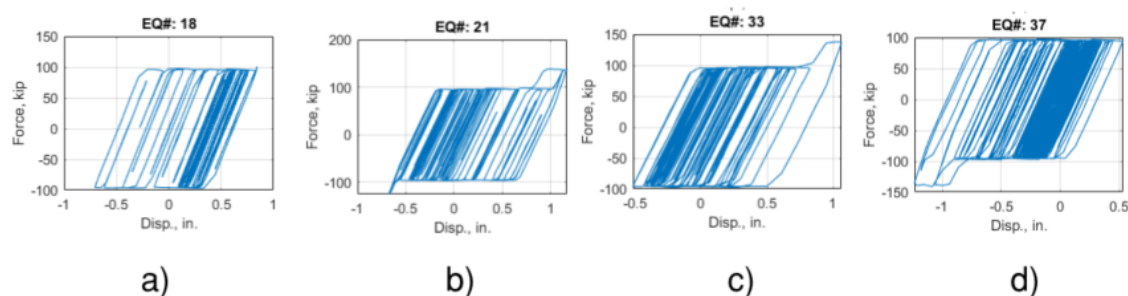


Figure 3.6-2: MCE 1.0 Scaled Outputs. a) ground motion EQ_1_18, b) ground motion EQ_1_21, c) ground motion EQ_2_11, d) ground motion EQ_2_15

Acknowledging the second stage not being enacted within some of these scaled trials, the damper slip values were decreased in their design. To achieve this, the first and second stage interaction values, P1 and P2 were reduced. This allowed the friction

dampers stages to be engaged at lower levels, making for both a conservative design and allowing the full use of the two-stage damper. Trials with scale factors of 0.8, 0.6, and 0.4 were conducted. Using the 0.8 trial as an example, the values of the P1 and P2 values, or the lateral force applied to slip at stages 1 and 2 of the dampers, were reduced to 80% of their calculated values. For the first stage, the P1 slip value was reduced from 47.25 kips to a value of 37.8 kips. The same was done for the P2, second slip force, value, reducing it to 54.0 kips from the original 67.5 kips. The reduced value required new ETABS© link inputs. Those new values can be found in Table 3.6-2.

Table 3.6-2: Link Input Values for 0.8 Scaled Two-Stage Friction Damper.

| ETABS Input Values | | | | |
|--------------------|------------------|------------------|----------------|--------------|
| | Lin Stiffness | Nonlin Stiffness | Yield Strength | Open |
| | lb/in | lb/in | lb | in |
| FD1 | 979735.73 | 979735.73 | 53457 | --- |
| FD2 | 979735.73 | 979735.73 | 76368 | --- |
| Hook1 | 979735.73 | 979735.73 | --- | 0.505 |
| Hook2 | 979735.73 | 979735.73 | --- | 2.57 |
| Gap1 | 979735.73 | 979735.73 | --- | 0.505 |
| Gap2 | 979735.73 | 979735.73 | --- | 2.57 |

Once the slip forces had been scaled down, the new inputs were placed within the links and the analysis was run again. Looking at Figure 3.6-3 and comparing the results to those shown for the 1.0 trials shown in Figure 3.6-2 although slipping slightly more often, most trials did not reach or barely reached the second stage of the damper. The trials were then repeated for reduced values of 0.6 using the same process as depicted above for 0.8.

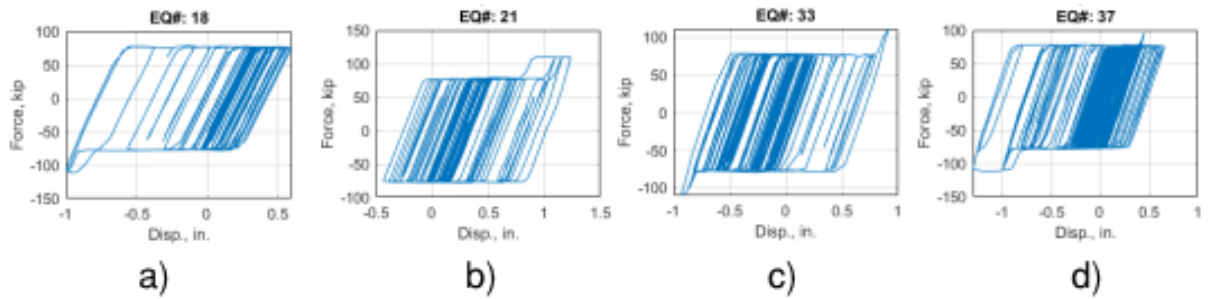


Figure 3.6-3: MCE 0.8 Scaled Outputs. a) ground motion EQ_1_18, b) ground motion EQ_1_21, c) ground motion EQ_2_11, d) ground motion EQ_2_15

As can be seen, the value MCE level trials for the 0.8 trials began to show a slipping at the second stage for a larger number of the trials. However, most barely reached the value and did not fully slip at that value. To create the full benefit and testing of the damper, the desire was to ensure full engagement of both stages of the two-stage friction damper. To achieve this full effect, the trials were again scaled down, this time using a factor of 0.6. The results for the MCE trials for the 0.6 Scaled 4-bay test can be seen below in Figure 3.6-4. Now, nearly all ground motions enact the second stage of the two-stage friction damper, slipping significantly at that point.

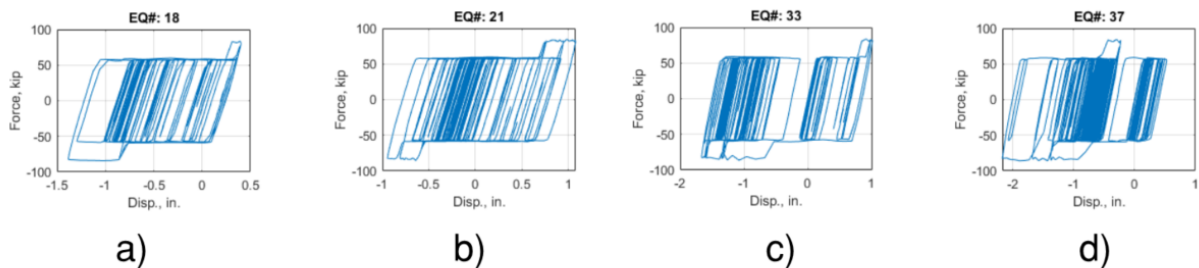


Figure 3.6-4: MCE 0.6 Scaled Outputs. a) ground motion EQ_1_18, b) ground motion EQ_1_21, c) ground motion EQ_2_11, d) ground motion EQ_2_15

Now that both stages have been enacted and the two-stage damper can be fully functional, this is where the design would be held at. This meant that the damper, designed to slip at values of 0.6 times the calculated service and ultimate loading values, would be conservatively designed. By enacting the damper at lower forces, also, the damper would be much more effective in damping and dissipating the energy away from the building LFRS.

The process was repeated once more for the 0.4 scale. As seen in Figure 3.6-5, the ground motions at the MCE scale nearly all reached the second stage of the damper application. This scale allowed both stages to be engaged and used to dissipate the forces seen during the seismic event. It was determined that the 0.4 scale of the damper would be used on all following trials to ensure that the 2nd stage of friction dampers could be reached to dissipate energy at MCE level.

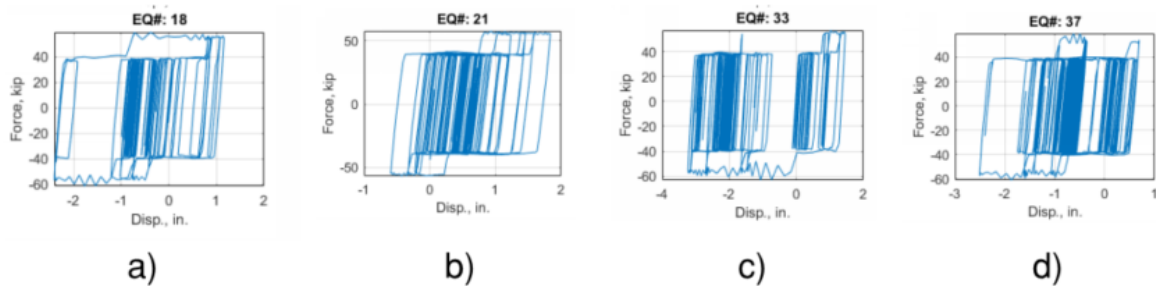


Figure 3.6-5: MCE 0.4 scaled outputs. a) ground motion EQ_1_18, b) ground motion EQ_1_21, c) ground motion EQ_2_11. d) ground motion EQ_2_15

3.7. 4-Story Analysis Setup

Using the 0.4 scaled damper properties and the link inputs found in the 4-bay single story trials, the model was expanded. The 4-bay, two damper model was copied up

to create a four-story structure to conduct the final testing and development of the two-stage friction damper. The model structure, similar to before, consisted of a building with two braced frames at each end. These frames, spaced 75 feet apart, contained the 4-bay damper setup ran within the past trials. Figure 3.7-1 and Figure 3.7-2 show the building geometry of the model building that was employed in this Capstone project.

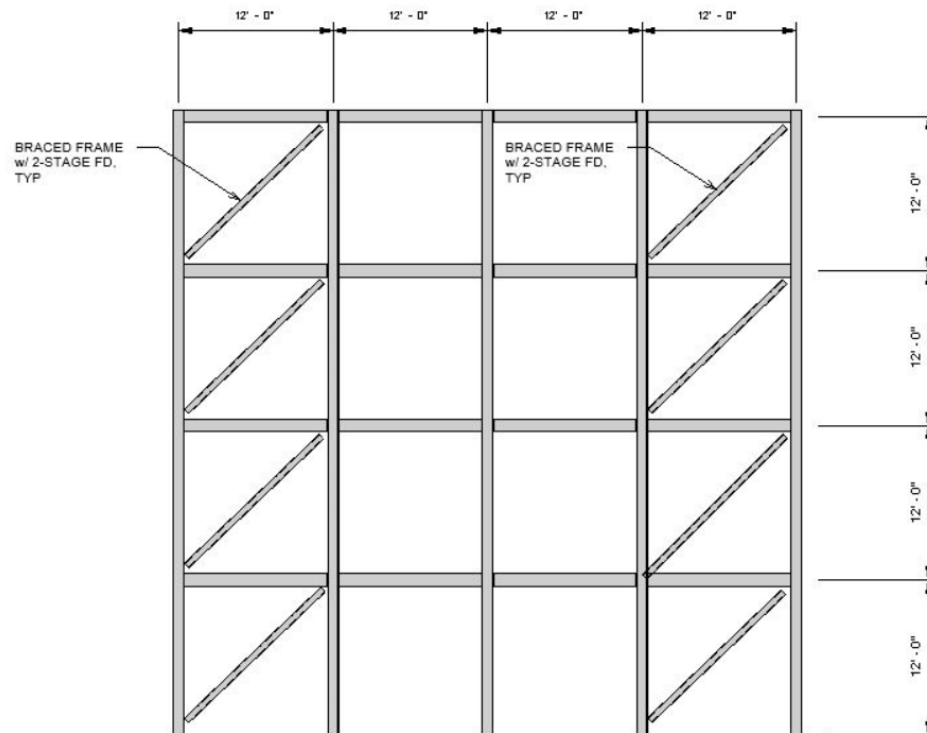


Figure 3.7-1: 4-Story, 4-Bay Friction Damper Model Building Elevation.

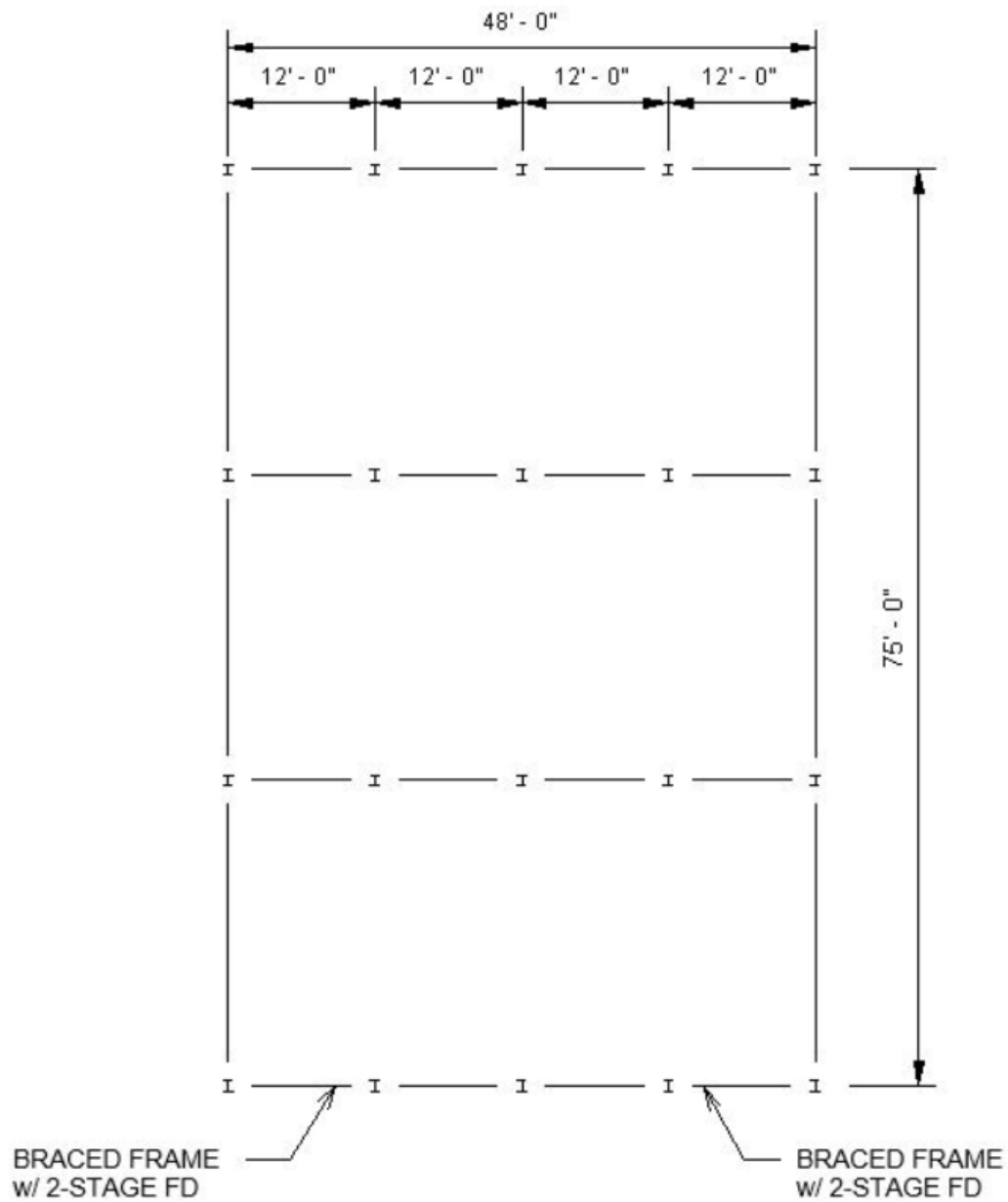


Figure 3.7-2: 4-Story, 4-Bay Friction Damper Model Plan View.

With the 4-story model, the limiting factor for the design will be to limit the inter-story drift between each of the floors in the structure. The values of the limits, determined from the performance-based criteria govern the drift values for both the structure at an SLE loading level and the ultimate MCE loading level. Since the floors

are modeled at the same height for each level of the structure, this number was able to be held consistent throughout. From the criteria, the drift limit of the upper level, found to be 0.5%, determined the maximum deflection desired at the end of the first stage. This value, created by the SLE loading applied to the building, includes the overall drift of the structure at that time. This maximum value is where the damper will be designed to stop at the first stage. To achieve this, the damper had to be addressed for both the slip distance at the first stage, but also the axial deformation of the bracing member sustained before reaching the slip force. Using Equation (3.2-2), the axial deformation of the member due to the loading can be found, leaving the remainder to be the value of the D_1 or slip distance of the first stage of the damper.

This process was repeated for the second stage of the damper to determine the maximum drift for the second stage. Based on the criteria, the value for this stage, the drift at the ultimate or MCE loading was found to be 3% of the floor-to-floor height of the structure. Having the consistent floor height this value was calculated to be 4.32 inches. In the same way, this determined the slip distance D_2 for the second stage of the damper. The difference for stage two was that in addition to the axial deformation and slip distance of the second stage, the same values from the first stage needed to be included in this total drift value.

To accurately determine the input values for the link parameters, a bracing section needed to be defined. To achieve this, the maximum forces that would be applied to the brace needed to be found. This design was approached using the design forces that were calculated in the beginning of the test setup, the SLE force of 47.25 kips and the MCE ultimate force of 67.5 kips. To ensure that the bracing member would be able to fully

handle forces up to this maximum force, at which point the second stage of the damper would begin to be engaged, the value of 67.5 kips was used for these members' design. Consulting the *AISC Steel Manual* 14th Edition, a member that both sufficiently and efficiently could handle this force for tension and compression was found. This member, at an unbraced length of 17 feet was determined to be an HSS6x6x1/2. This member would be redesigned at the end the trials, given the realistic and maximum force from the ground motions.

Chapter 4: Analytical and Numerical Results

Using the testing modeling and setup discussed above, the experimental analysis was ready to be conducted. This trial, a four-story, four bay structure with two-stage friction dampers within a braced frame LFRS was exposed to the suite of ground motions in order to determine its base shear, inter-story drift, and overall deflection values. These values would allow for both the comparison to the normal elastic values of a normal braced frame system to justify the use of the two-stage damper and for the further development of the two-stage damper in the future.

4.1. Initial Final Trials

The trials were conducted via the previous methods used in the single-story trials. Each ground motion, both at the SLE and MCE levels, were applied to the model structure. The dampers modeled using the same parameters as the single-story trials, were consistent at each of the floors of the structure. The critical results that were desired from the inter-story drift at the SLE and MCE levels stayed below the 0.5% and 3% of floor height, respectively. When the trials were analyzed as approached in the previous tests, the story displacement and story shear values were exported from the ETABS© model. When the values were analyzed and graphed, the overall values were averaged and compiled. Looking at Figure 4.1-1, the values for the maximum drifts of the structure were found to be 2.136 % at the MCE level, meeting the limit justified by the code of 3%. However, when looking at the drift values for the SLE level, the maximum drift was unable to meet this desired value, coming in at 1.3% drift, well above the 0.5% recommended.

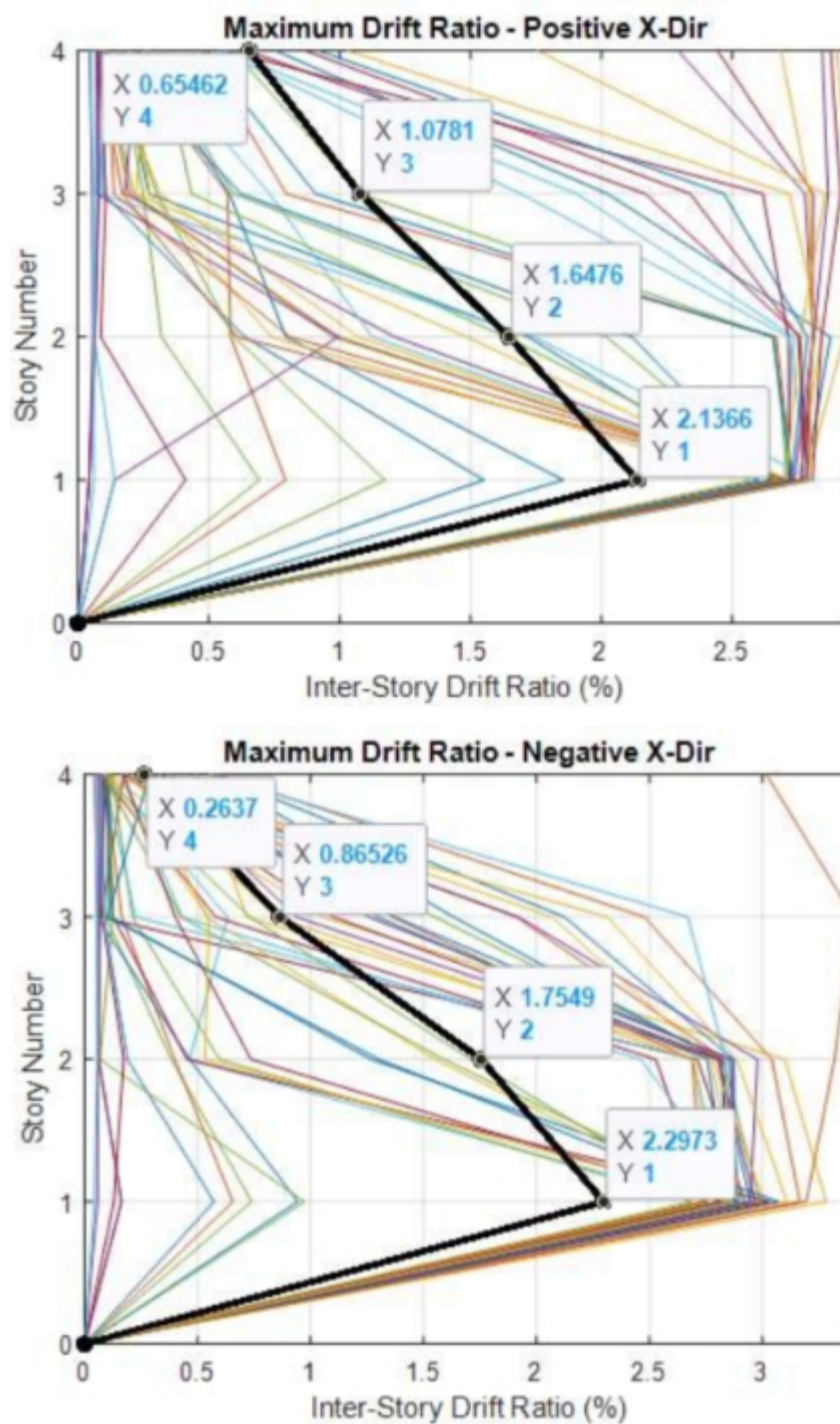


Figure 4.1-1: MCE Initial Final Trial Inter-Story Drift Ratios – 0.4 Scaled.

Looking at the ratios, and specifically, the SLE ratio, it was seen that the current modeling of the two-stage friction damper did not meet the code desired values for drift of the structure.

4.2. Adjusted SLE Values

To combat the current issue of the model not achieving the desired results, a solution was needed to be able to adjust the inter-story drift values of the trials without sacrificing the integrity of the model and its accuracy to a true building performance and loading.

Exploring a few options was place on the table when looking to reach the desired values. The first option was to adjust the displacement values of the damper itself to achieve a smaller overall slip for the system. This solution, while decreasing the slip values, would only increase the forces applied on the bracing member, defeating the purpose of the damper itself. By decreasing the amount of slip in the damper, the engagement of the friction pad would be less, attributing to a lessened energy dissipation in the system. The second solution was to increase the SLE force applied to the damper at stage one. This would allow for the frame to elastically deform to a higher force until slipping, thus decreasing the slip distance needed for stage one. In the same way, this process defeated the purpose of the damper and ultimately did not change the values achieved following the running of the forces through the damper.

The final solution was to look at the forces applied on the SLE trials. As mentioned in the experimental set up, all of the 44 ground motions used were scaled to

their accurate SLE and MCE levels. At this stage, the SLE, or service level, ground motions were scaled from the DBE, or design level, response spectrum values for San Diego. This scale, a factor of 0.7, was conservatively applied to the design values achieved from the ATC Hazards database. To decrease the displacements and ultimately the story drifts, the forces applied on the structure at the SLE level could be decreased. To appropriately decrease the current scale and apply a more accurate factor the design level loads, research was conducted to find a standard value used within the industry practice.

Using the research and the data provided from several projects conducted, a value of the SLE to DBE ratio was able to be determined. Two articles, one by I Wayan Sengara [9] and the other by Anwar *et al.* [10], show the investigative studies of performance-based and risk-targeted seismic design. The articles, along with discussion of several high-rise projects conducted by Bahmani [11], outlined several ratios for the value of SLE to DBE ratios used in seismic design. The results showed that most projects and research found the values used ranged to be from 0.28 to 0.41, with an average of approximately 0.32. To keep the design conservation and to allow for a more accurate application to all scenarios a value of 0.35 was chosen to be used for the SLE/DBE ratio for the trials conducted.

Within ETABS©, the San Diego-SLE response spectrum was adjusted, changing the S_s and S_1 parameters of the spectrum to match the newly determined SLE values of $0.35 \times \text{DBE}$, Figure 4.2-1 shows the new response spectrum generated.

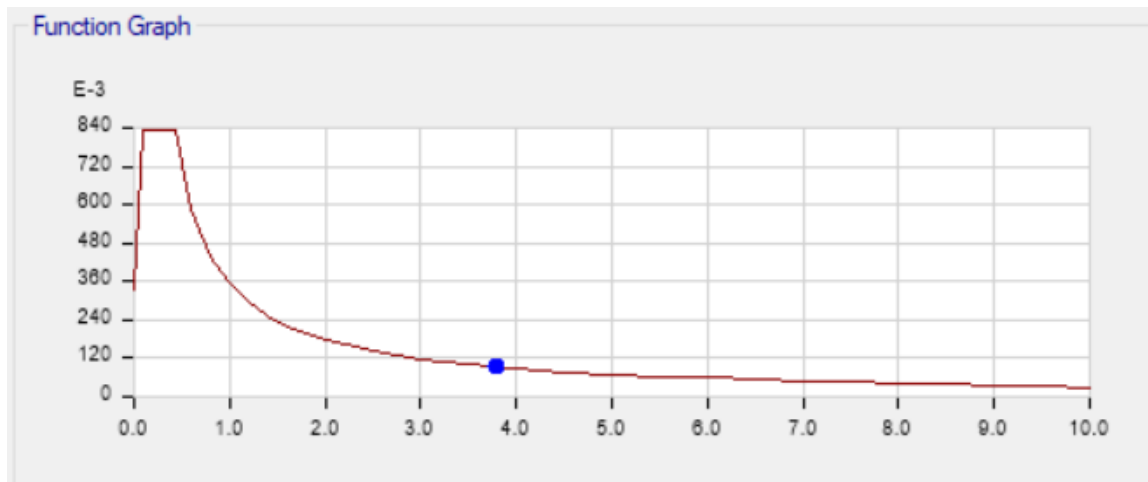


Figure 4.2-1: Adjusted SLE Response Spectrum (0.35*DBE) for San Diego, CA.

With the new adjusted SLE values, a final trial was able to run to determine the modeling, performance, and initial development of a two-stage friction damper.

4.3. Final Trial Displacement

Conducting the trials with the corrected SLE ratio, the displacement of the system was the key value to be determined. As shown in the initial trial, the SLE level ground motion using the first SLE ratio failed to meet the drift limit determined. Running the ground motions with the updated ratio, it was found that the maximum inter-story drift ratio of the structure in Figure 4.3-1 was around 0.65% on average. This figure, as all that follow like it show all ground motions ran, shown in various colors, and the average results of the multiple trials, shown as a thick black line with dots at each story. The average for this trial, while above the 0.5% target, allowed the damper to be deemed as a success in meeting the requirements set at the beginning of the design and testing.

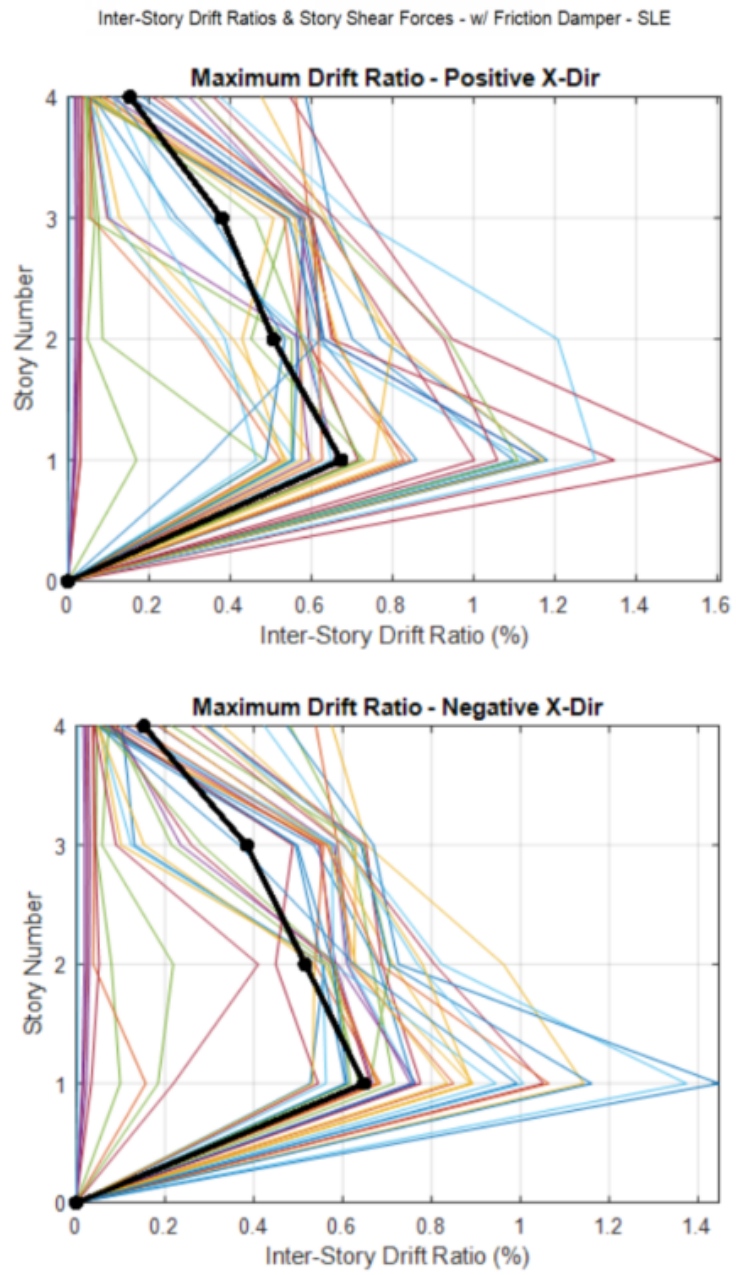


Figure 4.3-1: Updated SLE Trials Inter-Story Drift Ratio Plots.

The SLE drift did not fall under the predetermined limit of 0.5%, however it was deemed to be okay (0.65% for the first story, and less than 0.5% for the upper stories). The justification behind this decision falls in the category of engineering judgement. When looking at the design of the structure, the damper, and the loads applied, it can be seen that a conservative approach was taken at nearly every step. In the start of design for the damper and its model, the trials were run at scaled intervals in terms of the slip forces at stage one and two, defined as P1 and P2. In reducing these values by the intervals tested; 0.8, 0.6, and 0.4, the damper slip values and overall capacity was conservatively designed. In the same way, when looking at the adjusted SLE ratio, the value of 0.35 was taken even though the average of the studies found was less at a value of 0.32. Due to these conservative values, in addition to the SLE limit being a service condition rather than an ultimate or failure condition, it can be justified that the damper met the conditions that were determined and desired.

4.4. Final Trial Base Shear

One of the main goals of implementing the two-stage friction damper within a typical braced frame system is to reduce the loading on the braced frame and the overall base shear and overturning moment on the building structure. Within the trials conducted, a shape was selected preliminarily in order to conduct the trials and test the model for adequacy. Once the final parameters were determined and the overall base shear was found, an actual shape could be found for the framing member. This would then allow for the comparison to the shear values seen by the LFRS in the building with the two-stage friction damper implemented in the frame and a frame not containing the damper.

Running the model for the ultimate forces, MCE, allowed for the overall maximum base shear of the 4-story structure with the damper applied to be found. Given the 44-trials, it was found that the base shear, along with deflection and drift, varied for all ground motions. To allow for a damper that could be applied in all earthquake scenarios, along with keeping the theme of a conservative design, the average of these values was used for the comparison. As seen in Figure 4.4-1, the average base shear found while running the ground motions for the MCE level trials with the two-stage friction damper applied was found to be approximately 160 kips.

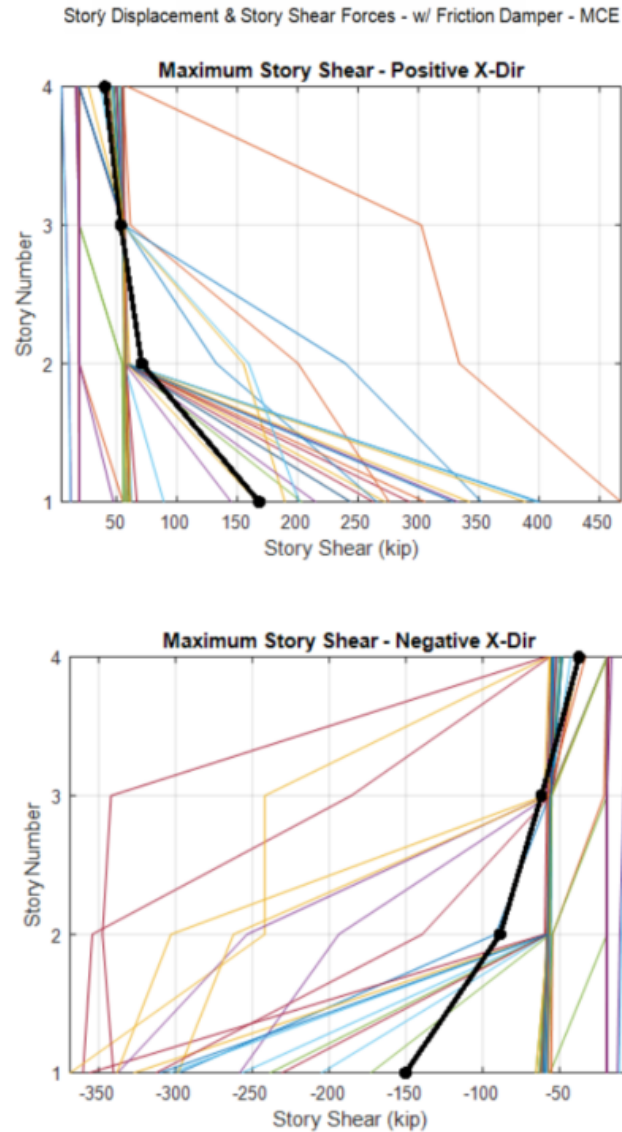


Figure 4.4-1: Final Trials MCE w/ Two-Stage Friction Damper Base Shear Plots.

A key aspect to determining the performance of the two-stage friction damper is to compare the base shear results to the elastic results of the same structure without the friction dampers applied. This structure, ran using the same bracing member as the

damper trials, will show the reduction factors of the damper in terms of base shear for both quake levels, SLE and MCE. Figure 4.4-2 shows the SLE forces achieved running the trials with the dampers. The average base shear for the trials, at 51 kips, was then to be compared to its elastic braced frame equivalent.

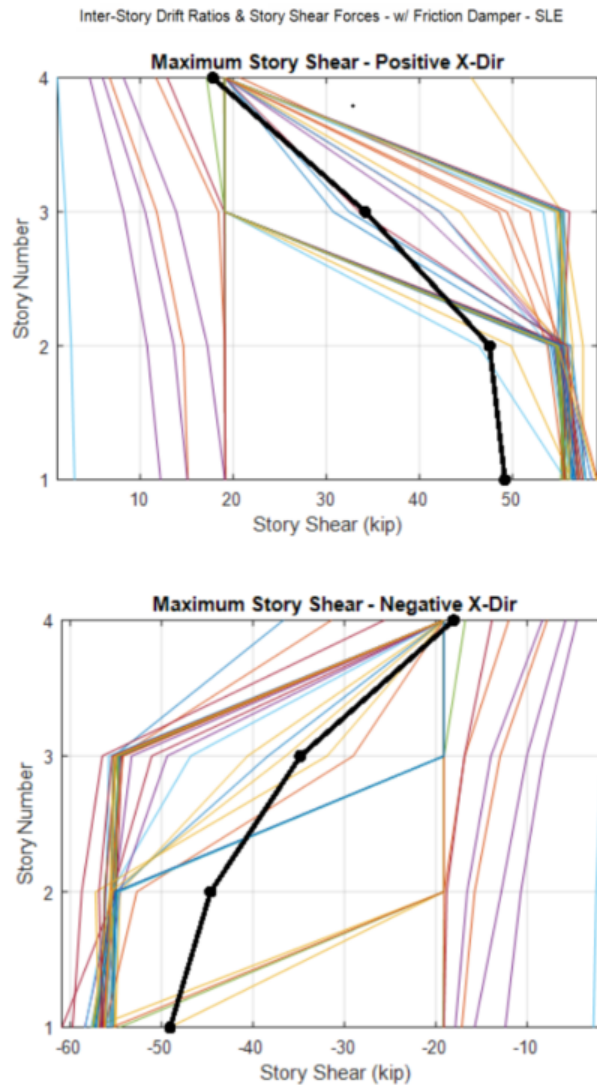


Figure 4.4-2: Final Trials SLE w/ Two-Stage Friction Damper Base Shear Plots.

The dampers were removed, and a simple bracing member was placed in their place to create a traditional braced frame LFRS. These trials produced results for base

shear that were much higher than that of the structure featuring the dampers. The average base shear for the elastic SLE trials, as shown by Figure 4.4-3, came in to an average value of approximately 255 kips. This value is seen to be significantly higher than the damper applied equivalent. The reduction for the structure using the two-stage damper at the SLE level was determined to be 5.0

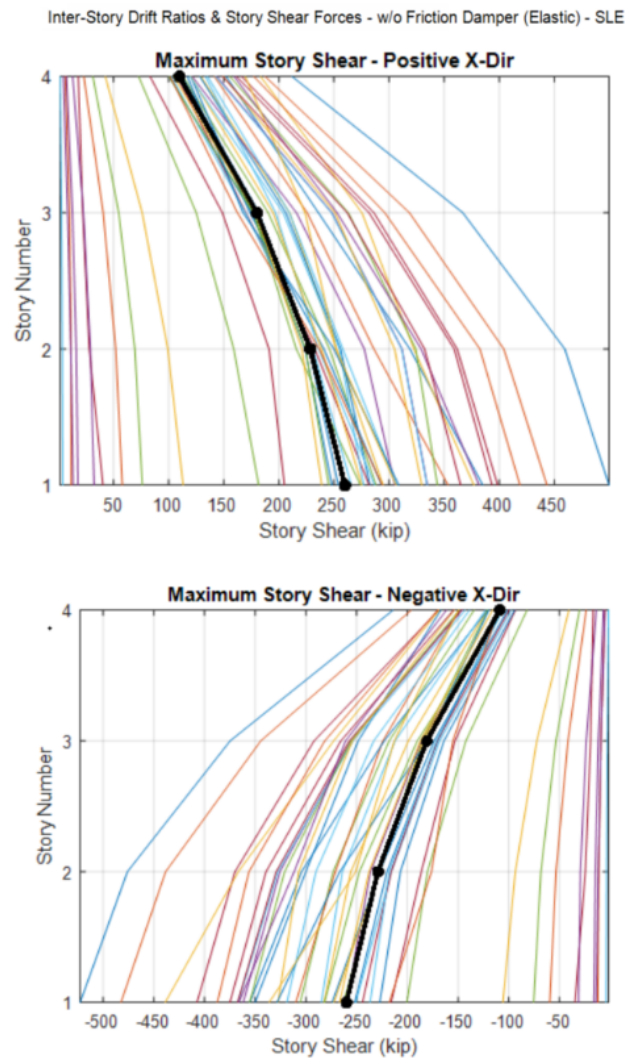


Figure 4.4-3: Final Elastic SLE Trials without Two-Stage Friction Damper Base Shear Plots.

The reduction, seen at the SLE level of the trials, was also seen at the MCE level. The ultimate trials, MCE, were the desired results of the research. These values are the key application of a damper within a structural system. Reducing the ultimate values allows the members that are used to design the structure to be reduced and become more economical as the ultimate loading is the governing factor for the member design. Figure 4.4-4 shows the output values for the base shear of the MCE trials ran without the dampers. The average base shear of nearly 1000 kips is much larger than that found in the damper trials, showing a reduction factor to the typical elastic, braced frame approach of 6.5.

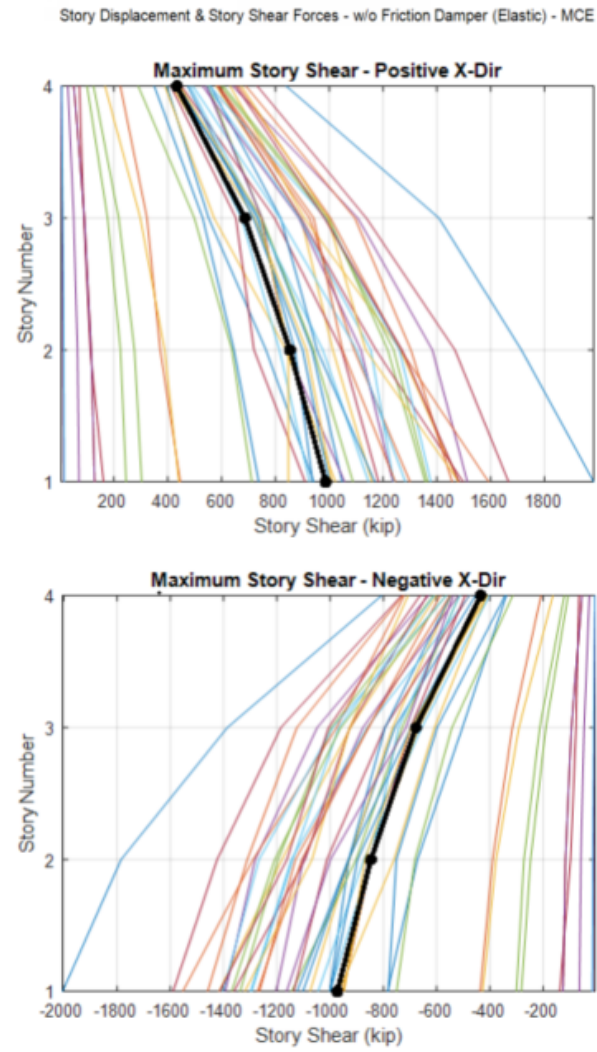


Figure 4.4-4: Final Elastic MCE Trials without Two-Stage Friction Damper Base Shear Plots.

Chapter 5: Discussion and Conclusion

The two-stage friction damper is a system that allows for the energy dissipation within a traditional braced frame lateral force resisting system in a building's structural frame. To consistently develop the damper and determine its performance under the suite of ground motions produced by earthquakes globally, an accurate model with a suite of ground motions needed to be analyzed. Within this study, a 4-story, 4-bay building was subjected to a suite of 44 ground motions at both the service, SLE, and the strength, MCE, loading. Limiting the inter-story drift of the structure, per the provisions in the current performance-based design guidelines, at each level allowed for a real-life simulation of the effects and performance of the damper. By creating a friction damper with a two-stage engagement, the loads at both stages can be dissipated, allowing for a much more efficient member design within the building. This efficient design allows for lower materials cost, additional space, and overall increase in safety within the structure itself.

The trials conducted, carried out within ETABS©, allowed for the comparison in performance of the structure with a damper to the traditional braced frame system found in structures industry wide.

5.1. Conclusions

5.1.1. Modeling within ETABS©

Using ETABS© for the modeling of the two-stage damper allowed for a much simpler process to develop the two-stage damper numerically. Using the links described

in Section 3.2 allowed for an ease of defining the slip distances, both in tension and compression, for the damper. These parameters allow an accurate model of the D_1 and D_2 values that are needed to be defined for the damper design and fabrication. In the same way, to define the slip forces, ETABS© Wen links provide a great opportunity to define this. Calculating the forces and being able to easily scale them as done with this research allowed for a streamlined process.

As it pertained to adding bays, floors and additional dampers, the replicate function within the program also expedited this process. This allowed for time to be spent elsewhere in the development of the damper and model. This application allows for all types of structure geometry and heights to be constructed and modeled using the two-stage friction damper.

5.1.2. Reduction Ratios

Following the trials conducted, both at the SLE and MCE levels, it was determined that the two-stage friction damper can be justified as a very effective damping system for building exposed to large seismic forces. The two-stage approach allows for a massive reduction in force applied to the structure, reducing base shear, and meeting performance criteria. By designing the dampers to meet these performance criteria limits as it pertains to inter-story drift, both the base shear values for the service load earthquakes, SLE, and the ultimate load earthquakes, MCE, were able to be reduced significantly. On the order of 5 and 6.5 reduction ratios, the suite of ground motions used proved that the two-stage friction damper, modeled within ETABS©, using the

combination of links described, allows for an accurate representation of a true structure behavior and model.

5.2. Future Work

5.2.1. Energy Dissipation

The development of the two-stage friction damper has many more steps that need to be taken following the model and analytical testing. Moving forward, the damper itself needs to be designed. Using the hysteresis curve generated when the building is subjected to the ground motions, the energy dissipation can be determined.

Energy dissipation within the friction damper is approached similarly to that in the dissipation of energy in a spring system involving a frictional resistance. Using this approach, the slip force within the braced frame can be found to size the friction pad needed for each condition and stage of the friction damper.

Looking into the typical approach to the above-mentioned spring system, it can be seen that a simple system is used to describe the system and its components. Within this system, an object with a mass (M) is subjected to a lateral force (F). This force causes a movement or displacement of the object (Δ). Two items resist this displacement, the spring stiffness (K) and the frictional force created from the frictional resistance of the object and the material below it. The spring stiffness is a given property and can be defined. It is used to find the displacement given a force or to find the force based on a given displacement. The second resistance, the frictional resistance, can be found using

the known friction coefficient (μ). This value is a known value based on the material of both the object and its interactive surface. Using this value, the relationship of this friction coefficient and the normal force (N), can be used to determine the friction force. The input energy can then be dissipated through work done by friction force between the objects. Therefore, the overall force in the system (F) can be found, stating that thus force is equal to the force of the system minus the frictional force of the system.

Applying this to the friction damper scenario, the result and the process are very much alike. Observing the system under increasing forces (F), the elongation of the frame member can be seen as the Δ in this scenario, shown in Figure 5.2-1. The elongation of the member is resisted by the stiffness of the bracing member. Once the force reaches the slip force (F_s), the friction damper is put in to affect, slipping the bolt and engaging the friction pad which has its own frictional coefficient (μ). This allows for the displacement of the system to happen with a desired value (D) derived by the slotted hole. Following this the system continues to deform based on the elongation of the member based on the stiffness (K) of the bracing member. As shown in the figure, the energy under the force-displacement curve for the displacement up to the point where the friction pad is not engaged (once the bolt has reached the end of the slotted bolt hole) is dissipated through the friction pad. From this, the force for that energy can be found, and can be back tracked to find the friction coefficient needed for the system to reach the desired deflection value.

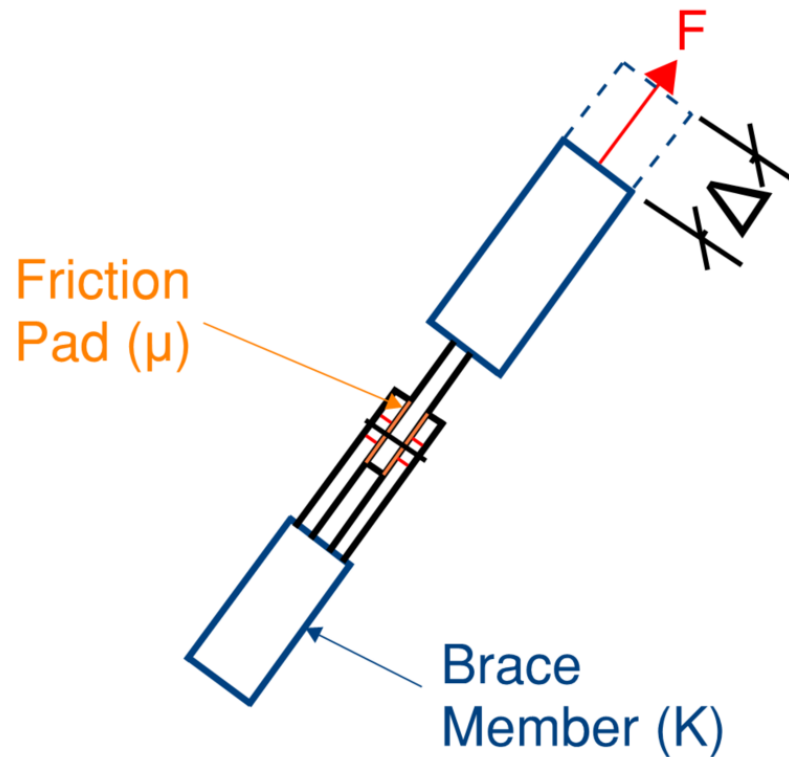


Figure 5.2-1: Bracing Member with Friction Damper Spring Properties.

Keeping with the spring approach, the two-stage friction damper's dissipated energy can simply be found by looking at the hysteresis of the results. The area under the curve for the plot is the energy dissipated within the given system. Figure 5.2-2 illustrates the approach and its comparison to the spring approach discussed above.

5.2.2. Design and Fabrication

Once the energy dissipation has been determined, the next steps are to actually design the damper itself. This design has several key steps and components. Those

components, including the damper construction, the friction pad design and selection, and the connection design. All of the aspects listed are crucial to the function and feasibility of the damper itself.

The damper construction includes both the material selection and make-up of the actual damper itself. Common to the design of any structural member, the integrity of the plates used within the damper need to be designed to be sufficient for the loads applied to the component. However, a key aspect with the two-stage damper is preventing buckling and hinge creation within the many locations of the bolts and weaker locations. These items cause for a intensive design approach to be determined and carried out. It is important that the damper functions as desired within a creation of hinges or out of plane forces that will add to the stresses applied at bolt and plate conditions. Figure 5.2-2 shows the damper design approach used in this Capstone project and modeling approach. As it is shown, the damper features several of the weak hinge points and further development will be needed to ensure local stability at the damper itself to ensure accurate performance.

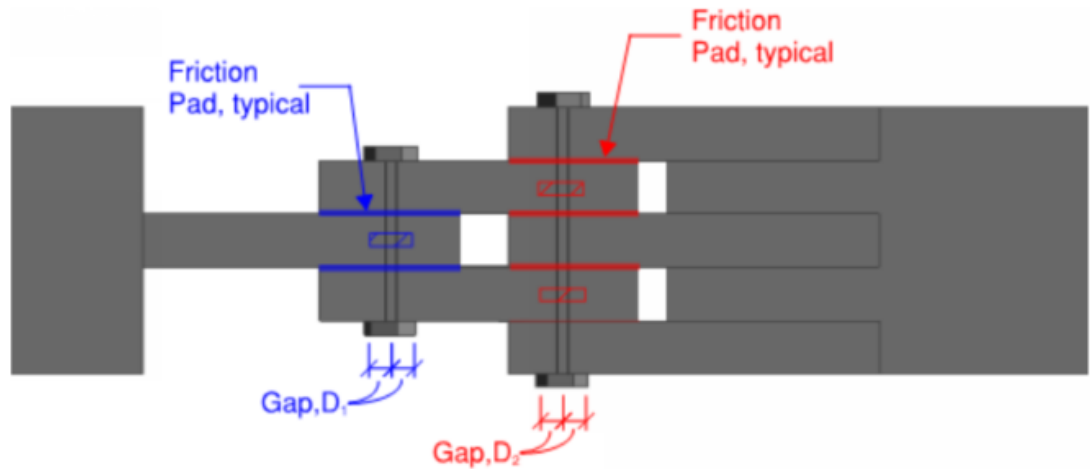


Figure 5.2-2: Two-Stage Friction Damper Preliminary Construction.

5.2.3. Optimization and Expansion

The current design approach was limited to a single two-stage damper applied to a 4-story model building. To further justify the damper's effectiveness and performance, two advancements of the study can be taken. These advancements allow for the damper to be used in a larger application of designs and building, as well as, to be more efficiently used in terms of material and cost savings within an individual project utilizing the system.

A common theme found within structural building design is the optimization of members within multi-story building. This can commonly be seen by using a tiered level of member sizes and strengths as needed throughout the height of the building. Not only a cost and installation savings, this allows for unnecessary loading and construction to be applied to upper, less loaded floors. This methodology can be used in the multi-story two-stage friction damper situation as well. By creating a grouping of like dampers or

designing a damper for each floor or scenario, several dampers can be used within the building's height. Shown in Figure 5.2-3, a grouping of less loaded dampers with smaller friction pads and members can be applied to the upper floors, and then increased as the structure moves towards the base, where it experiences the largest loads.

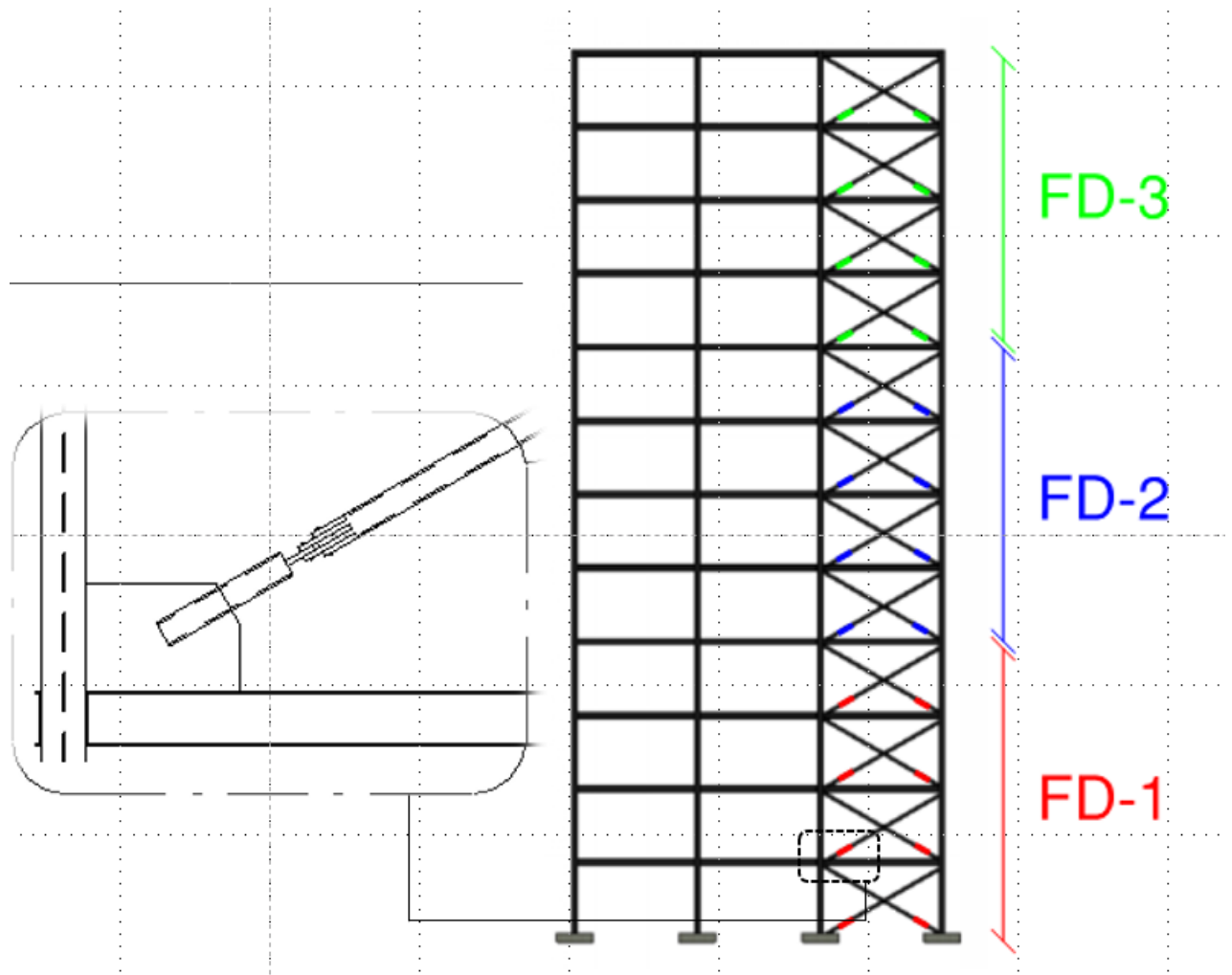


Figure 5.2-3: Optimized Two-Stage Friction Damper Building Diagram.

The second expansion of the study that can be done in future work, also shown in Figure 5.2-3 is testing the damper in larger buildings. Given the more widely used

practice of applying dampers to high-rise structures, a mid to high rise building would be an excellent approach to further developing the effectiveness of the two-stage friction damper. The optimization approach discussed would hugely benefit project costs and time for a structure as such.

References

- [1] Yeda, L; Xunan, Z.; Cherry, S. 2007. “Damping Characteristics of Friction Damped Braced Frame and its Effectiveness in the Mega-Sub Controlled Structure System”, *Earthquake Engineering and Vibration*, Vol 6, No 2, pp. 171-181. <https://doi.org/10.1007/511803-007-0732.4>

- [2] Aiken, Ian; Nims, Douglas; Whittaker, Andrew; Kelly, James 1993. “Testing of Passive Energy Dissipation Systems. *Earthquake Spectra*, Vol 9, No 3, pp. 335-370. <https://doi.org/10.1193/1.1585720>

- [3] Fu, Yaomin; Cherry, Sheldon. 1999, “Simplified Seismic Code Design Procedure for Friction-Damped Steel Frames”. *Canadian Journal of Civil Engineering*, Vol. 26, No. 1, pp. 55-71. <https://doi.org/10.1139/198-043>

- [4] Kaur, Naveet; Matsagar, V.A.; Nagpal, A.K. 2012, “Earthquake Response of Midrise to High Rise Buildings with Friction Dampers”. *International Journal of High-Rise Buildings*, December 2012, Vol 1, No 4. 311-332. <https://doi.org/10.21022/IJHRB.2012.1.4.311>

- [5] Chung, H.; Moon, B.W.; Lee, S.K.; Park, J.H. 2009, “Seismic Performance of Friction Dampers Using Flexure of RC Shear Wall”. *The Structural Design of Tall and Special Buildings*, Vol. 18, No. 7, pp. 807-822. <https://doi.org/10.1002/tal.524>

- [6] Malhotra, A.; Carson, D.; Gopal, P.; Braimah, A.; Di Giovanni, G.; Pall, D. 2004, “Friction Dampers for Seismic Upgrade of St Vincent Hospital, Ottawa”, 13th World Conference on Earthquake Engineering 2004, Paper No 1952. ADDRESS: https://civil1808.com/site/default/files/friction_dampers_for_seismic_upgrade_of_st_vincent_hospital.pdf

- [7] Pisal, A., Jangid, R.S. 2016. “Dynamic Response of Structure with Tuned Mass Friction Damper”. *International Journal of Advanced Structural Engineering*, Vol. 8, No. 4, pp. 363-377. <https://doi.org/10.1007/s40091-016-0136-7>

- [8] Applied Technology Council. June 2009. *Qualifications of Building Seismic Performance Factors* [FEMA P695. [Internet, WWW, PDF]. ADDRESS: <https://www.hsd1.org/?view&did=685496>

- [9] Sengara, I Wayan. 2012. “Investigation on Risk-Targeted Seismic Design Criteria for a High-Rise Building in Jakarta-Indonesia” , 15 WCEE, Lisboa 2012. ADDRESS: <https://www.iitk.ac.in/micee/wcee/article/WCEE2012-3636.pdf>

- [10] Anwar, N; Sy, Jose A., Aung, Thaung Htut; Talpur, Mir Shabir. 2015, “Effect of Using Performance-Based Approach for Seismic Design of Tall Building Diaphragms.” *Proceedings of the Second International Conference on Performance-Bases and Life-Cycle Structural Engineering (PLSE 2015)*. <https://doi.org/10.1426/uql.2016.683>

- [11] Bahmani, Pouria, April 2021. Personal Communication.

APPENDIX A
CYCLIC LOADING TRIALS

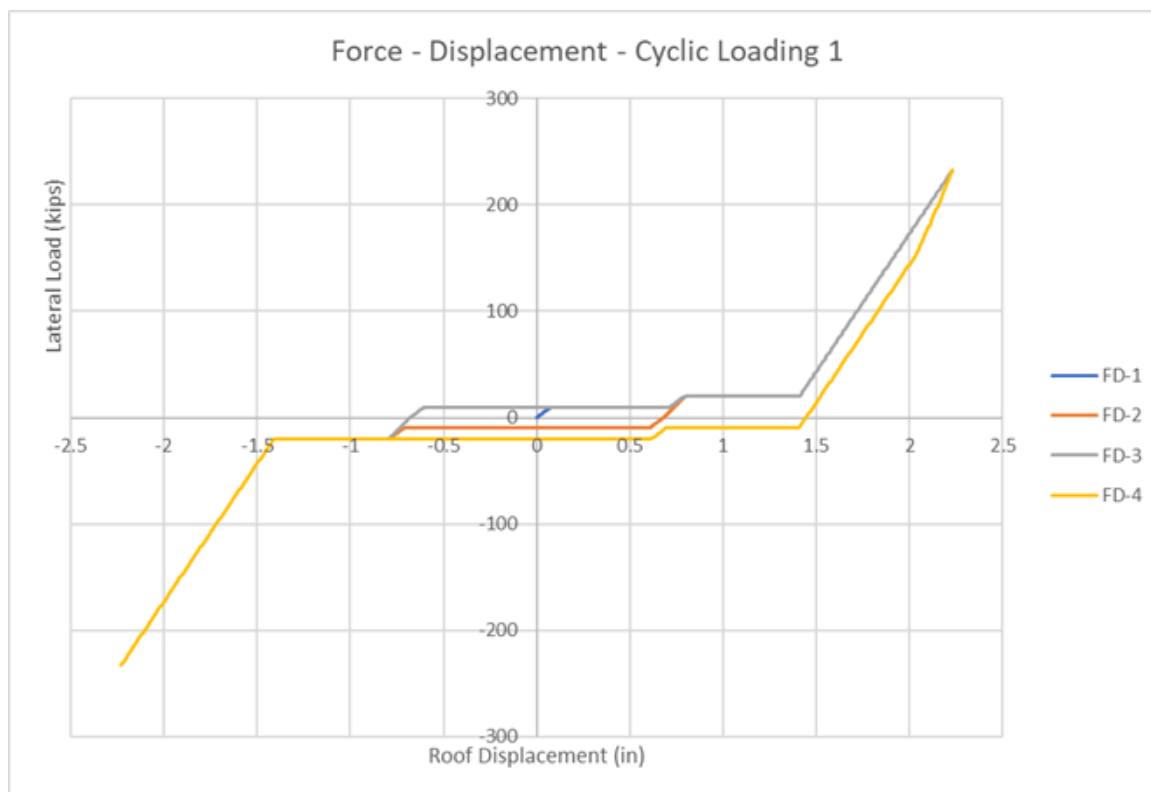


Figure A-1: Force-Displacement - Cyclic Loading 1.

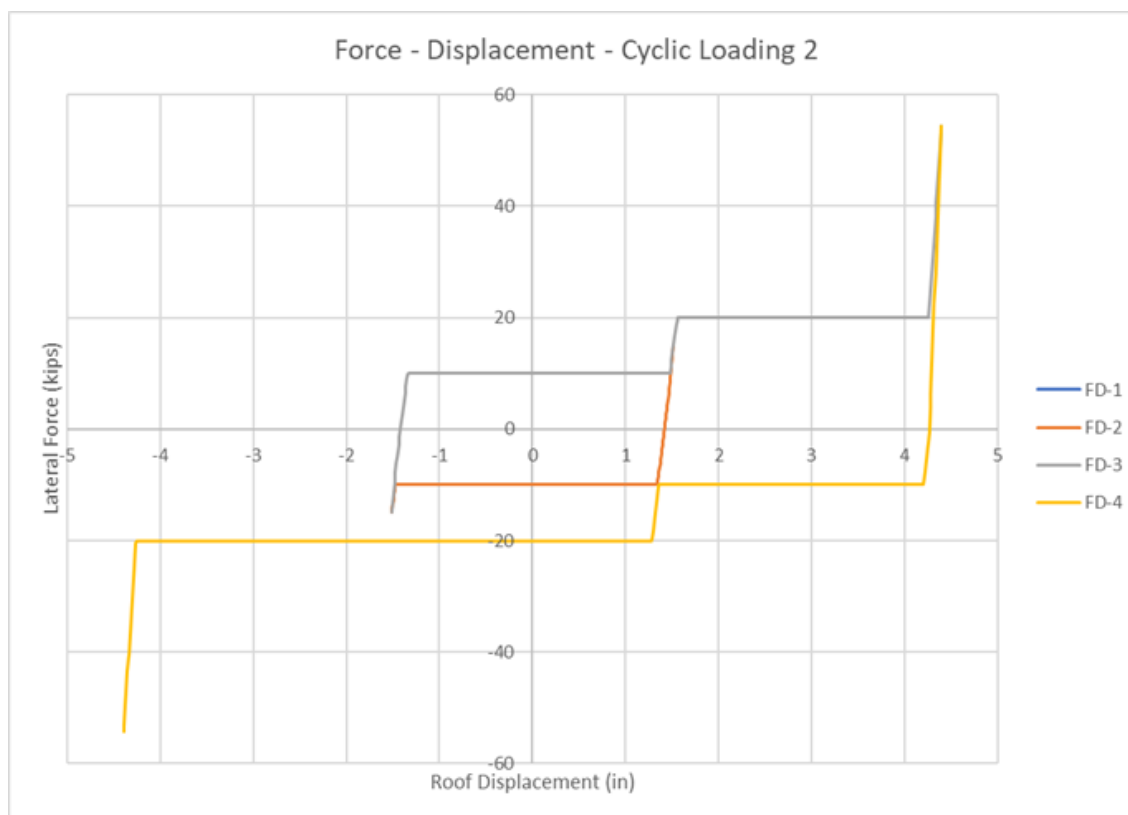


Figure A-2: Force-Displacement - Cyclic Loading 2.

APPENDIX B
1-STORY, 1-BAY INITIAL UNSCALED GROUND
MOTION TRIALS

Table B-1: Unscaled Damper Design Values.

| Global Parameters (Per Frame) | | | Local Parameters (Per Frame) | | |
|-------------------------------|-------|---------|------------------------------|-------------|--------------------|
| P1= | 47.25 | kips | SLE Foce | Member: | HSS6X6X5/16 |
| P2= | 68 | kips | MCE Force | E= | 29000 ksi |
| P3= | | kips | Max Force | | |
| H= | 12 | ft | 144 inches | D1= | 0.43 inches |
| L= | 12 | ft | 144 inches | D2= | 1.5 inches |
| D1= | 0.43 | inches | | a= | 6.43 square inches |
| D2= | 1.5 | inches | D2=Total drift at Stg 2 | l= | 203.6468 inches |
| θ= | 45 | degrees | 0.785 radians | Override a= | square inches |

| | | |
|--------------|------|--------|
| Δ1= | 0.71 | inches |
| Δ2= | 2.88 | inches |
| MAX Δ= | 2.88 | inches |
| Drift Limit= | 5 | inches |
| Status? | OK | |

| Force (k) | Disp. (in) |
|-----------|------------|
| 0 | 0 |
| 47.25 | 0.103 |
| 47.25 | 0.711 |
| 68 | 0.76 |
| 68 | 2.88 |
| 0 | 2.73 |

| | | |
|-----|--------|-----------|
| f1= | 66.8 | kips |
| f2= | 96.2 | kips |
| d1= | 0.073 | inches |
| d2= | 0.032 | inches |
| d3= | -0.105 | inches |
| δ1= | 0.50 | inches |
| δ2= | 2.04 | inches |
| δ3= | 1.93 | inches |
| k= | 915.65 | kips/inch |
| f1= | 66.8 | kips |
| f2= | 96.2 | kips |
| f3= | 0.0 | kips |

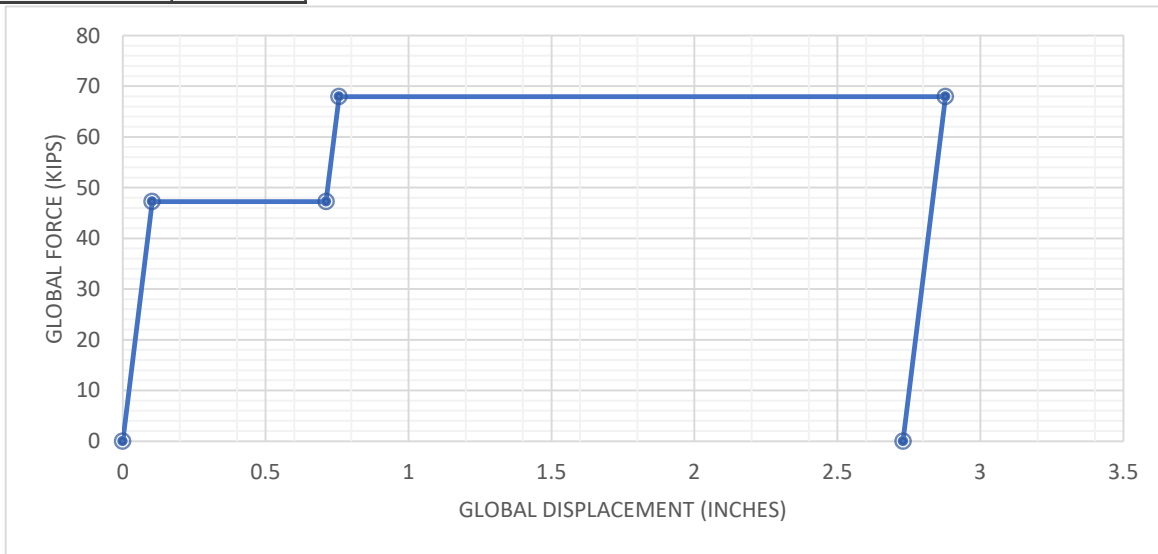


Figure B-1: Force-Displacement of Unscaled Two Stage Friction Damper.

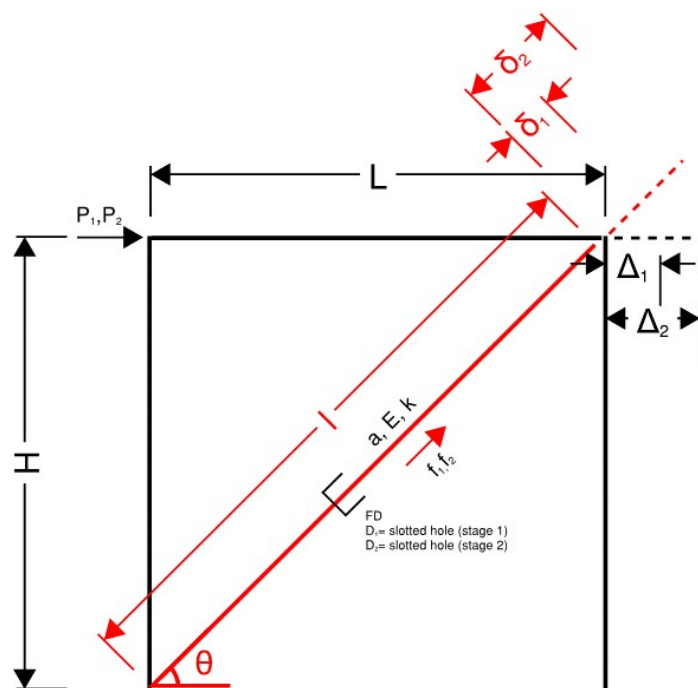


Figure B-2: Design Parameter Diagram for Two Stage Friction Damper.

Table B-2: ETABS Input Values for Unscaled Two-Stage Friction Damper.

| ETABS Input Values | | | | |
|--------------------|---------------|------------------|----------------|-------|
| | Lin Stiffness | Nonlin Stiffness | Yield Strength | Open |
| | lb/in | lb/in | lb | in |
| FD1 | 915654.18 | 915654.18 | 66822 | --- |
| FD2 | 915654.18 | 915654.18 | 96167 | --- |
| Hook1 | 915654.18 | 915654.18 | --- | 0.503 |
| Hook2 | 915654.18 | 915654.18 | --- | 2.04 |
| Gap1 | 915654.18 | 915654.18 | --- | 0.503 |
| Gap2 | 915654.18 | 915654.18 | --- | 2.04 |

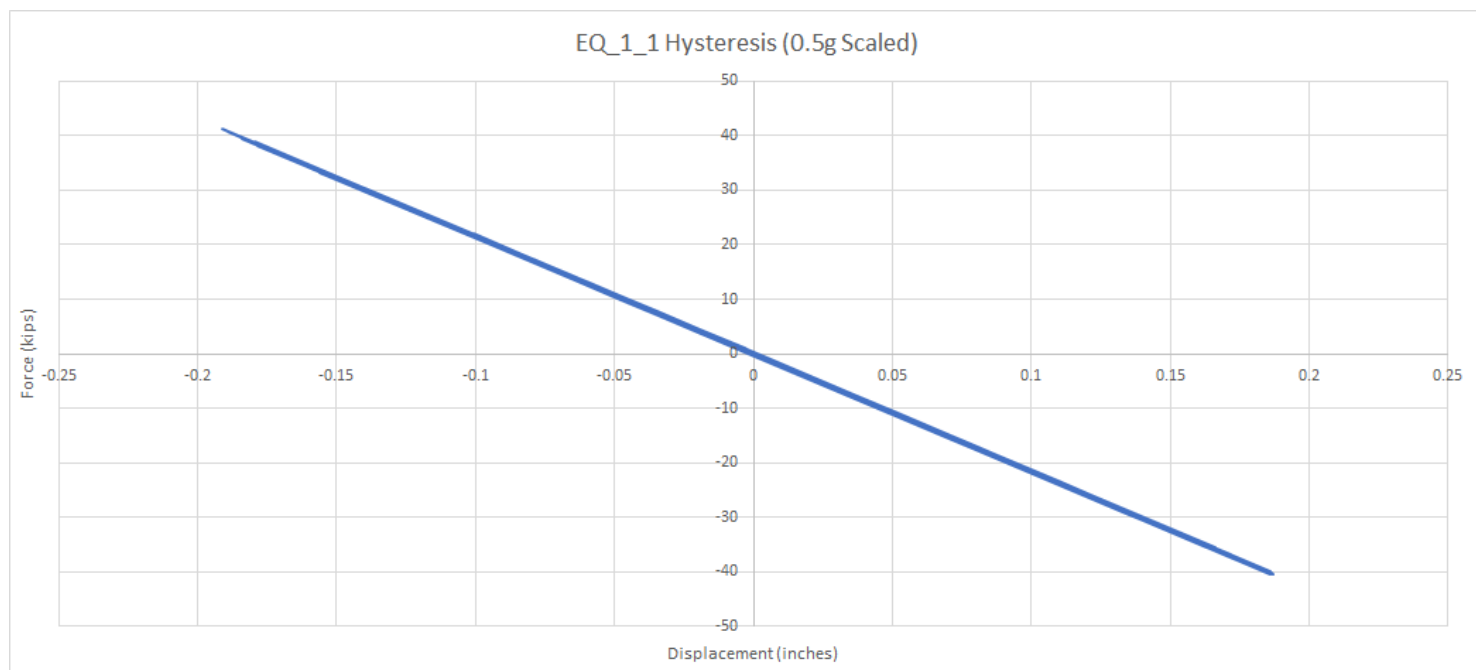


Figure B-3: Hysteresis Plot for 0.5g Scaled Analysis.

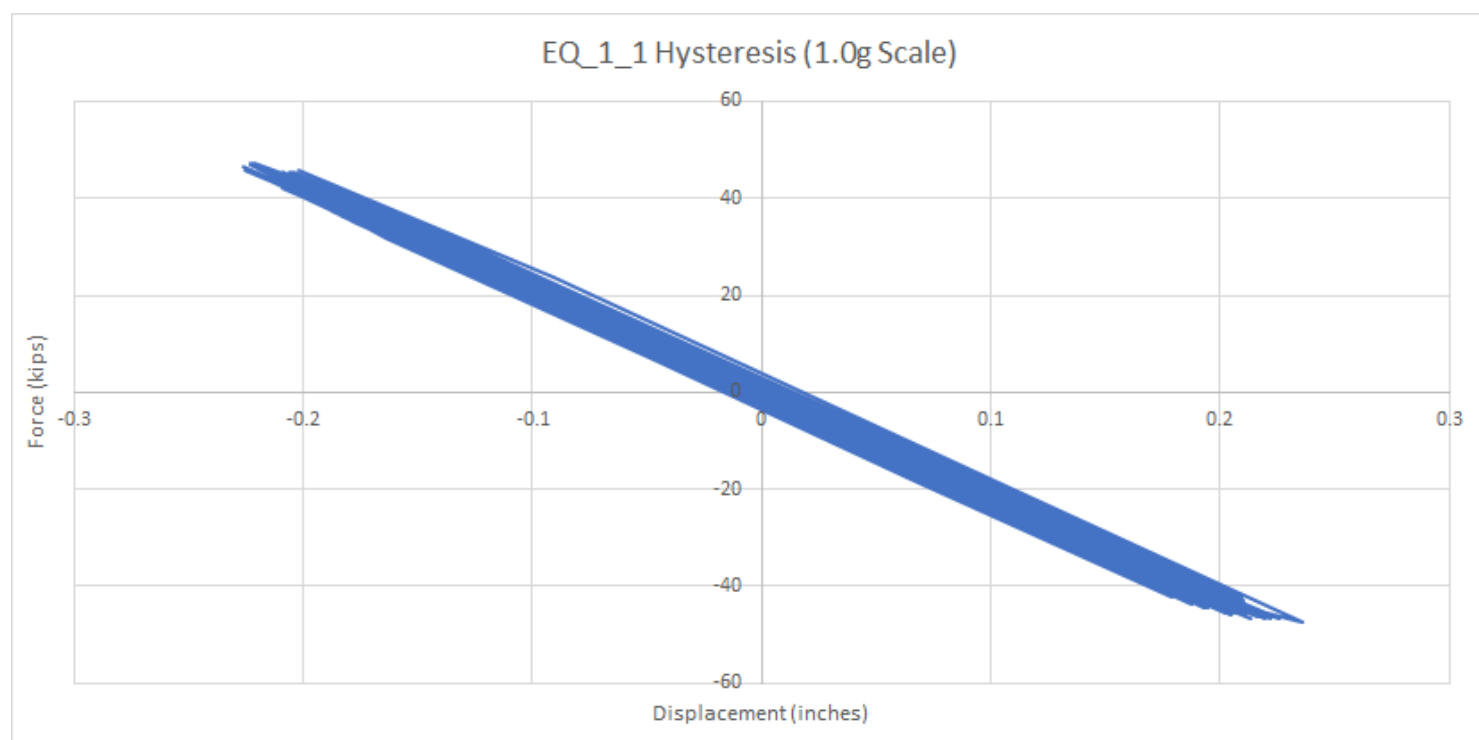


Figure B-4: Hysteresis Plot for 1.0g Scaled Analysis.

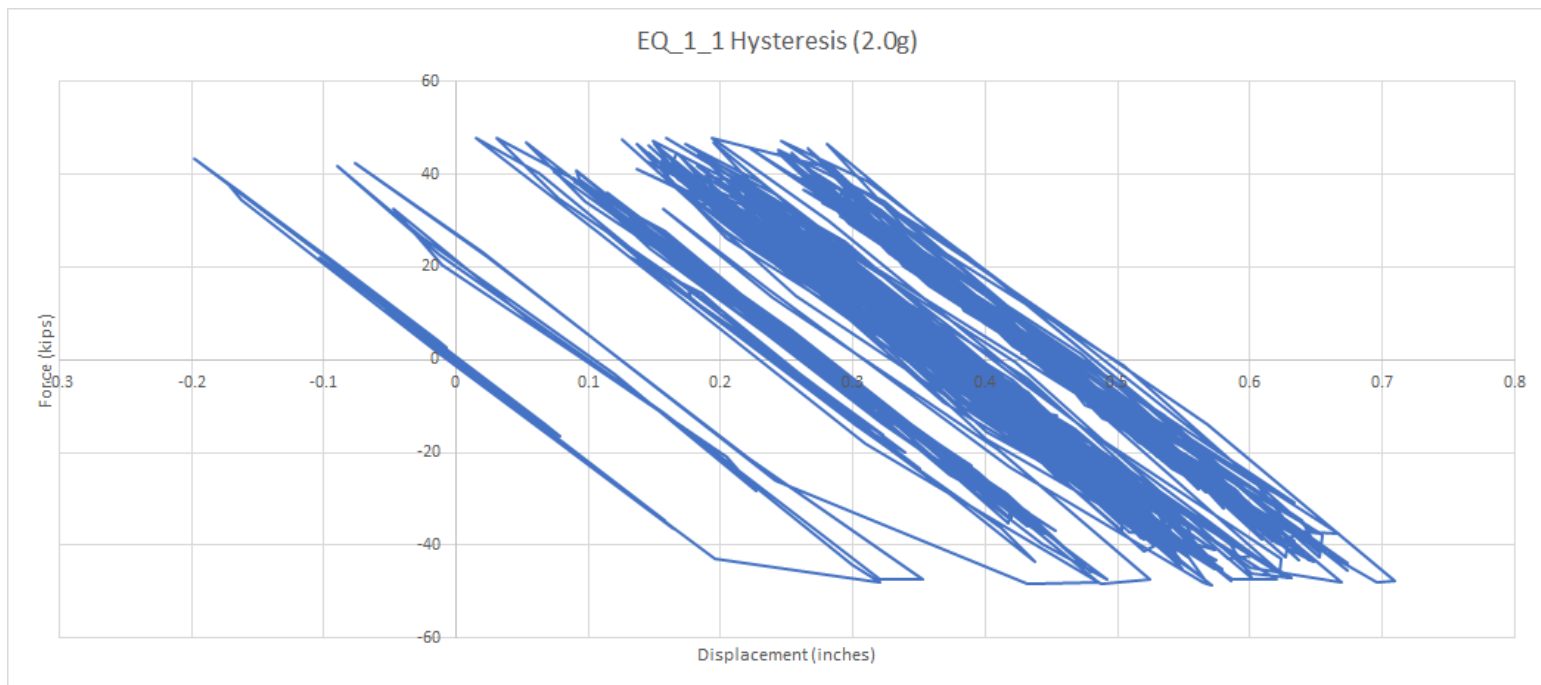


Figure B-5: Hysteresis Plot for 2.0g Scaled Analysis.

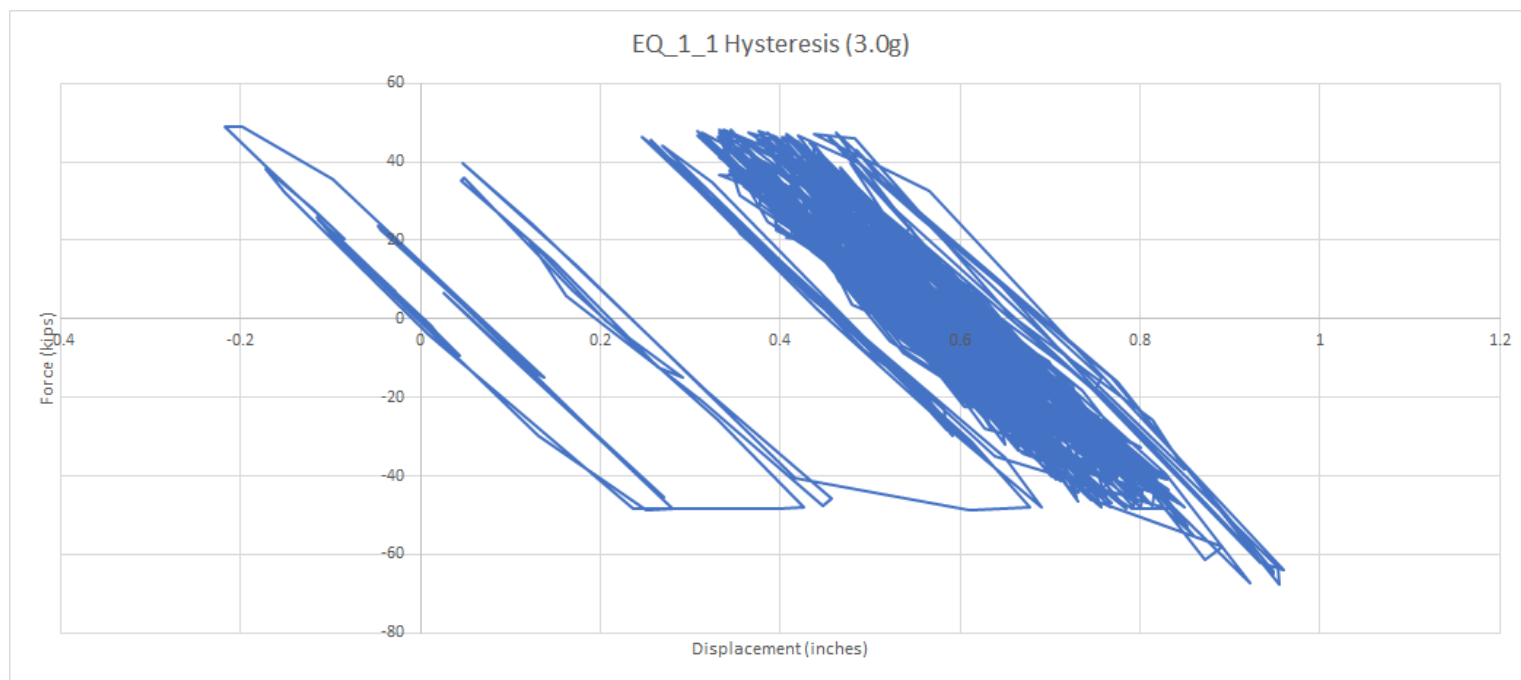


Figure B-6: Hysteresis Plot for 3.0g Scaled Analysis.

APPENDIX C
1-STORY, 4-BAY INITIAL SCALED GROUND
MOTION TRIALS

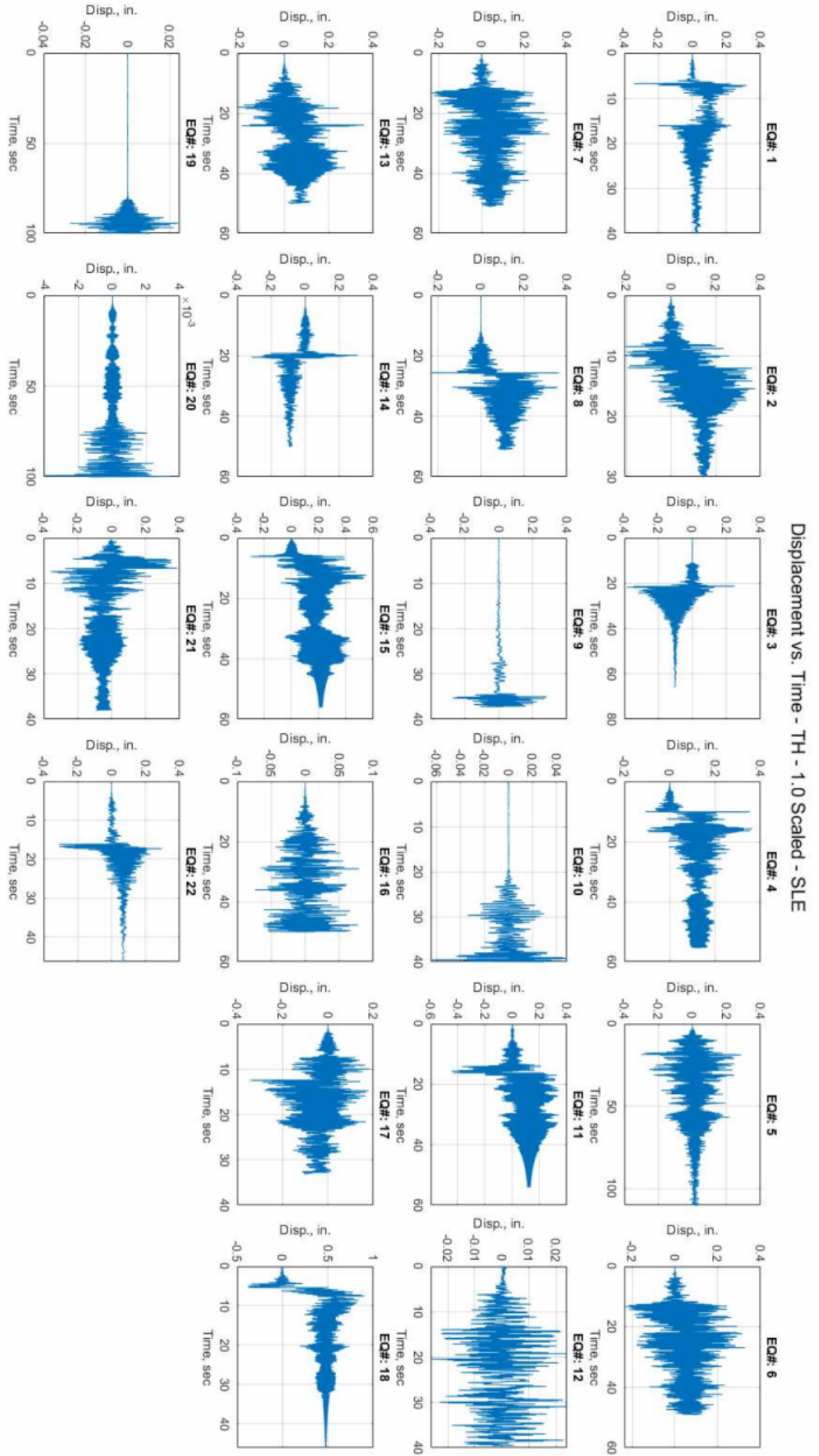


Figure C-1: Displacement versus Time Results for 1.0g Scaled SLE Trials - Ground Motions 1-22.

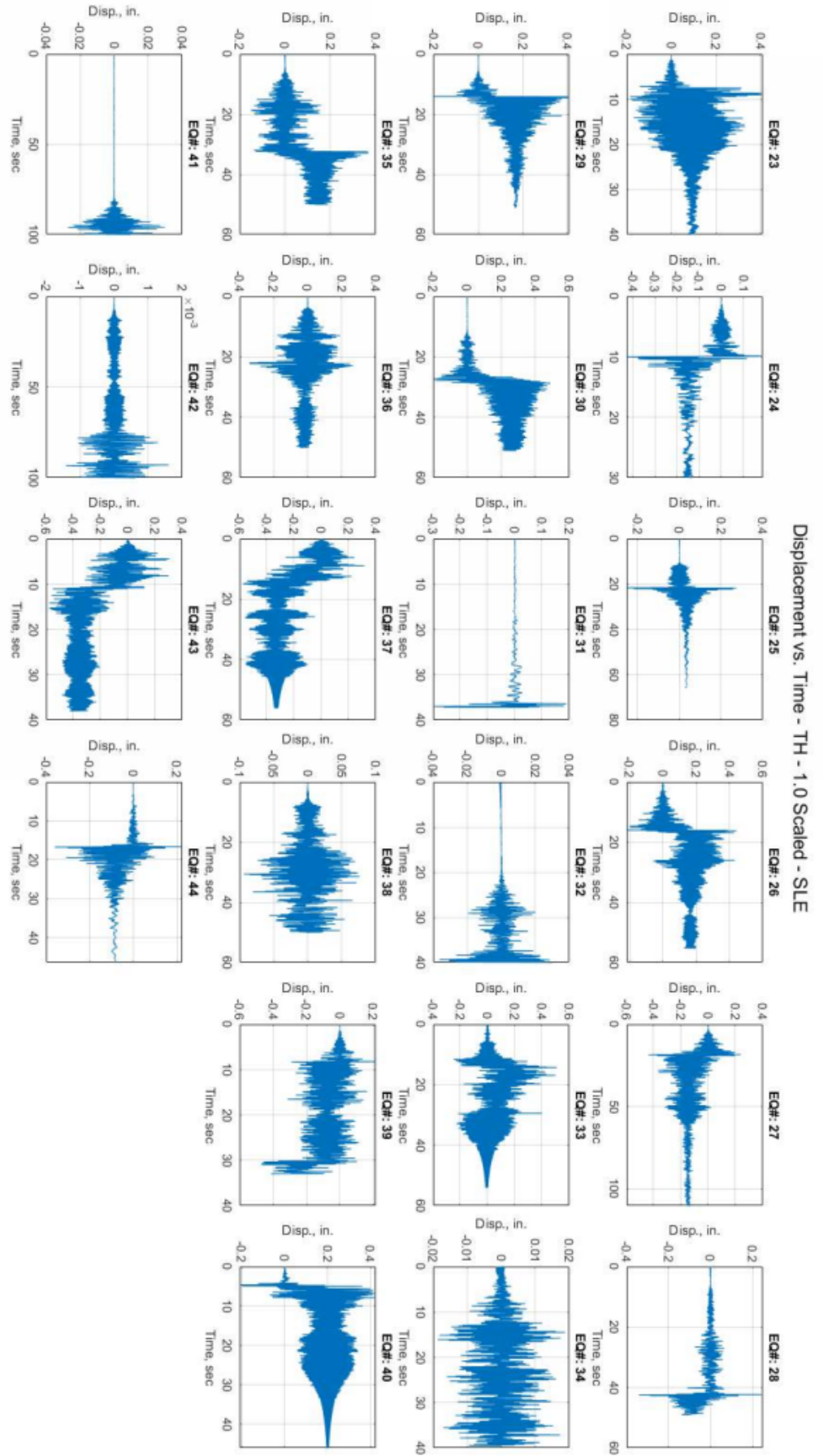


Figure C-2: Displacement versus Time Results for 1.0g Scaled SLE Trials - Ground Motions 23-44.

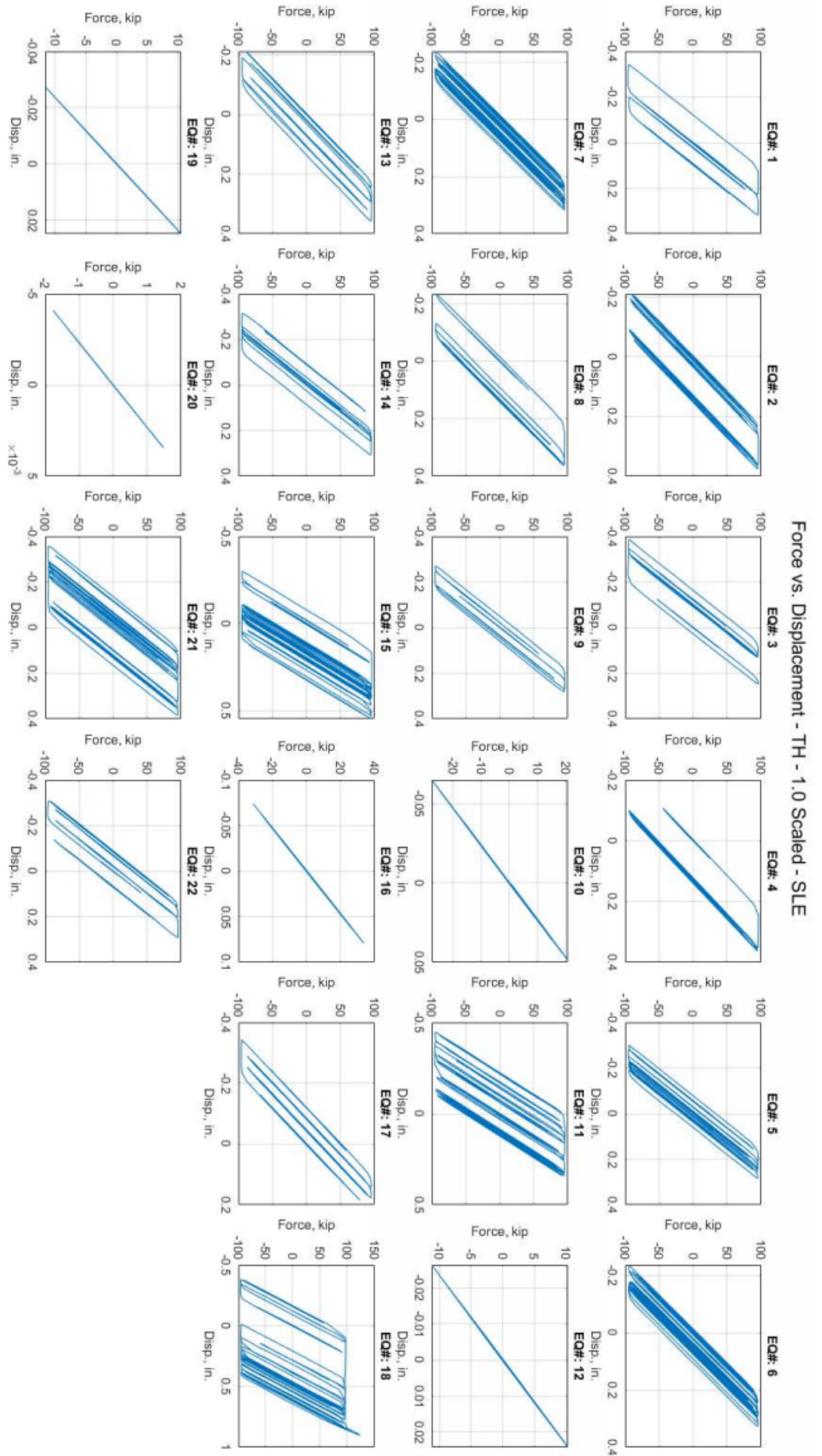


Figure C-3: Force versus Displacement Results for 1.0g Scaled SLE Trials - Ground Motions 1-22.

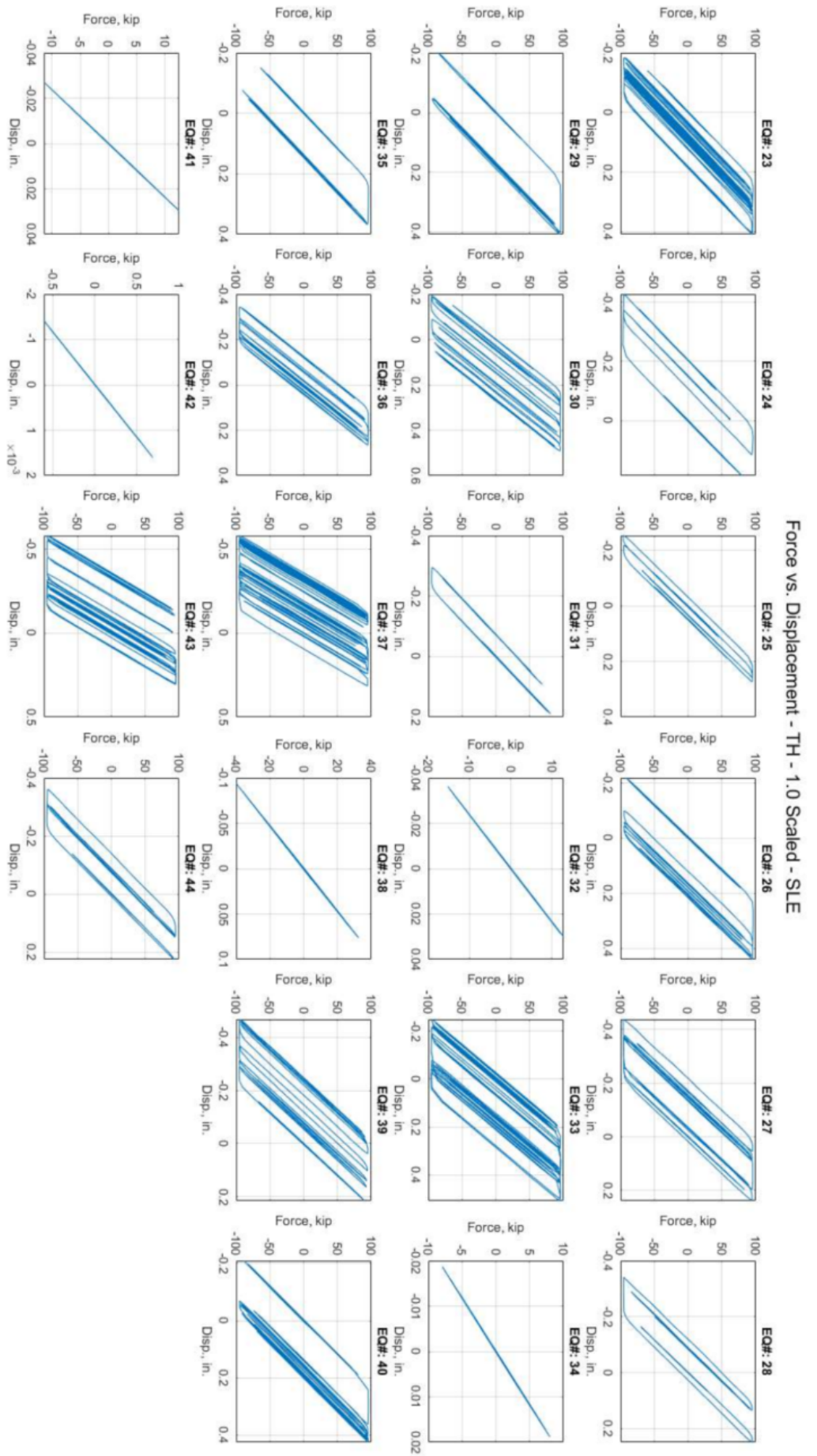


Figure C-4: Force versus Displacement Results for 1.0g Scaled SLE Trials - Ground Motions 23-44.

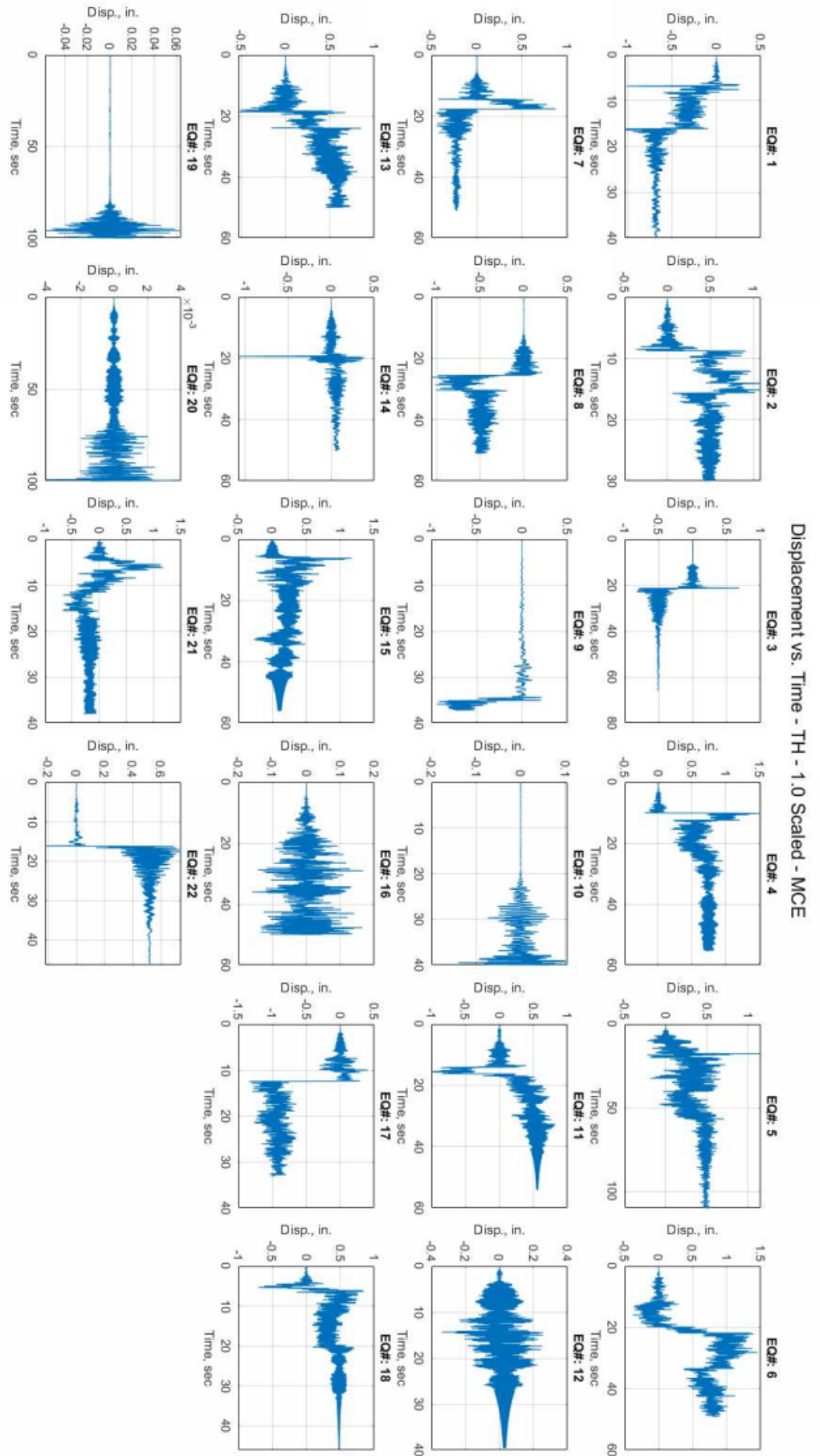


Figure C-5: Displacement versus Time Results for 1.0g Scaled MCE Trials - Ground Motions 1-22.

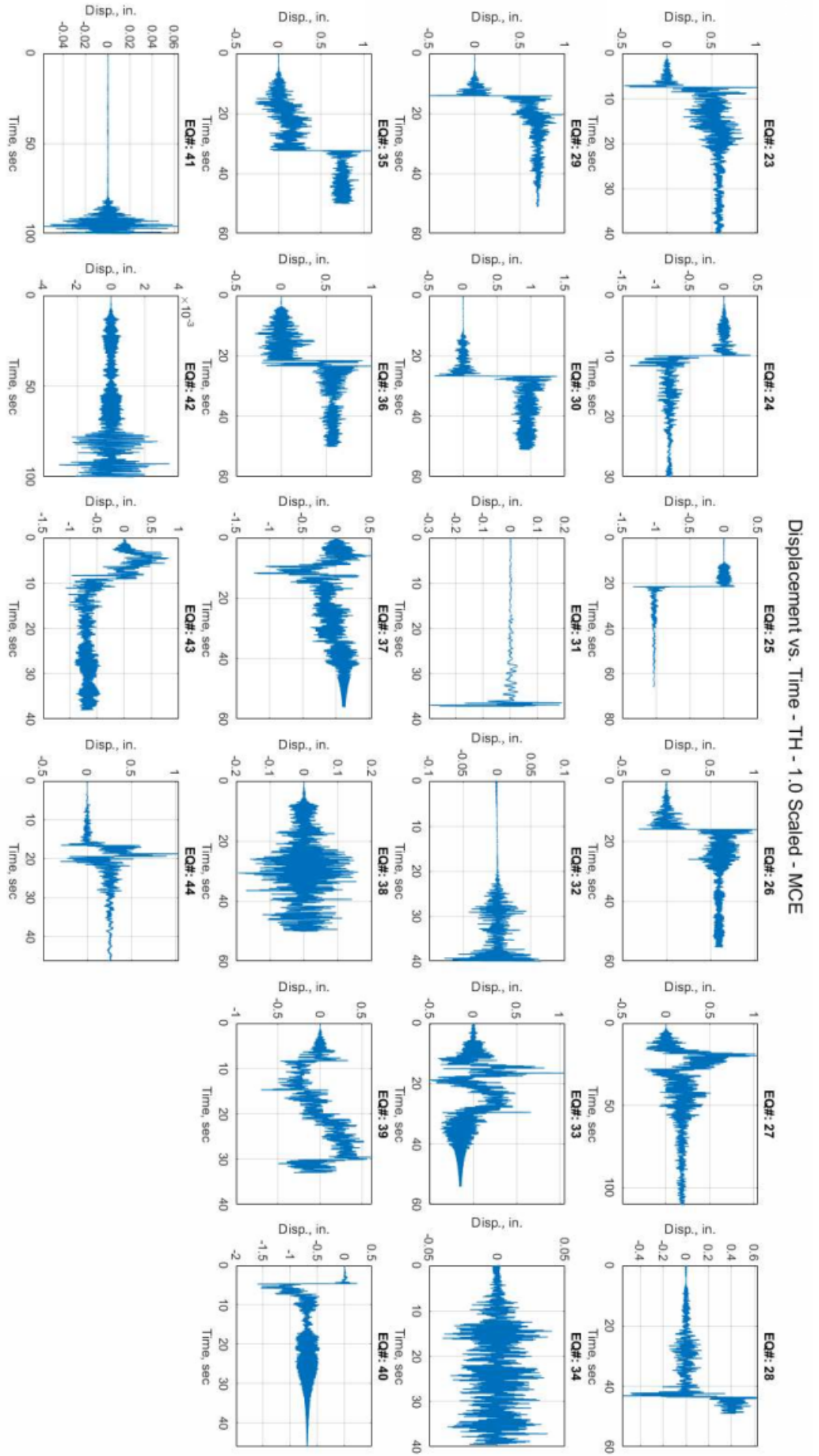


Figure C-6: Displacement versus Time Results for 1.0g Scaled MCE Trials - Ground Motions 23-44.

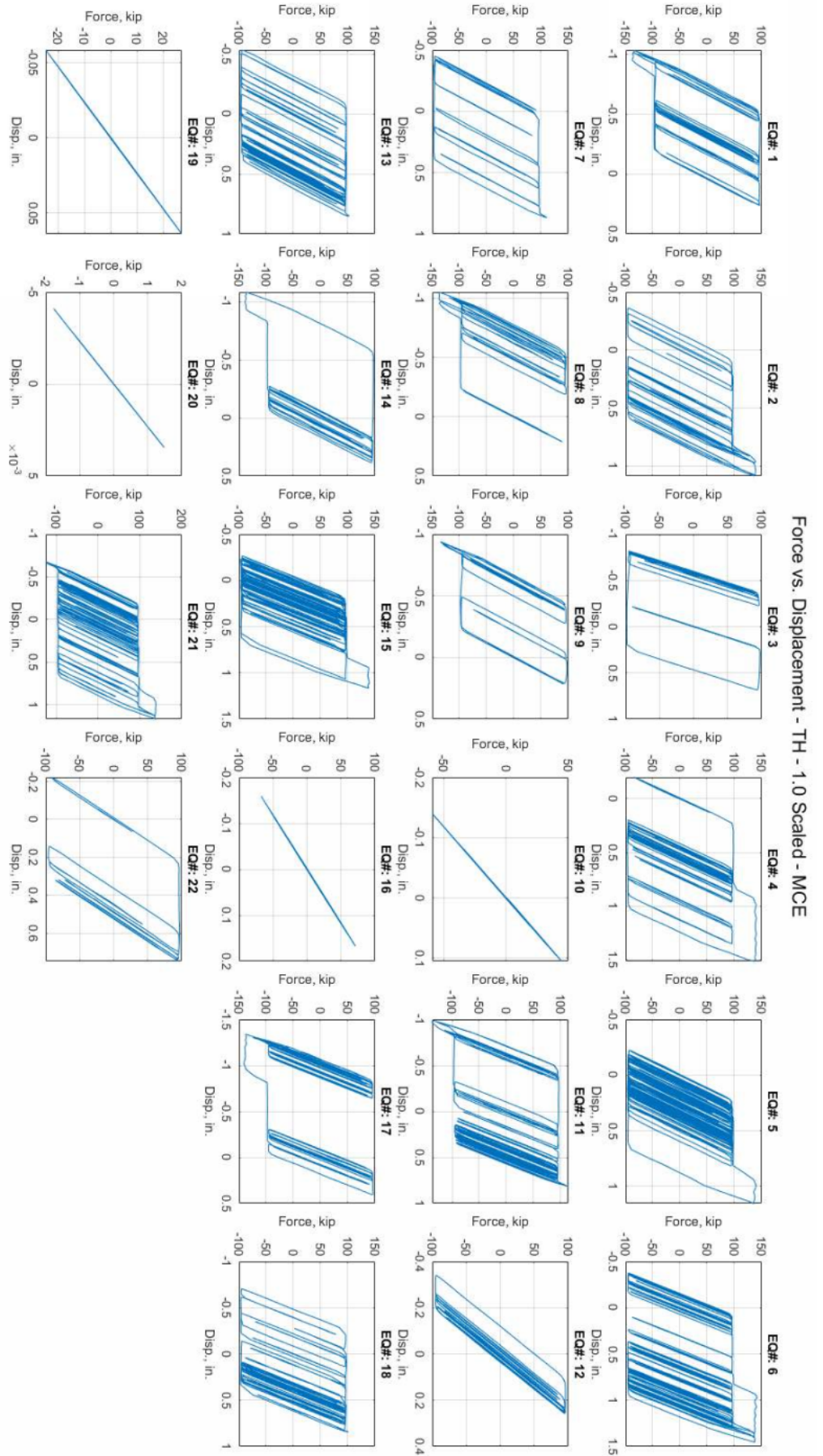


Figure C-7: Force versus Displacement Results for 1.0g Scaled MCE Trials - Ground Motions 1-22.

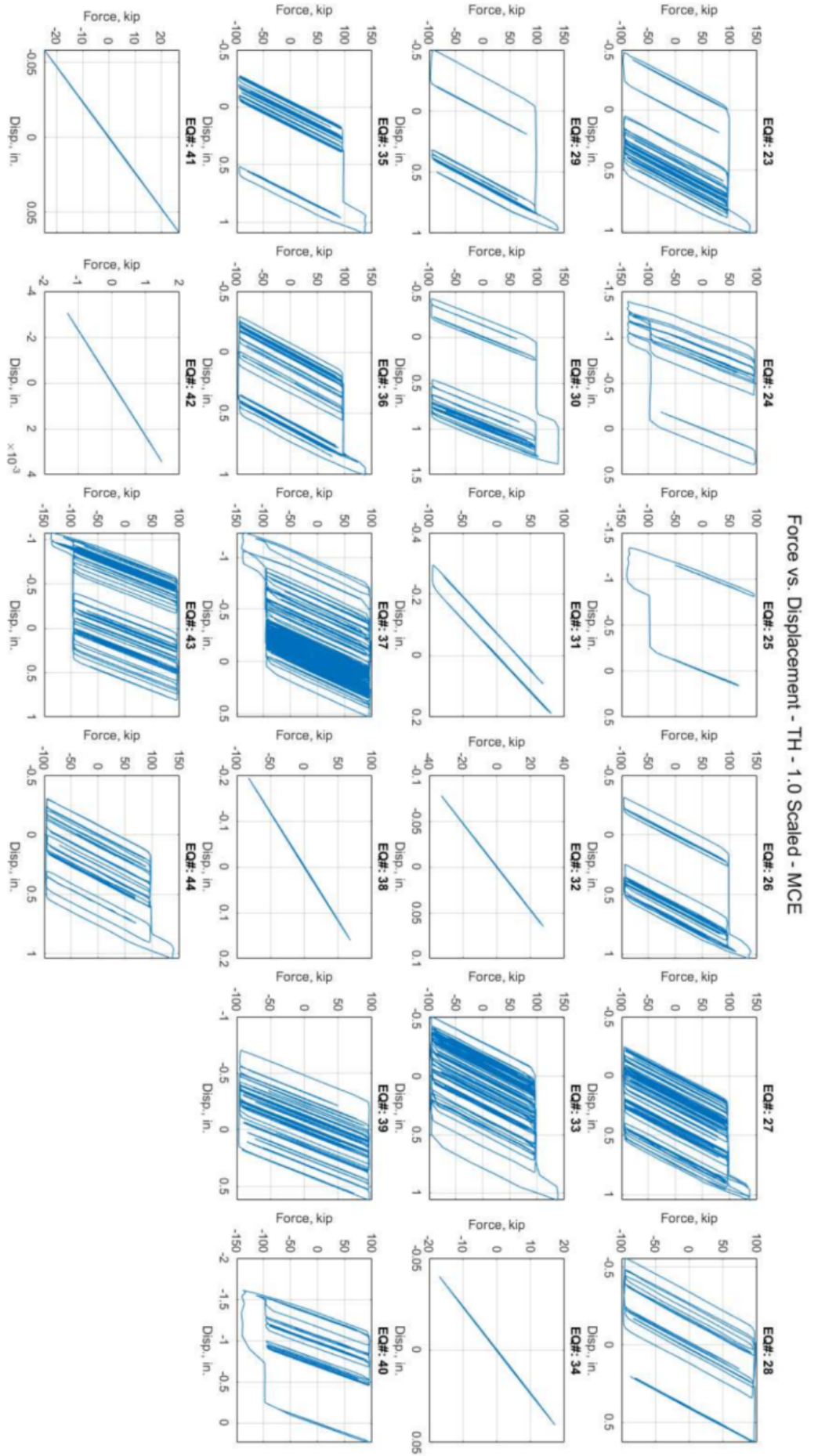


Figure C-8: Force versus Displacement Results for 1.0g Scaled MCE Trials - Ground Motions 23-44.

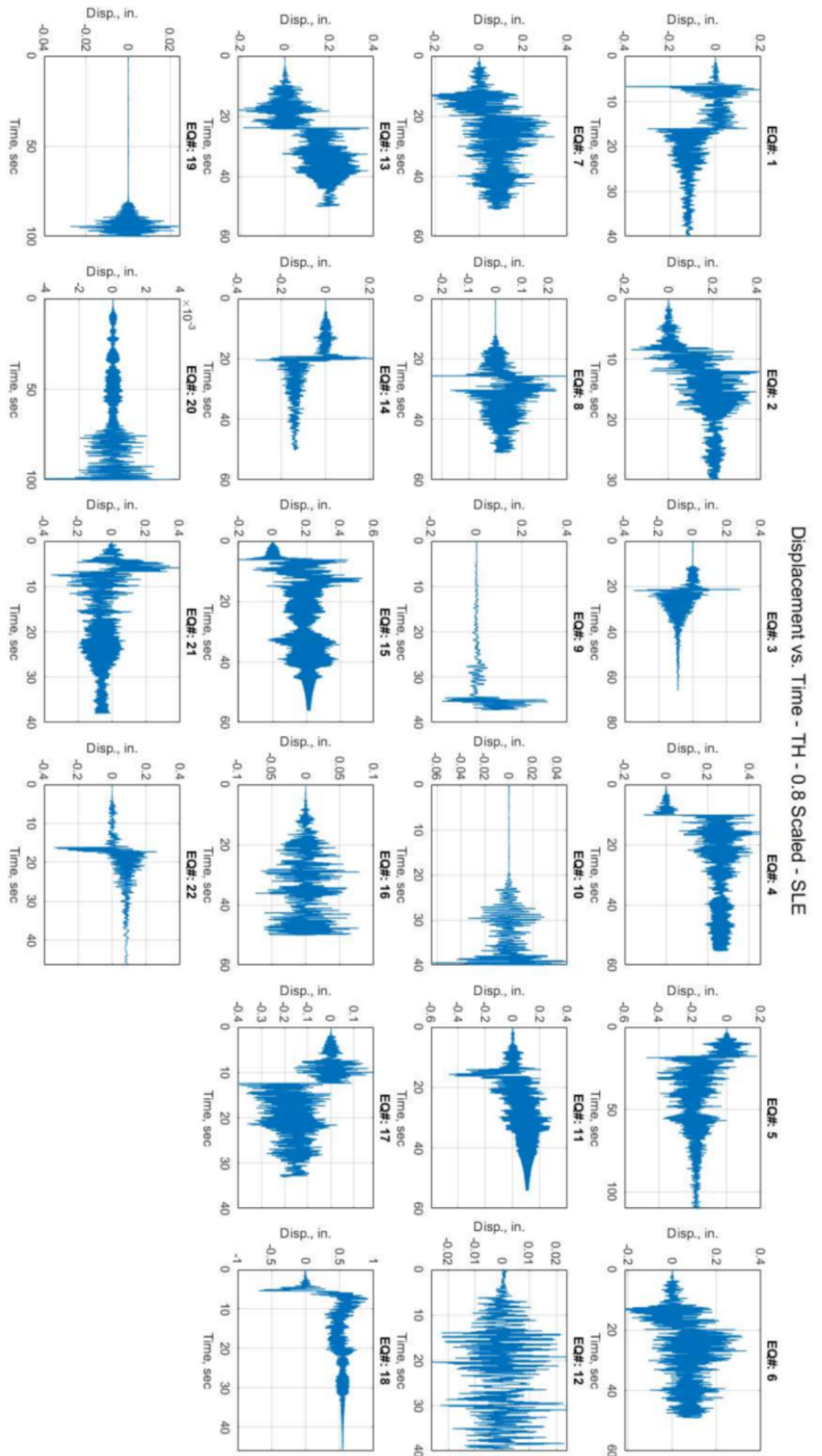


Figure C-9: Displacement versus Time Results for 0.8g Scaled SLE Trials - Ground Motions 1-22.

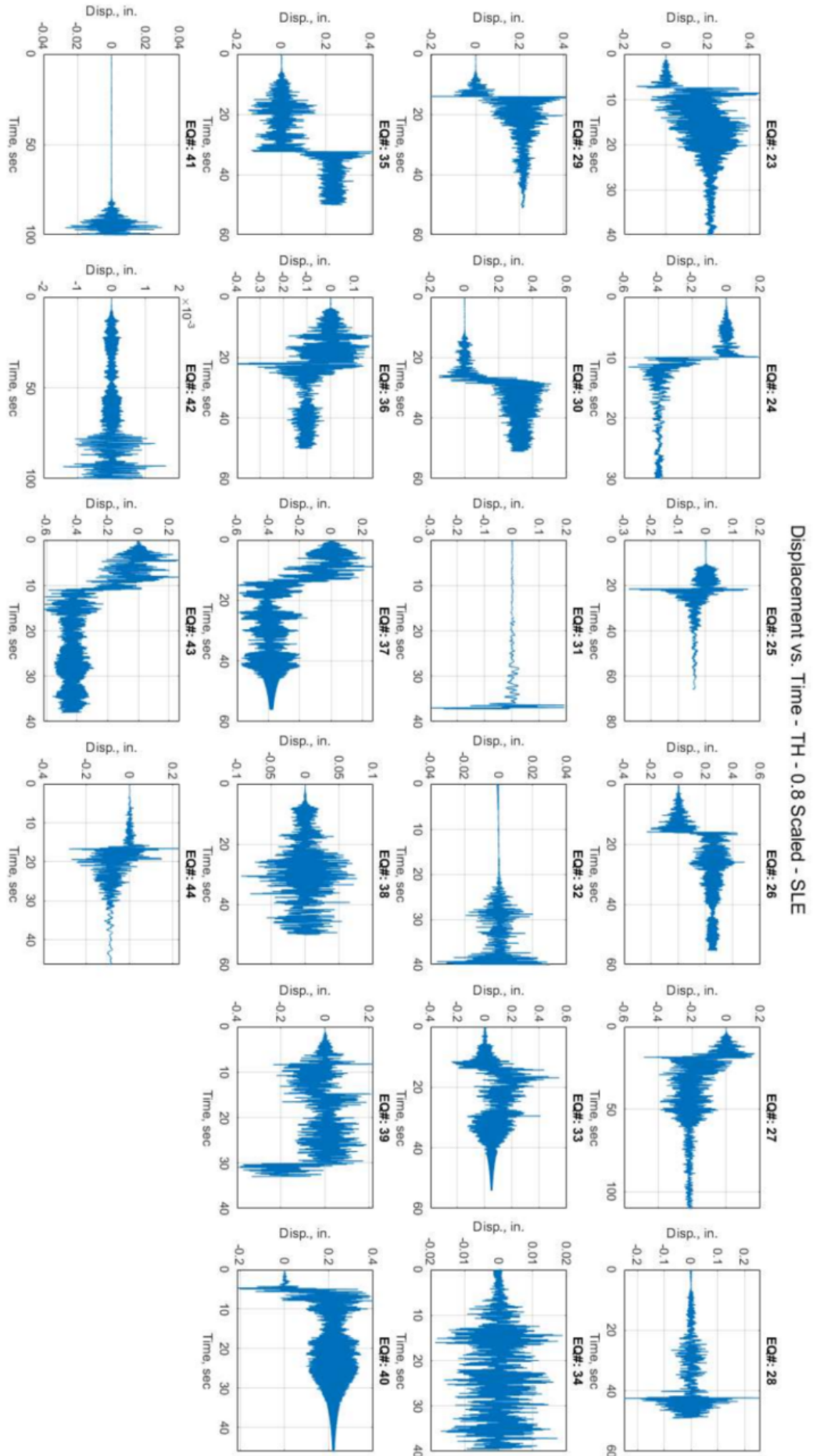


Figure C-10: Displacement versus Time Results for 0.8g Scaled SLE Trials - Ground Motions 23-44.

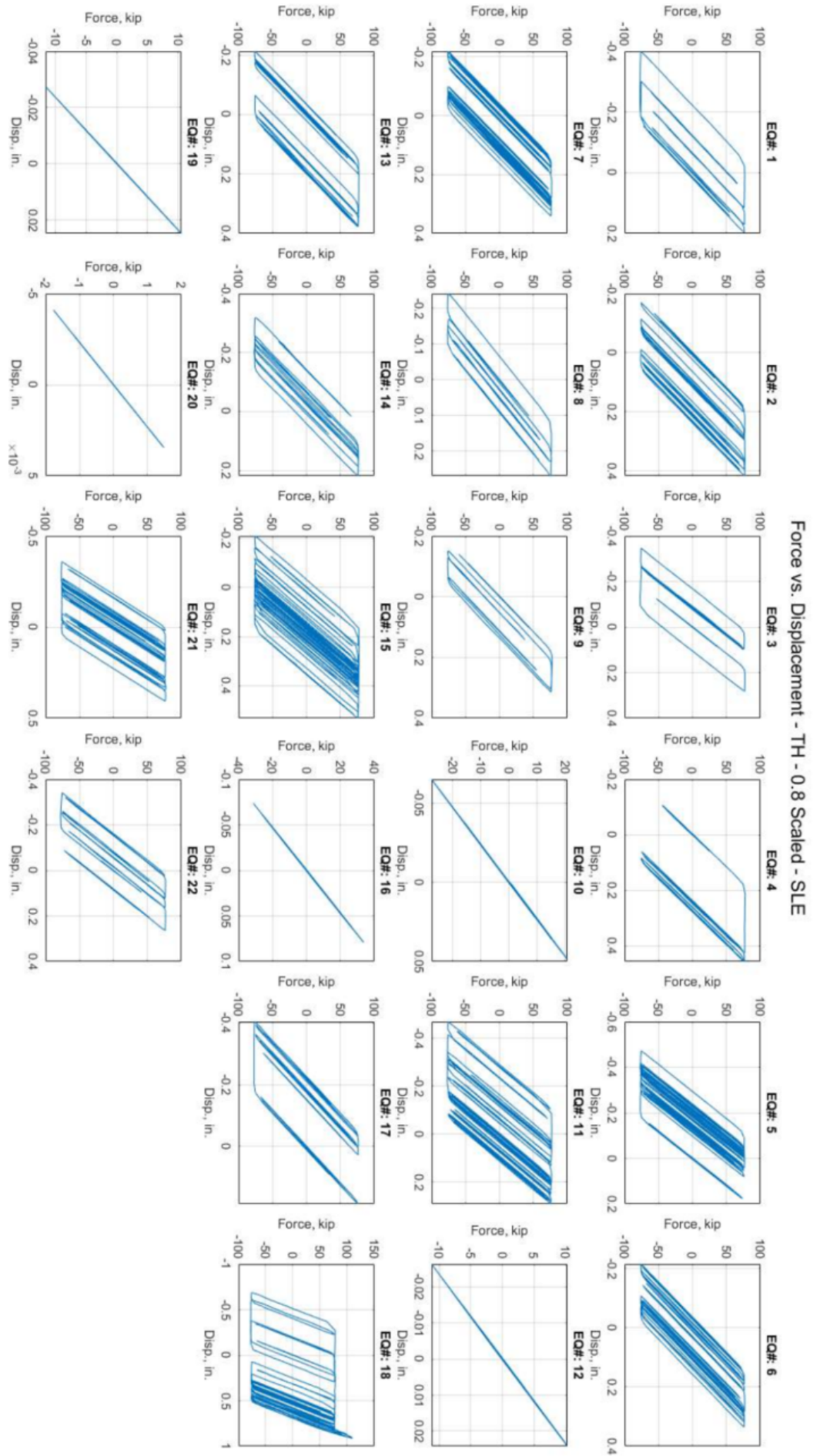


Figure C-11: Force versus Displacement Results for 0.8g Scaled SLE Trials - Ground Motions 1-22.

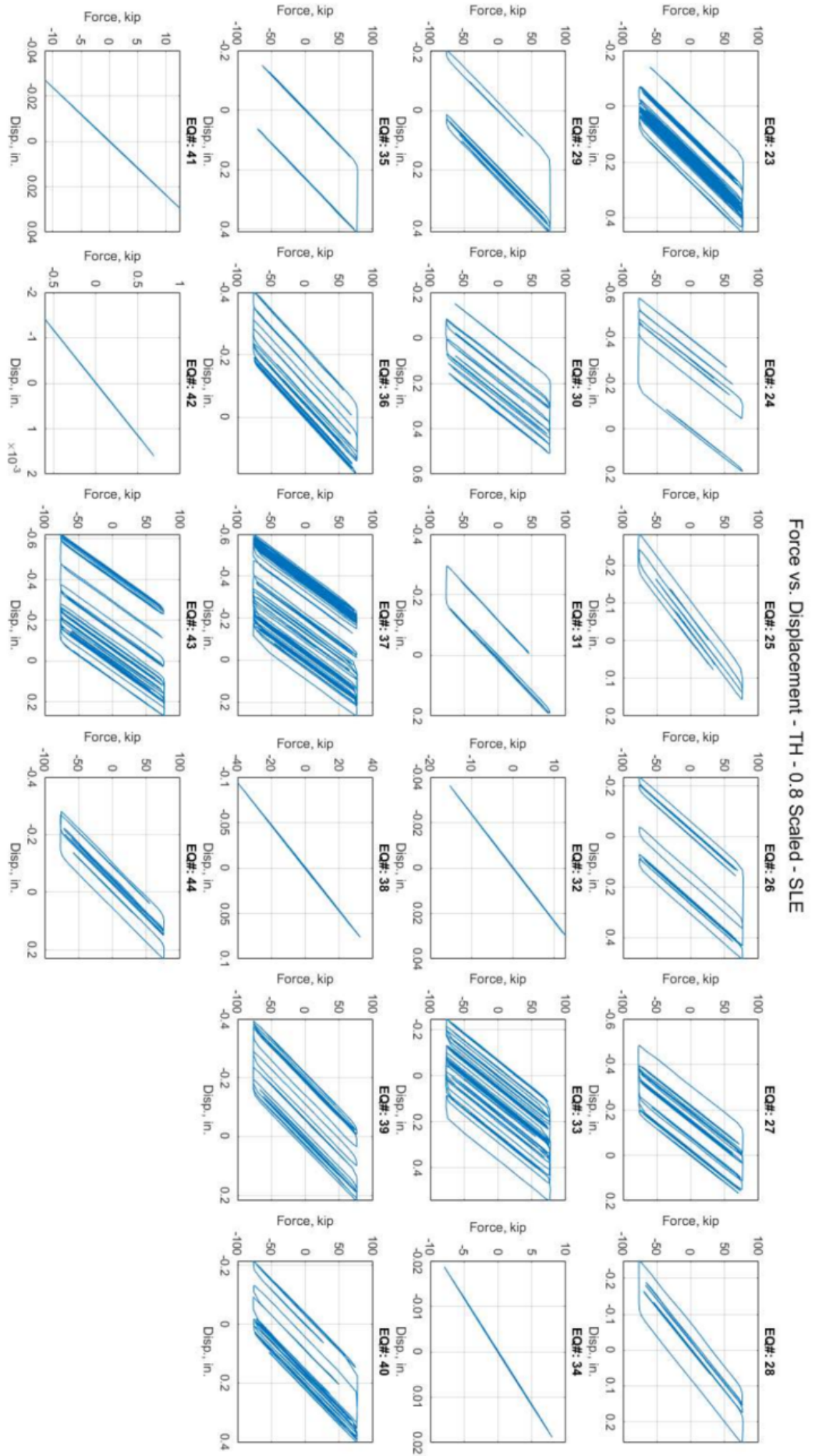


Figure C-12: Force versus Displacement Results for 0.8g Scaled SLE Trials - Ground Motions 23-44.

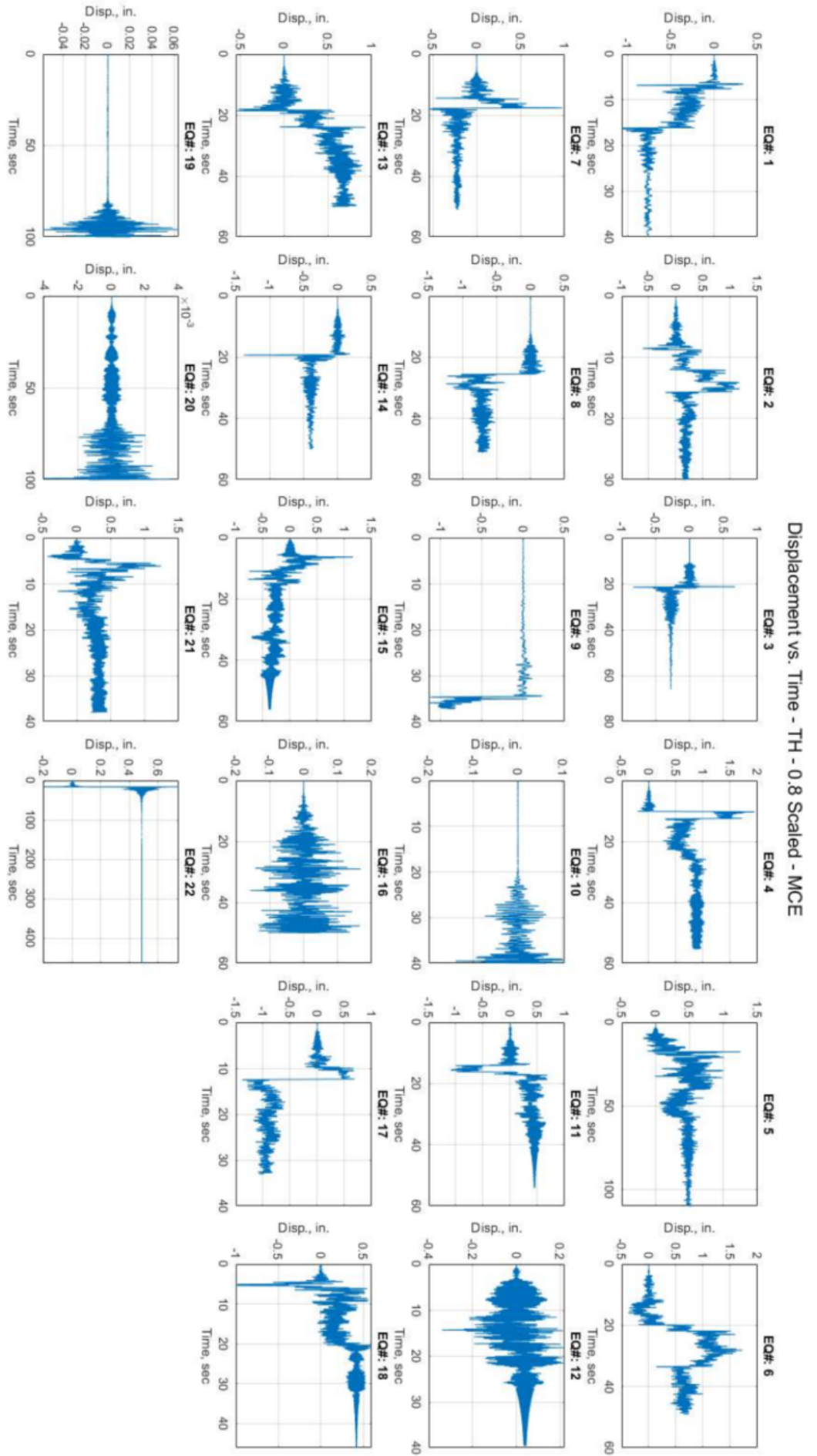


Figure C-13: Displacement versus Time Results for 0.8g Scaled MCE Trials - Ground Motions 1-22.

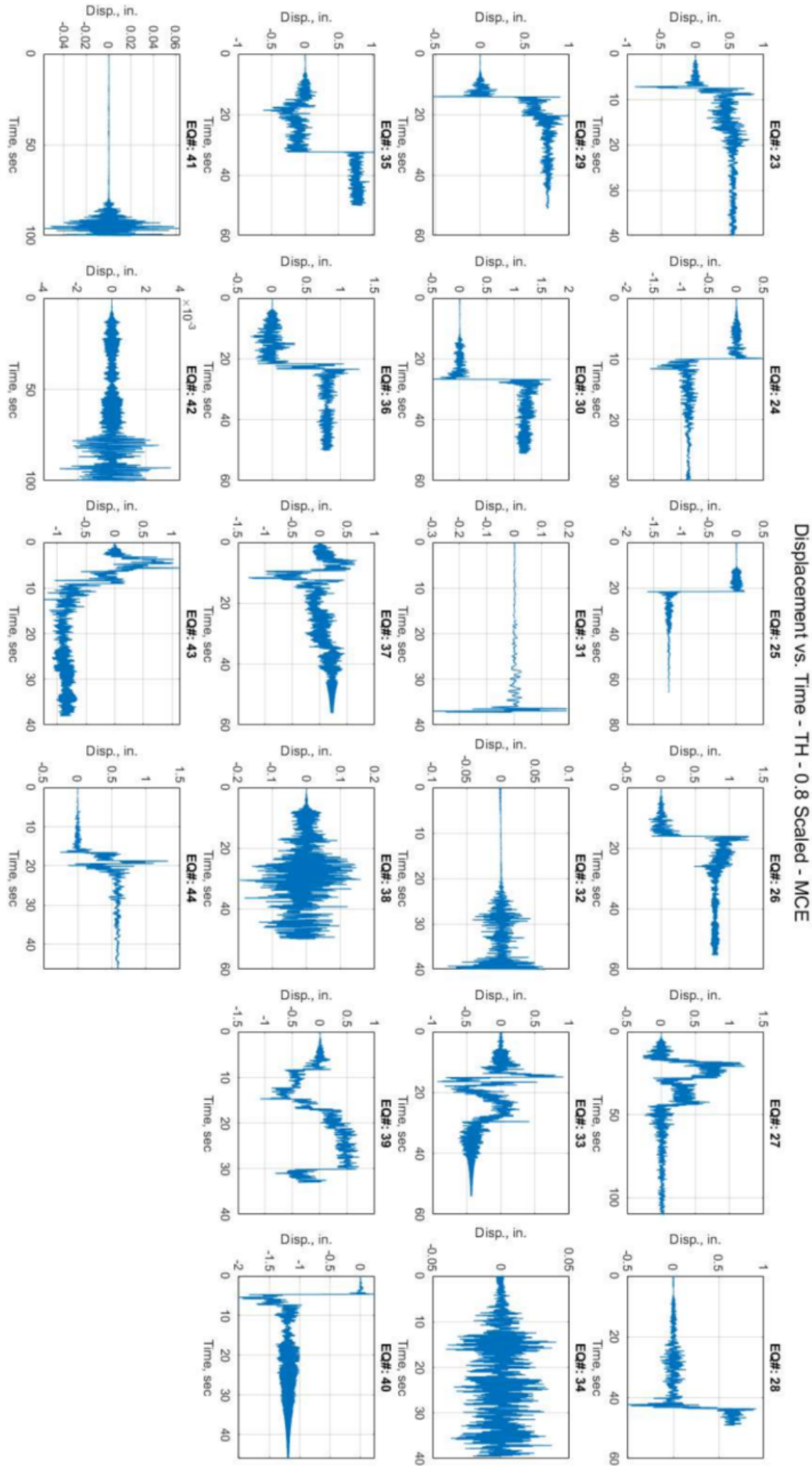


Figure C-14: Displacement versus Time Results for 0.8g Scaled MCE Trials - Ground Motions 23-44.

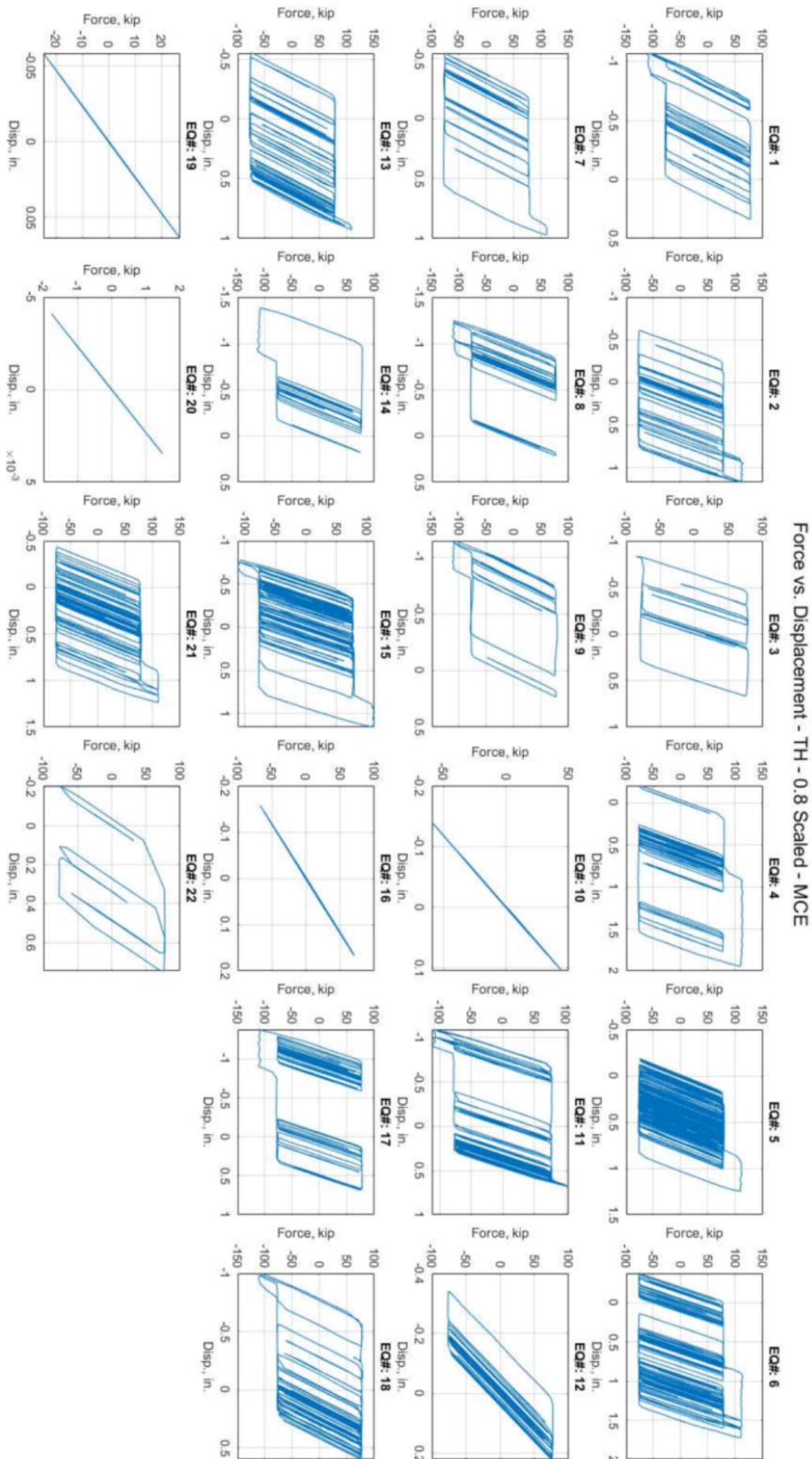


Figure C-15: Force versus Displacement Results for 0.8g Scaled MCE Trials - Ground Motions 1-22.

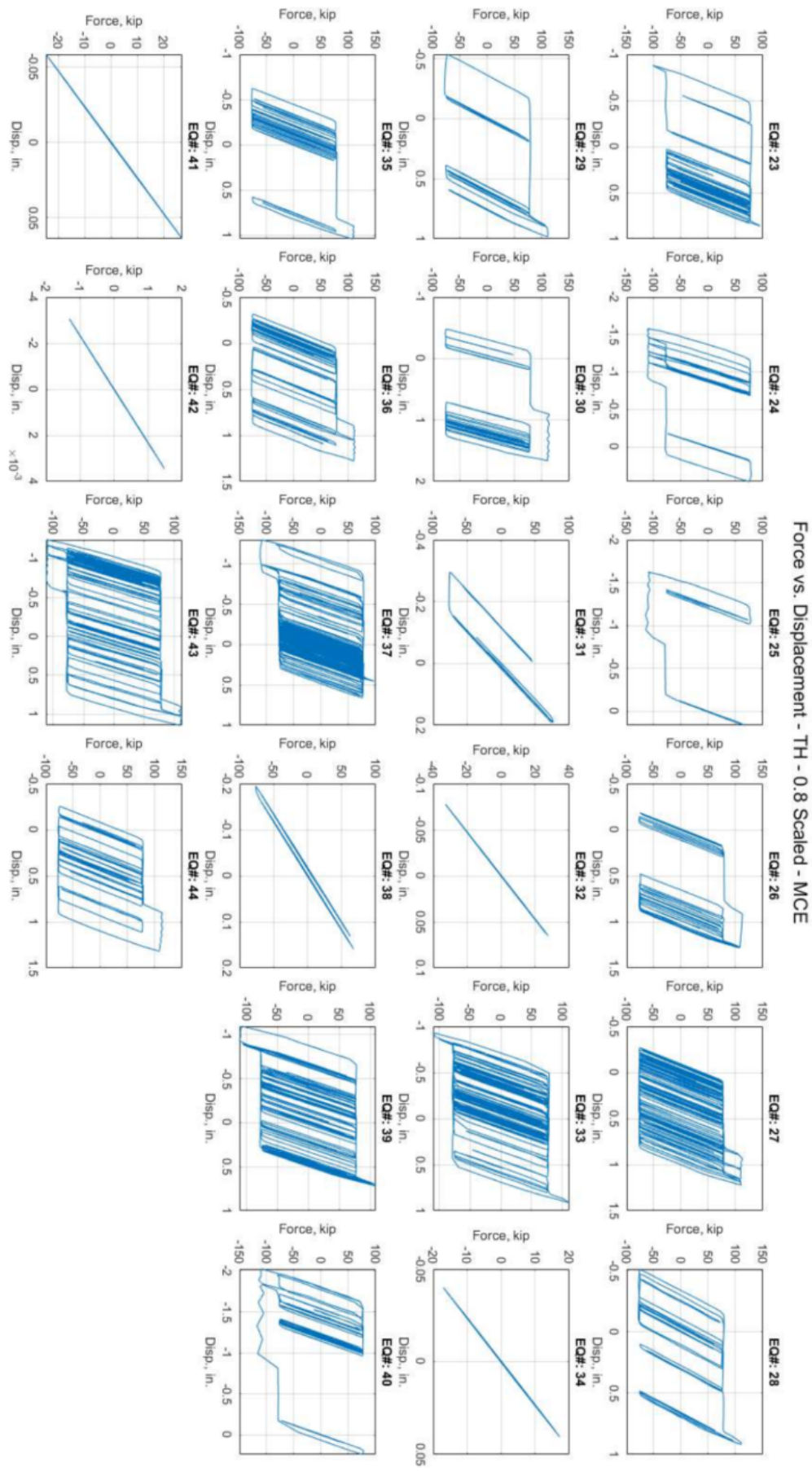


Figure C-16: Force versus Displacement Results for 0.8g Scaled MCE Trials - Ground Motions 23-44.

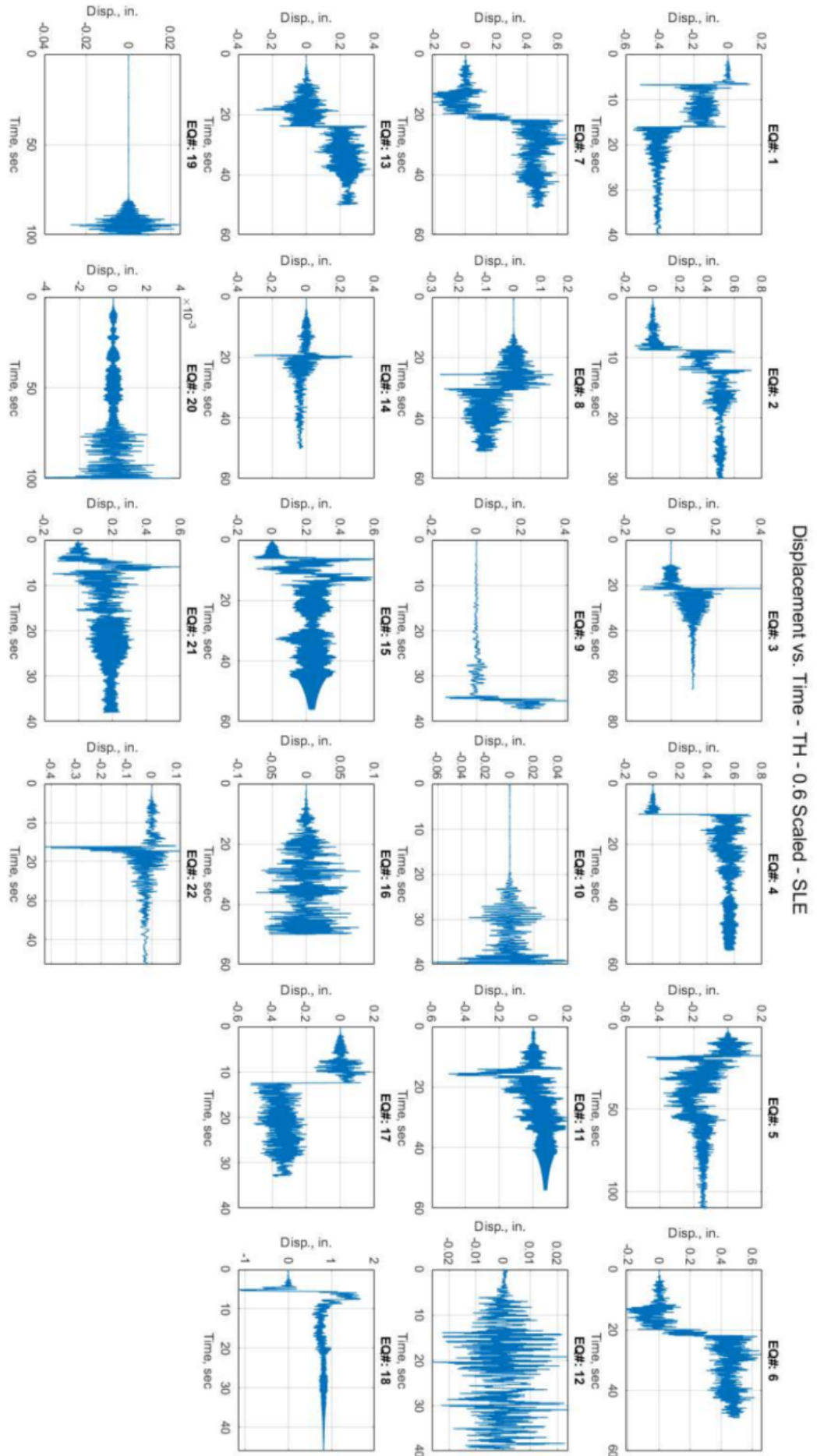


Figure C-17: Displacement versus Time Results for 0.6g Scaled SLE Trials - Ground Motions 1-22.

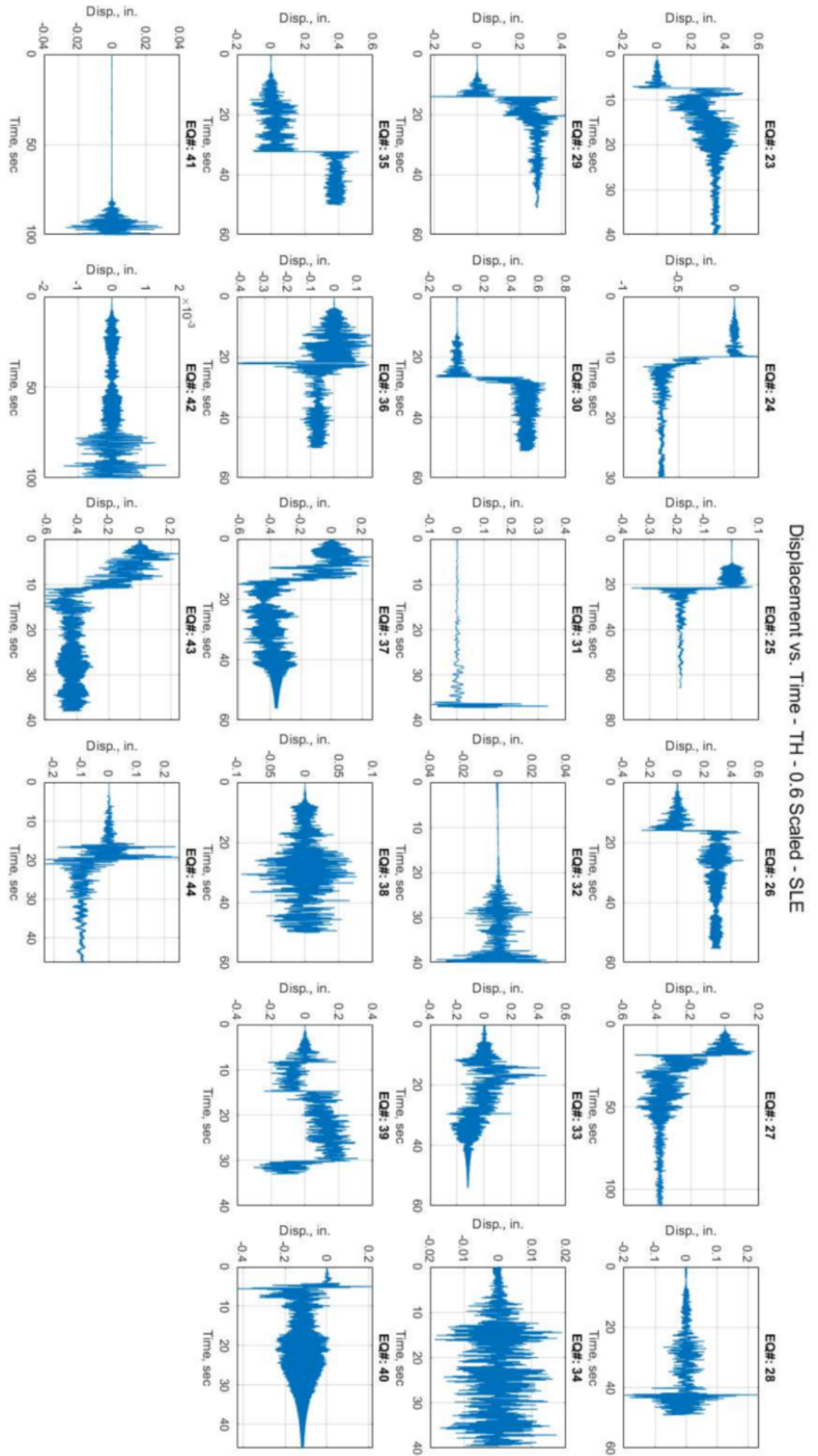


Figure C-18: Displacement versus Time Results for 0.6g Scaled SLE Trials - Ground Motions 23-44.

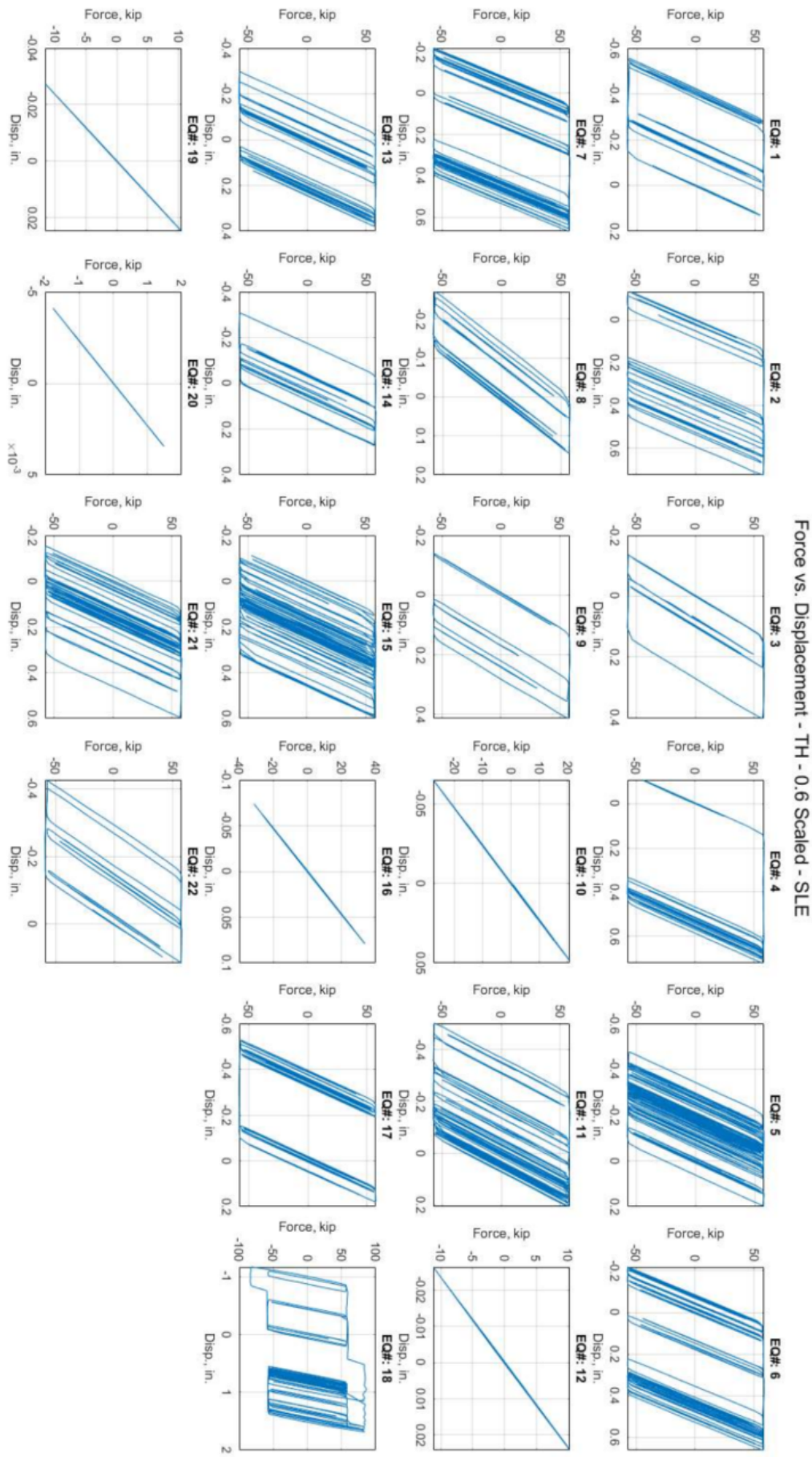


Figure C-19: Force versus Displacement Results for 0.6g Scaled SLE Trials - Ground Motions 1-22.

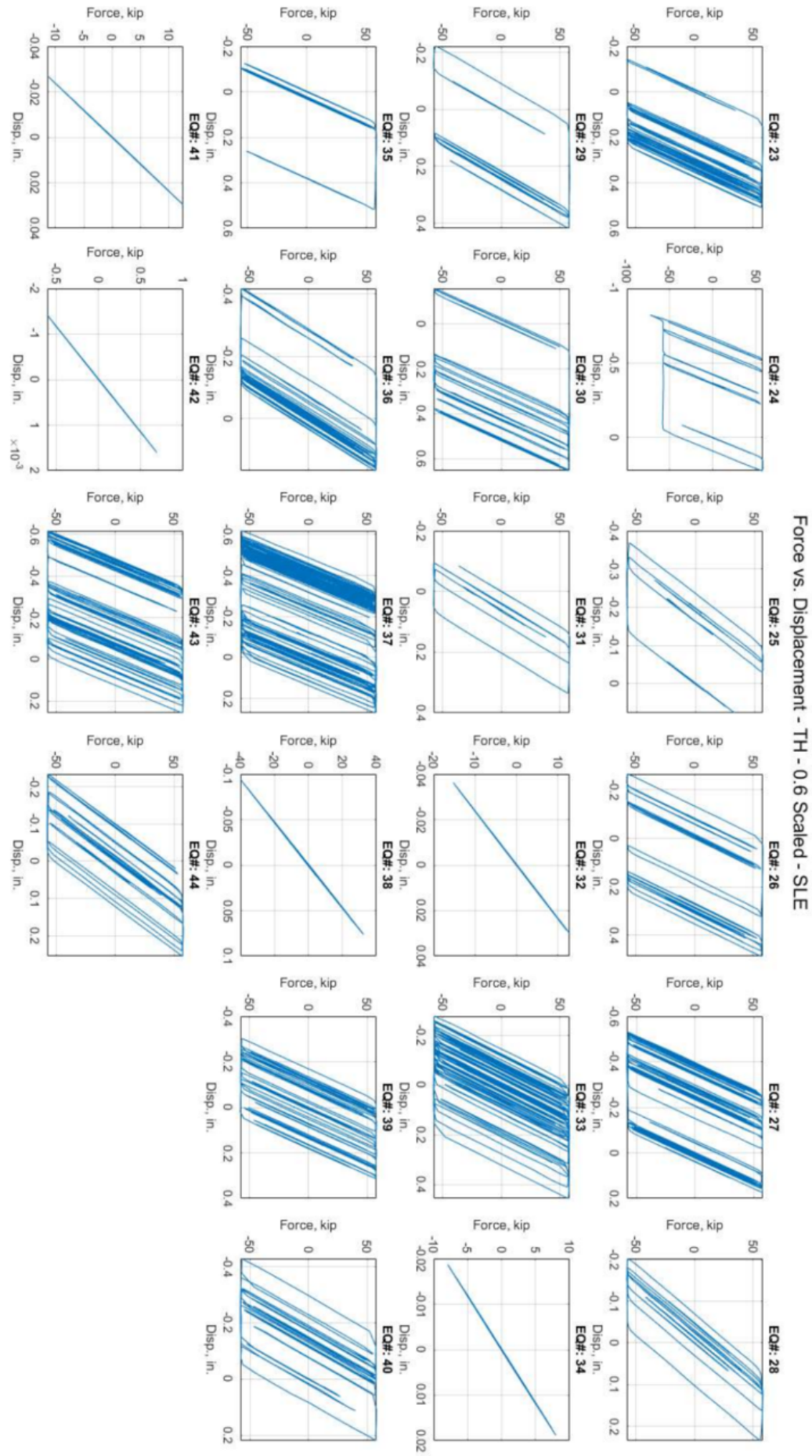


Figure C-20: Force versus Displacement Results for 0.6g Scaled SLE Trials - Ground Motions 23-44.

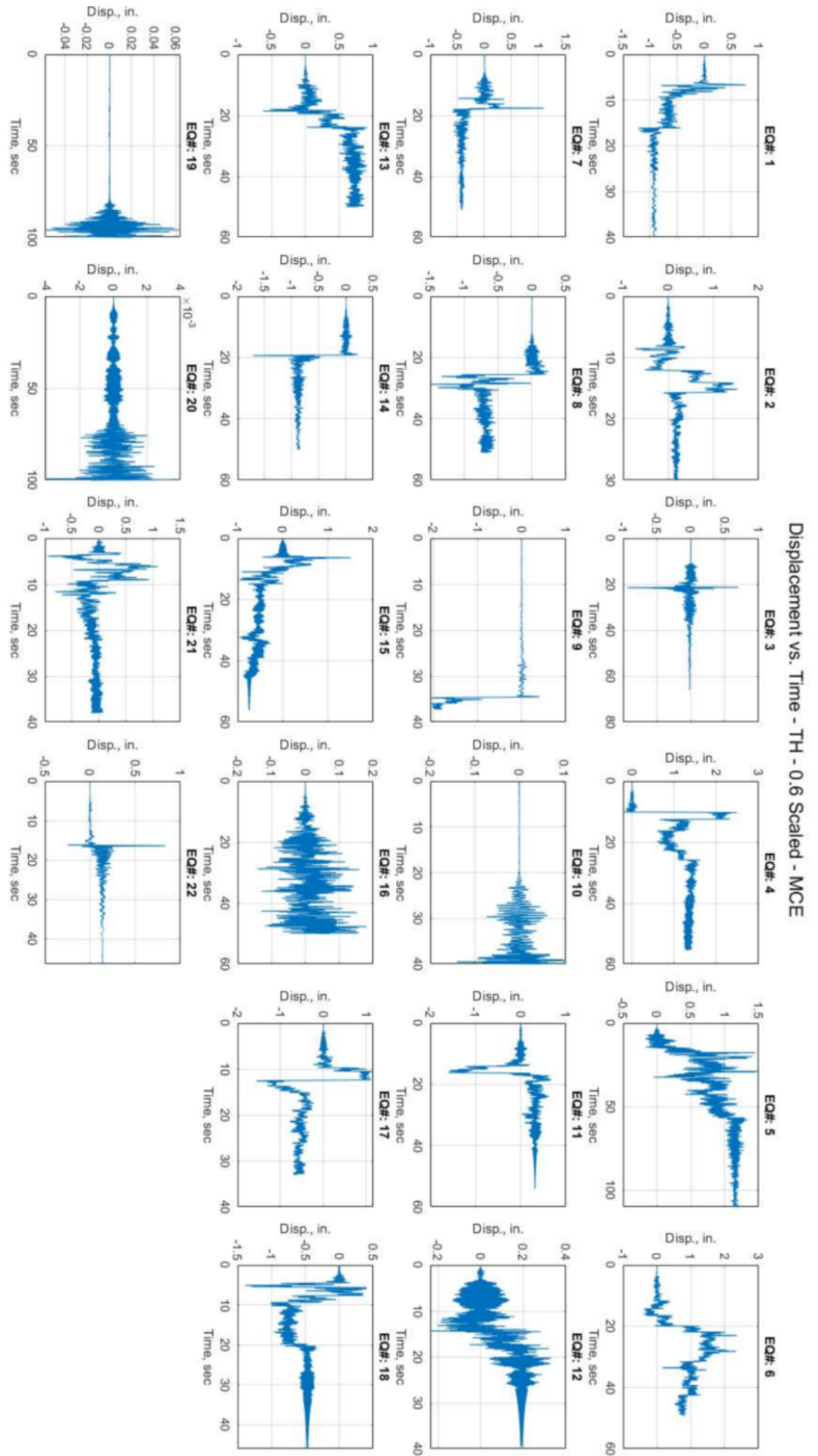


Figure C-21: Displacement versus Time Results for 0.6g Scaled MCE Trials - Ground Motions 1-22.

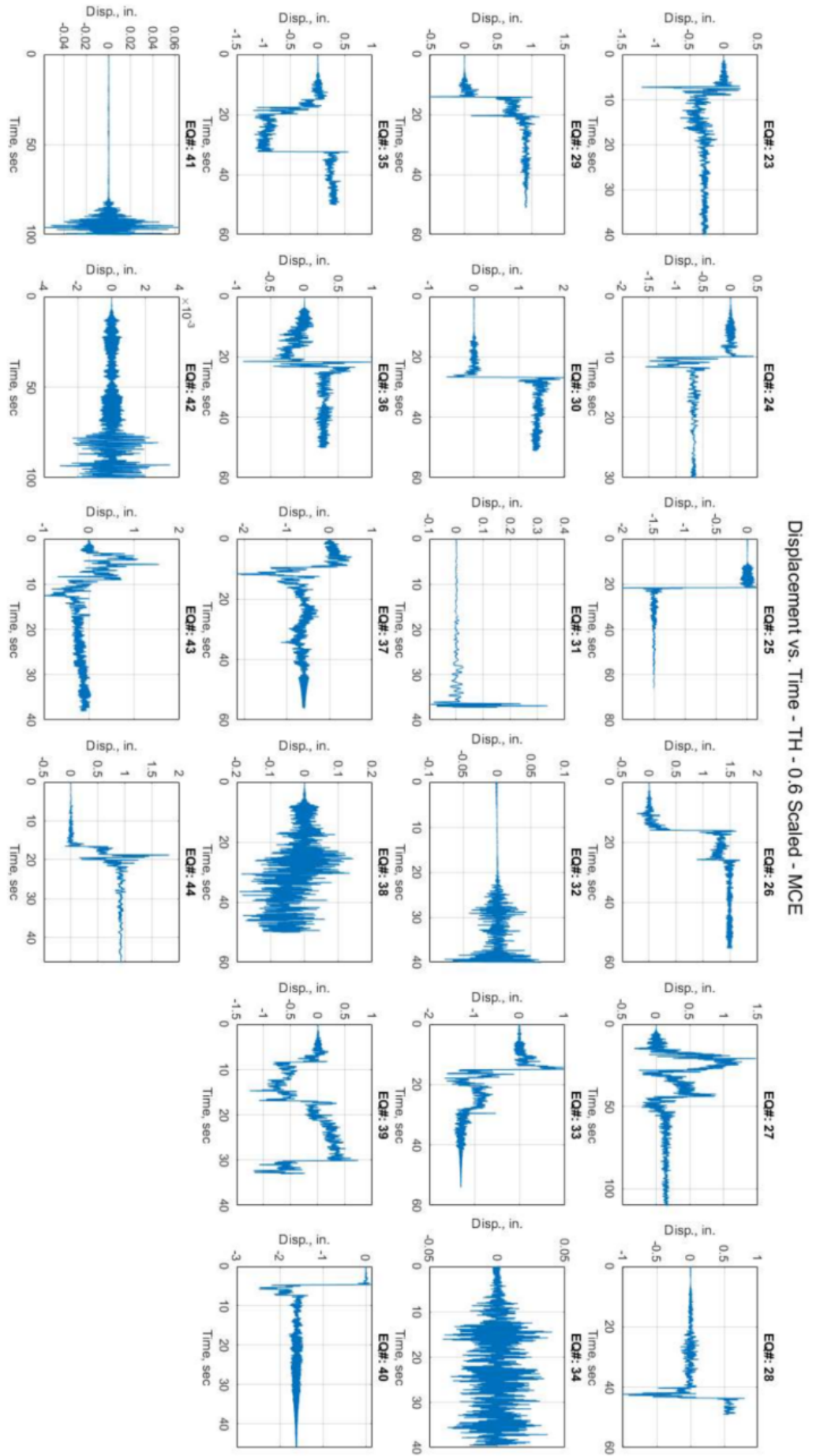


Figure C-22: Displacement versus Time Results for 0.6g Scaled MCE Trials - Ground Motions 23-44.

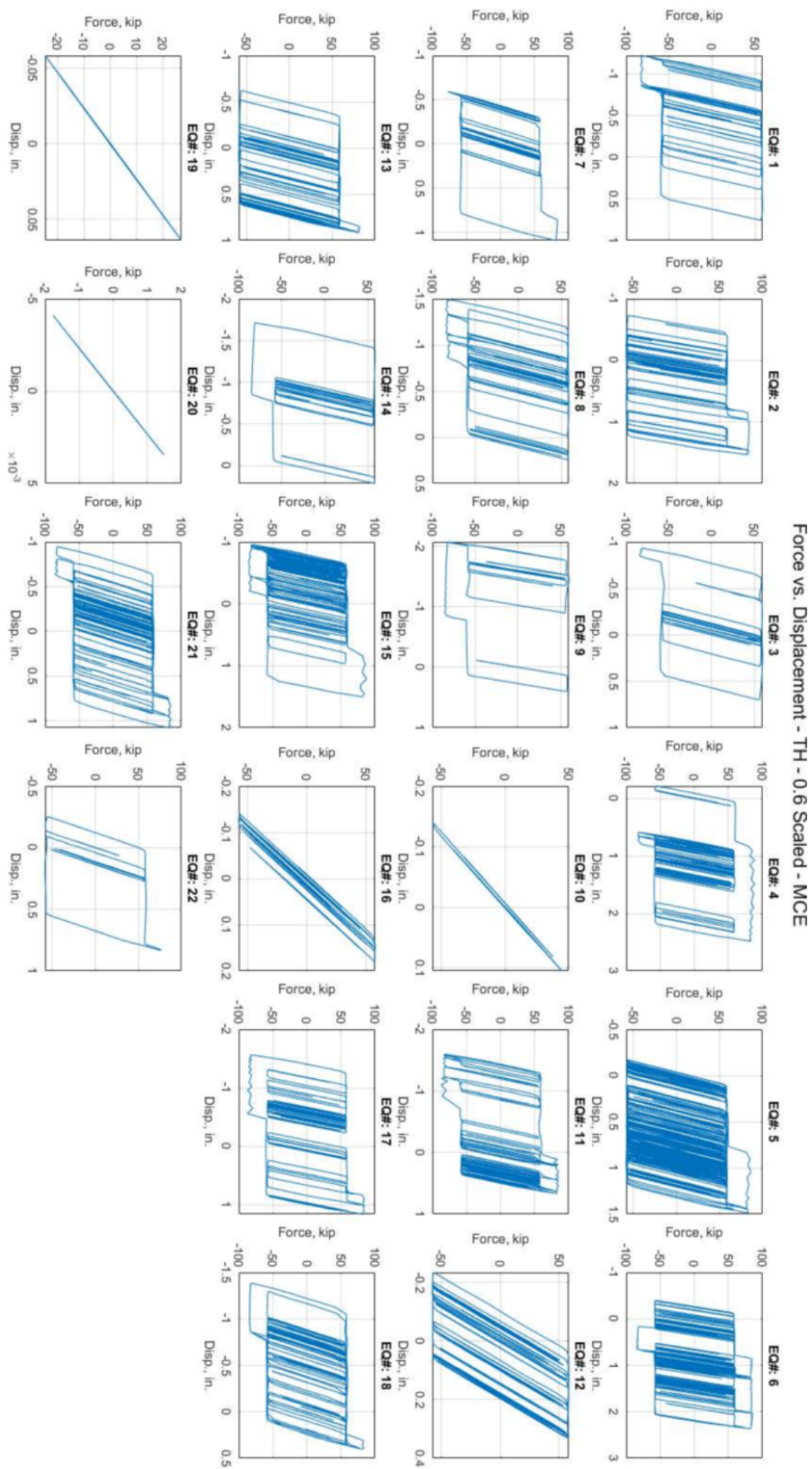


Figure C-23: Force versus Displacement Results for 0.6g Scaled MCE Trials - Ground Motions 1-22.

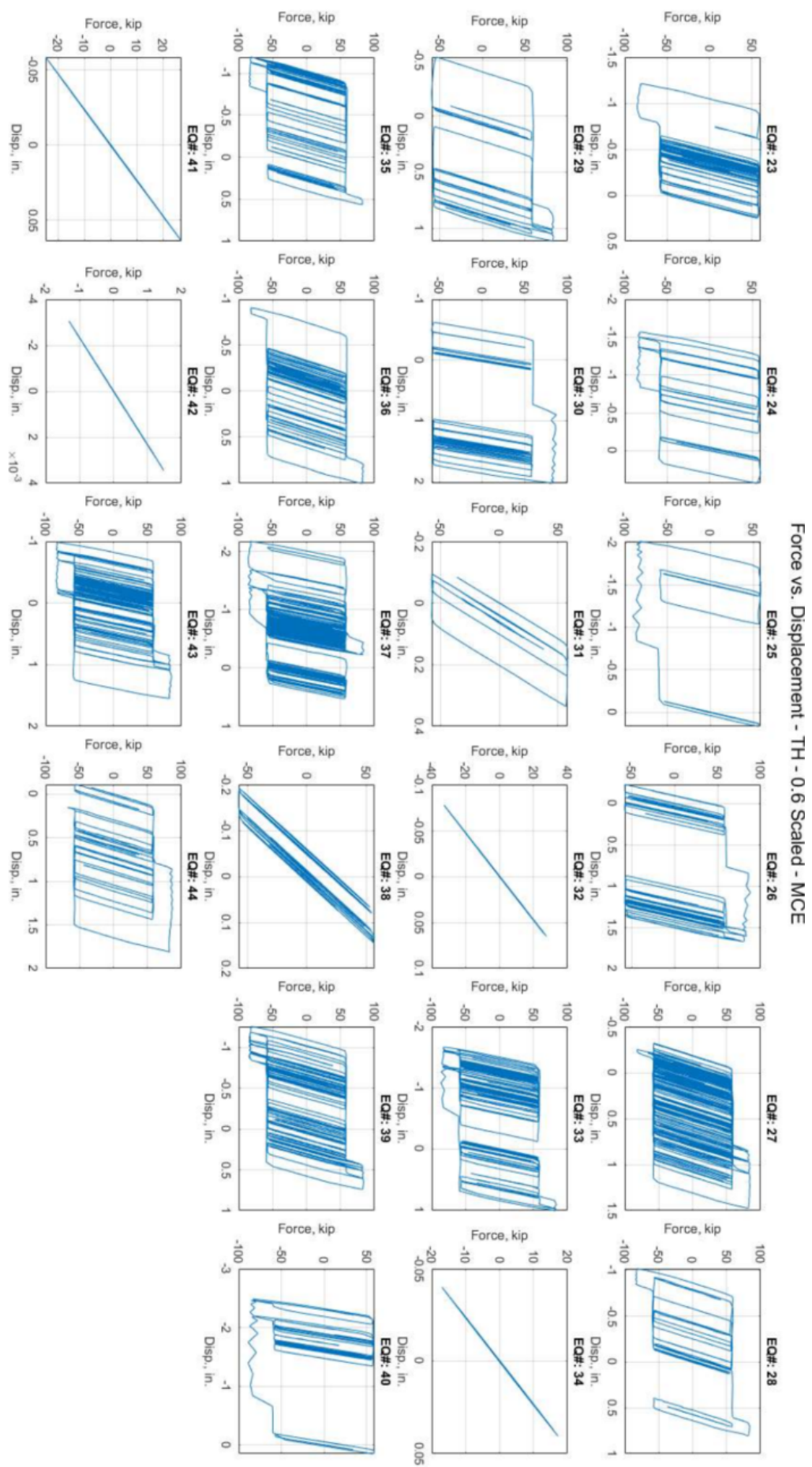


Figure C-24: Force versus Displacement Results for 0.6g Scaled MCE Trials - Ground Motions 23-44.

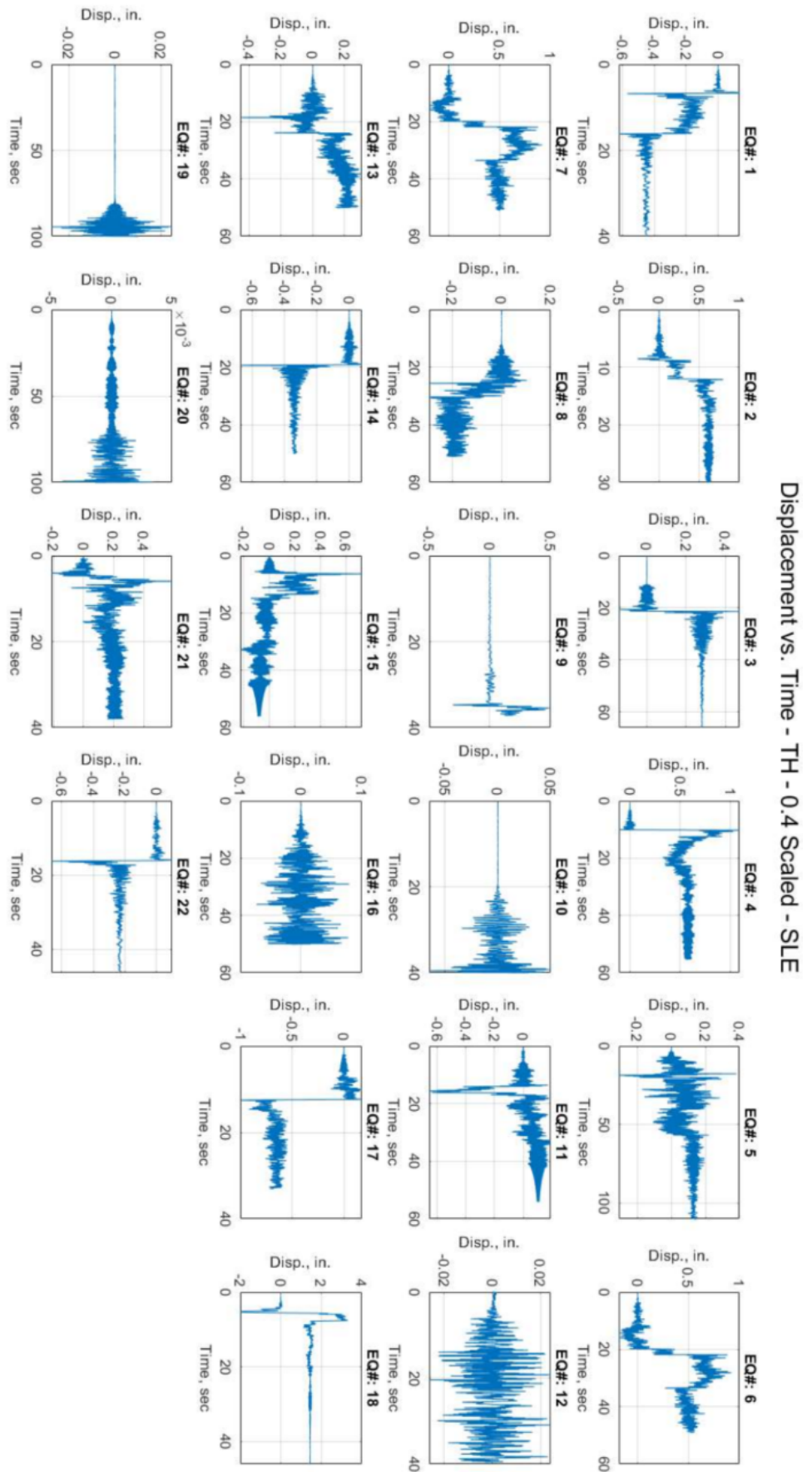


Figure C-25: Displacement versus Time Results for 0.4g Scaled SLE Trials - Ground Motions 1-22.

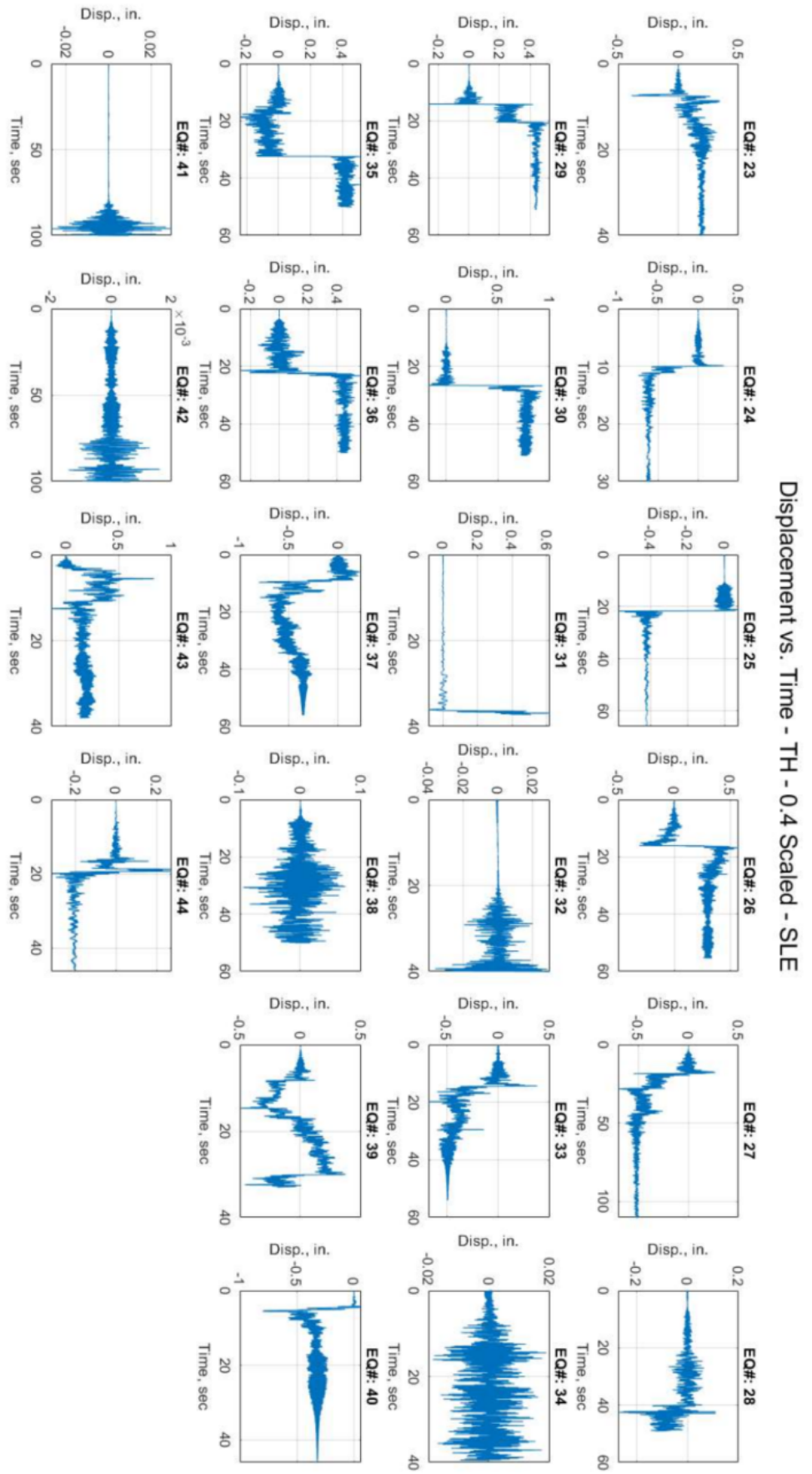


Figure C-26: Displacement versus Time Results for 0.4g Scaled SLE Trials - Ground Motions 23-44.

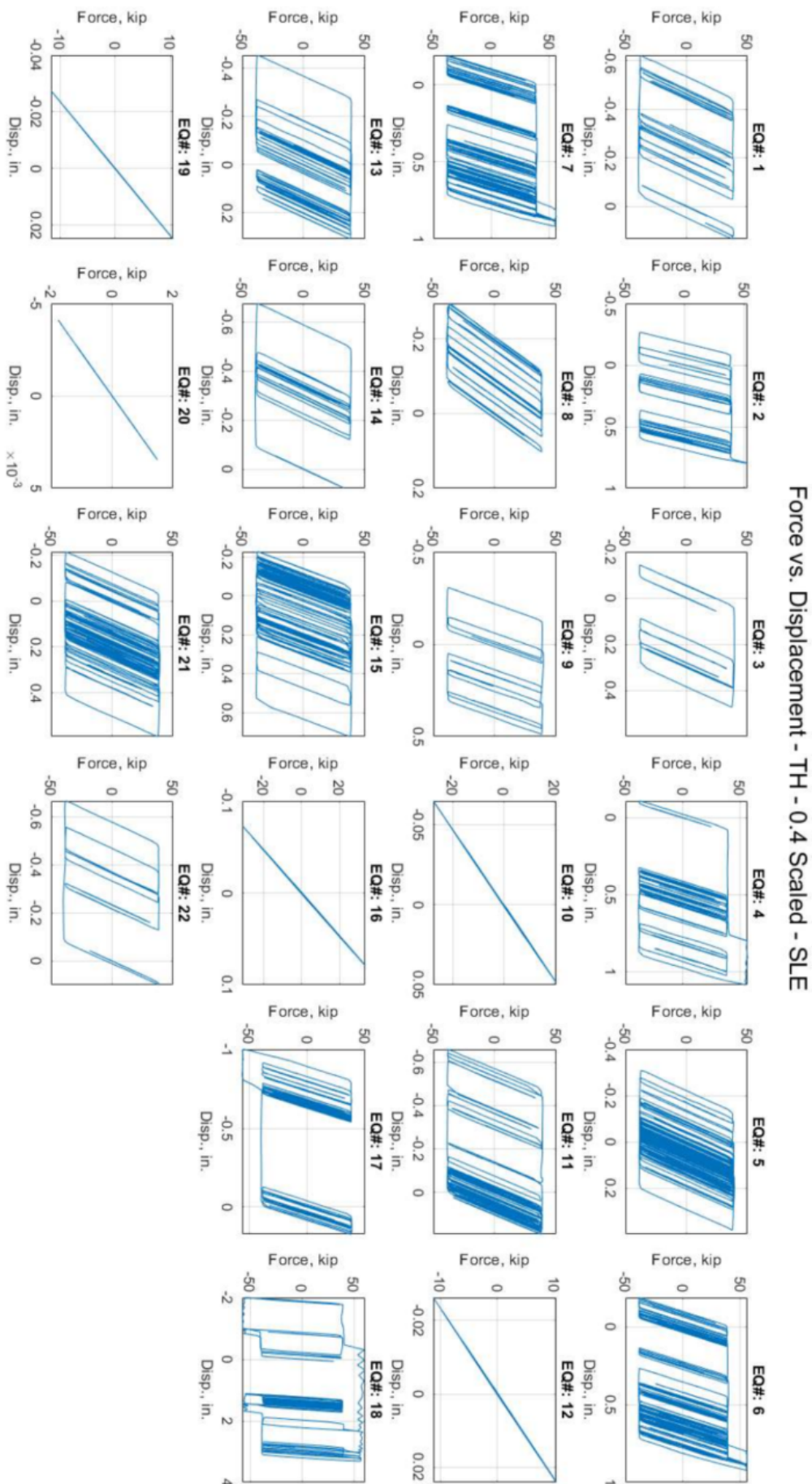


Figure C-27: Force versus Displacement Results for 0.4g Scaled SLE Trials - Ground Motions 1-22.

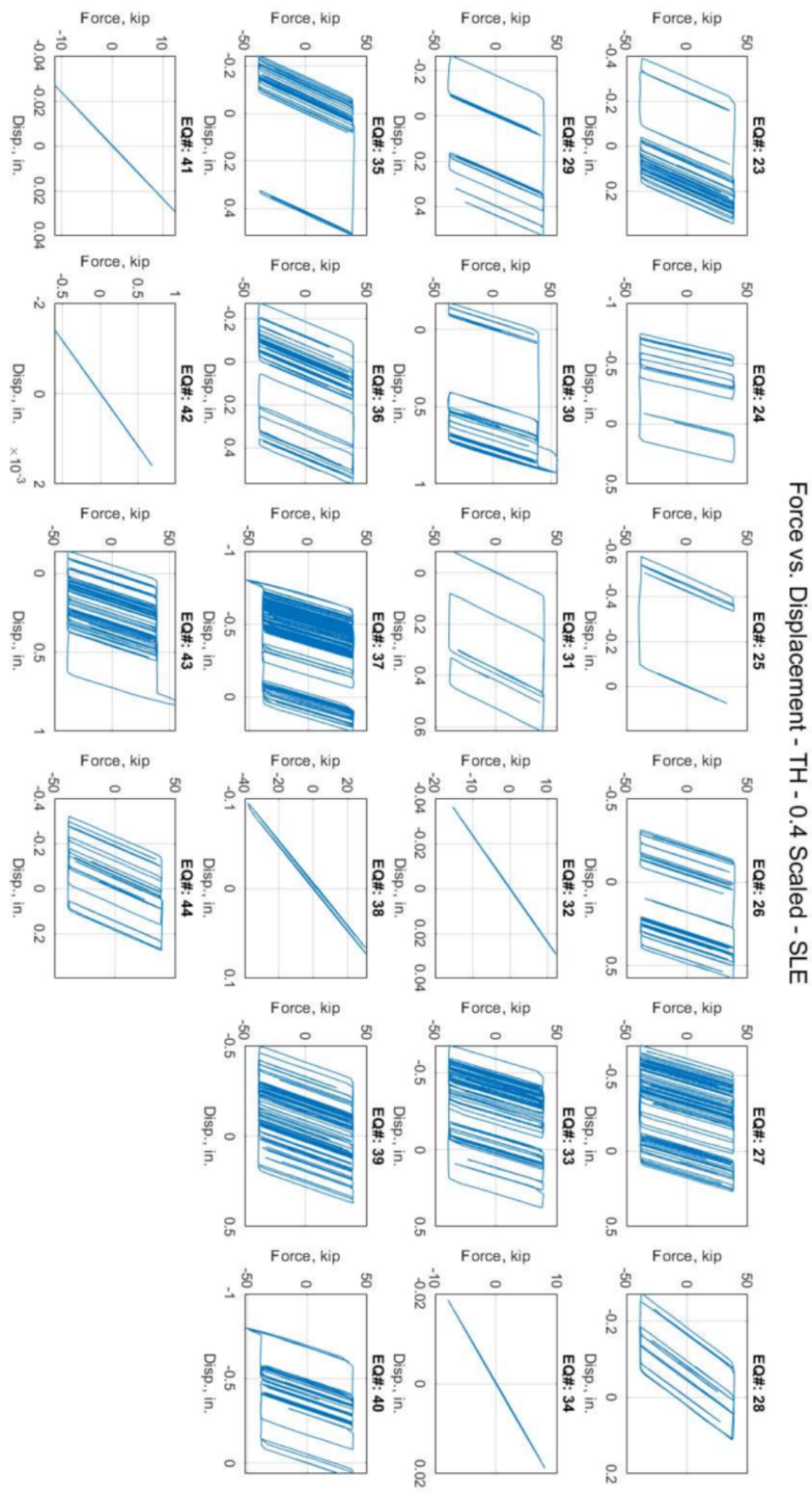


Figure C-28: Force versus Displacement Results for 0.4g Scaled SLE Trials - Ground Motions 23-44.

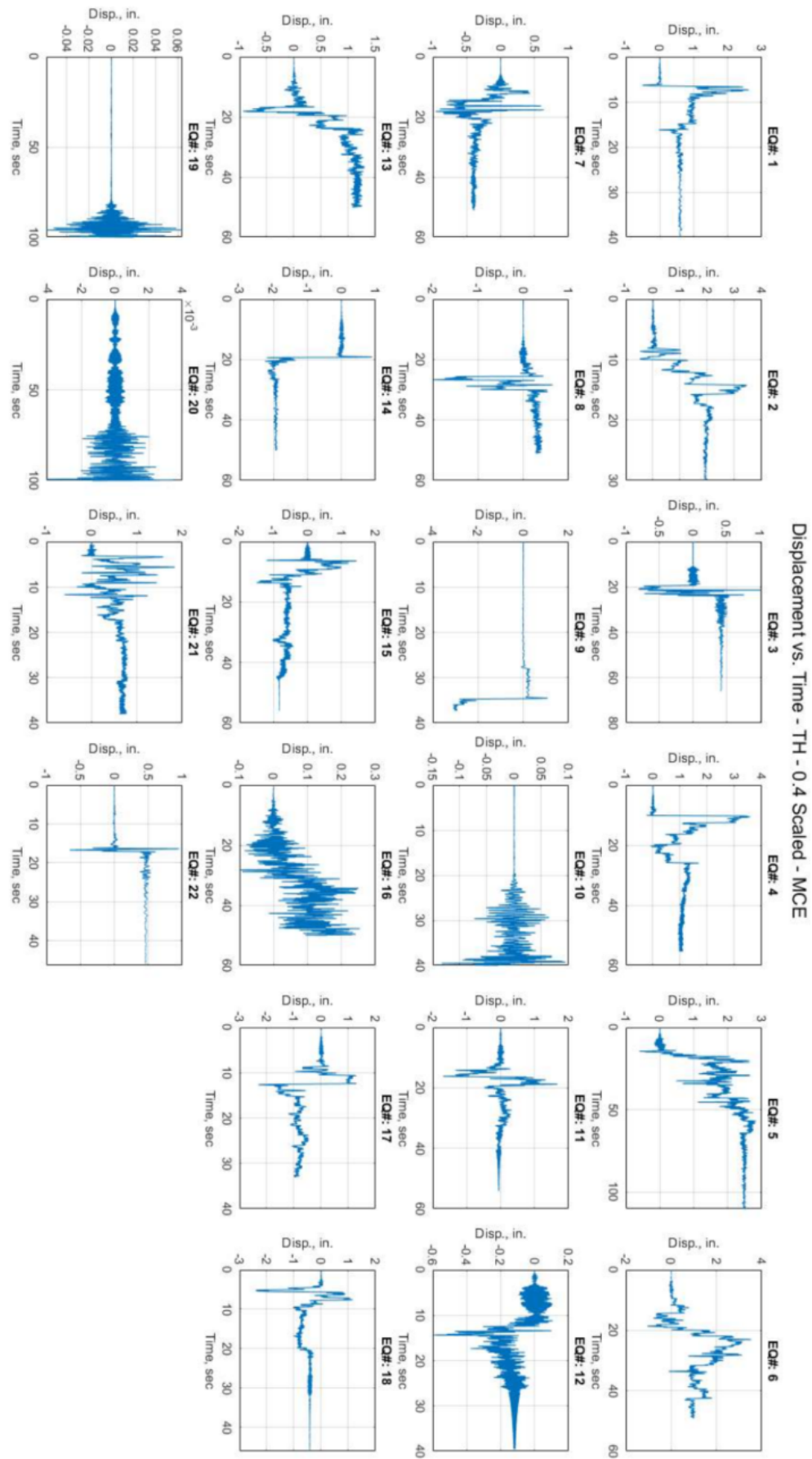


Figure C-29: Displacement versus Time Results for 0.4g Scaled MCE Trials - Ground Motions 1-22.

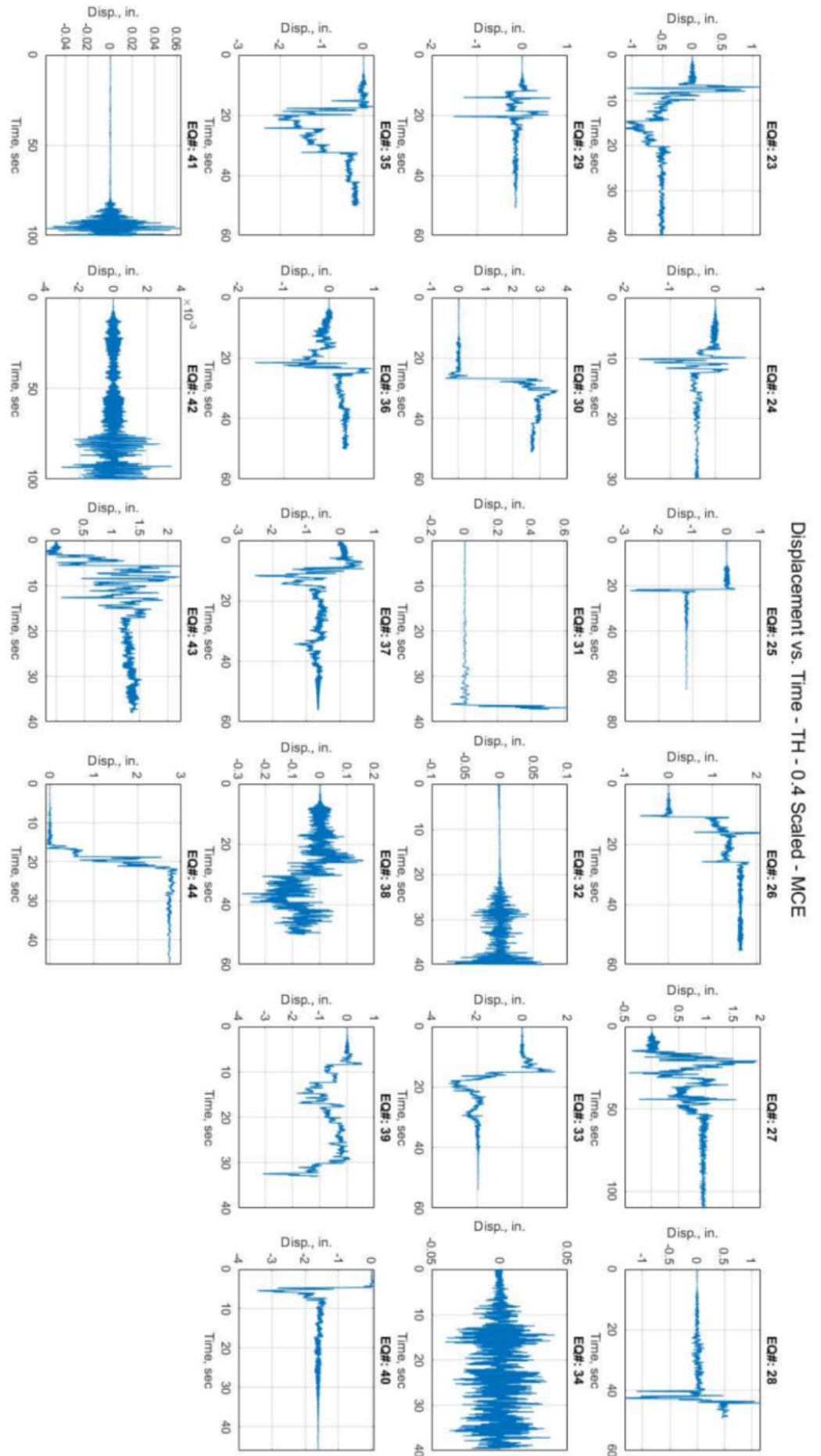


Figure C-30: Displacement versus Time Results for 0.4g Scaled MCE Trials - Ground Motions 23-44.

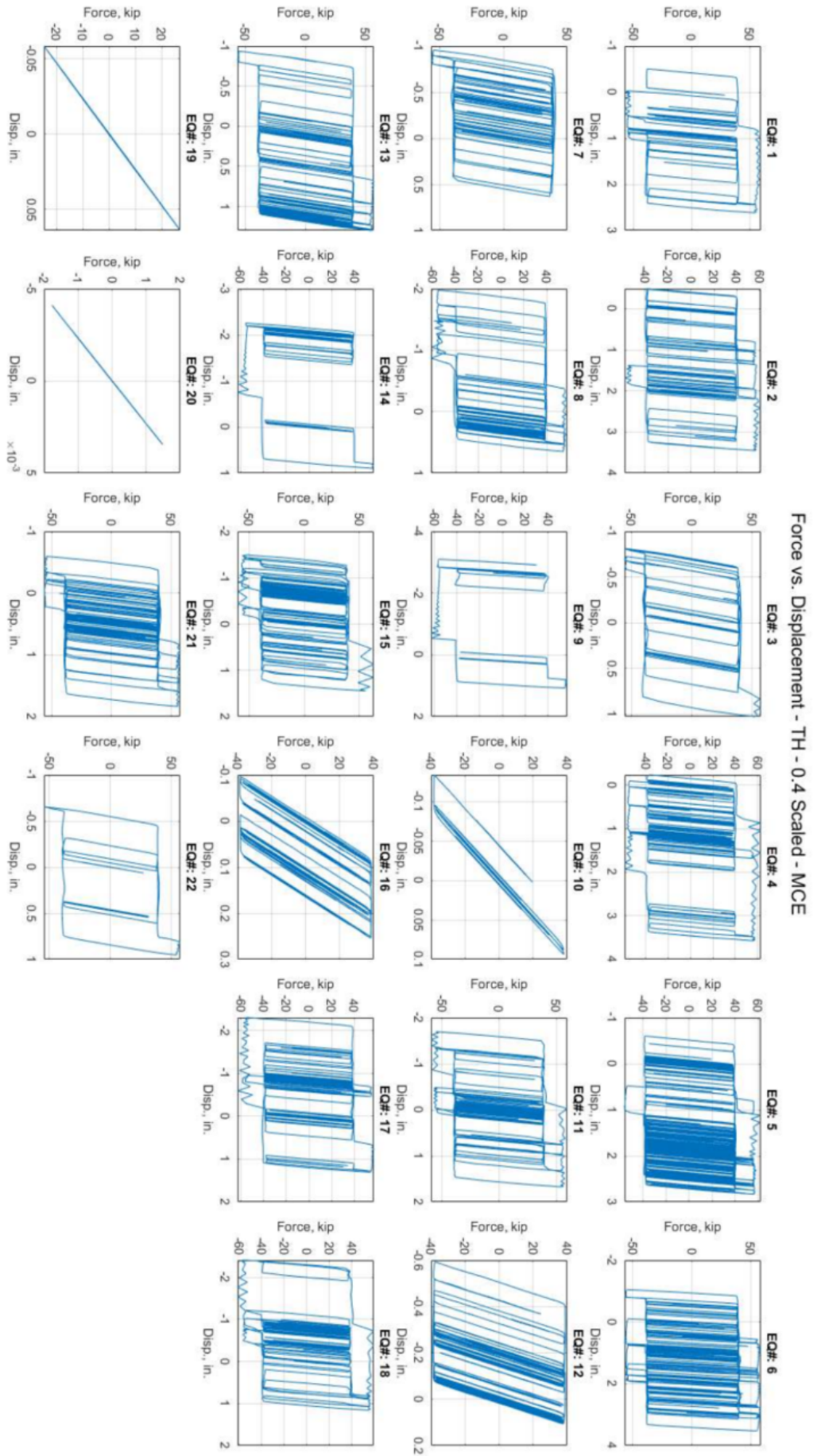


Figure C-31: Force versus Displacement Results for 0.4g Scaled MCE Trials - Ground Motions 1-22.

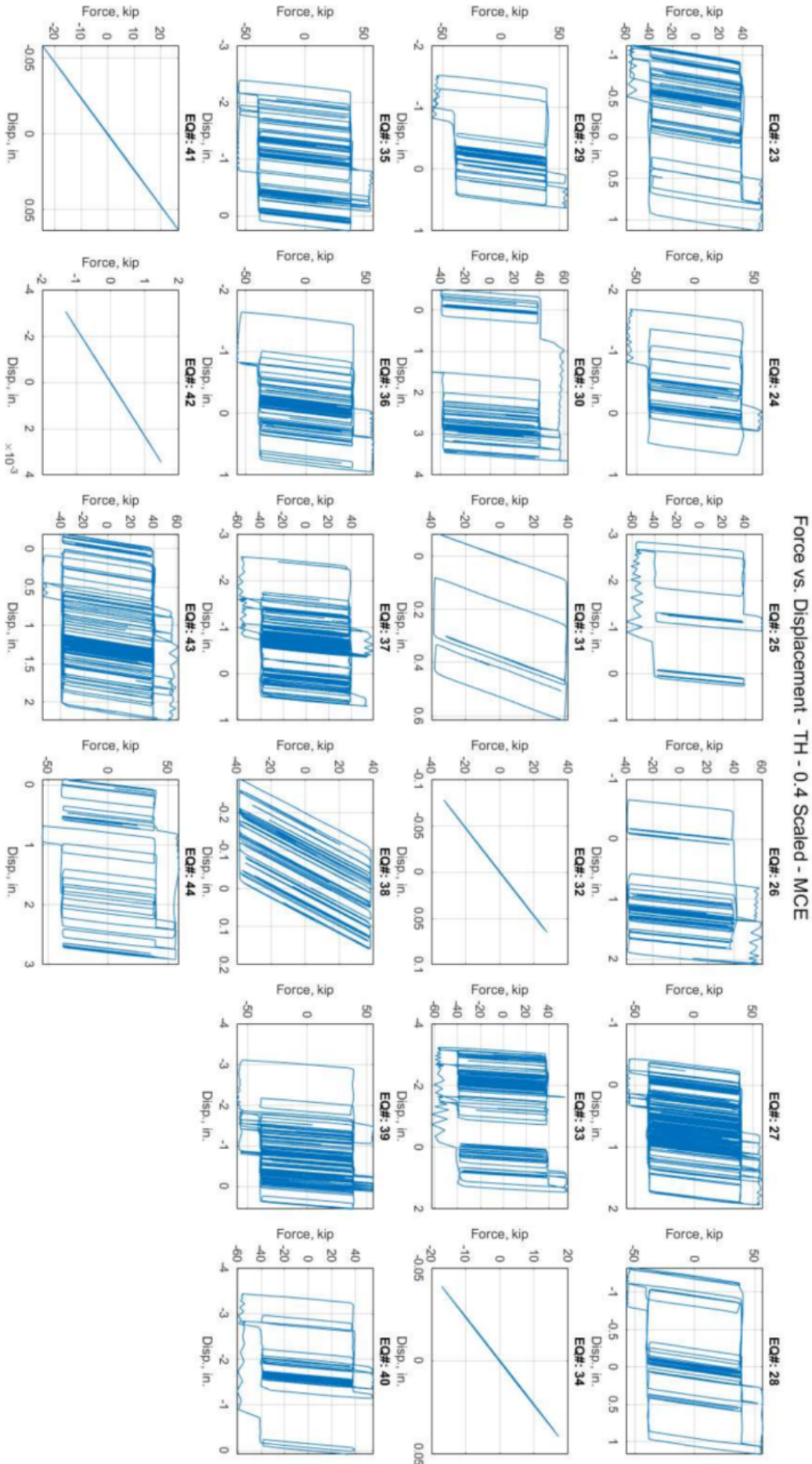


Figure C-32: Force versus Displacement Results for 0.4g Scaled MCE Trials - Ground Motions 23-44.

APPENDIX D
4-STORY, 4-BAY INITIAL FINAL TRIAL

Inter-Story Drift Ratios & Story Shear Forces - 0.4 Scaled

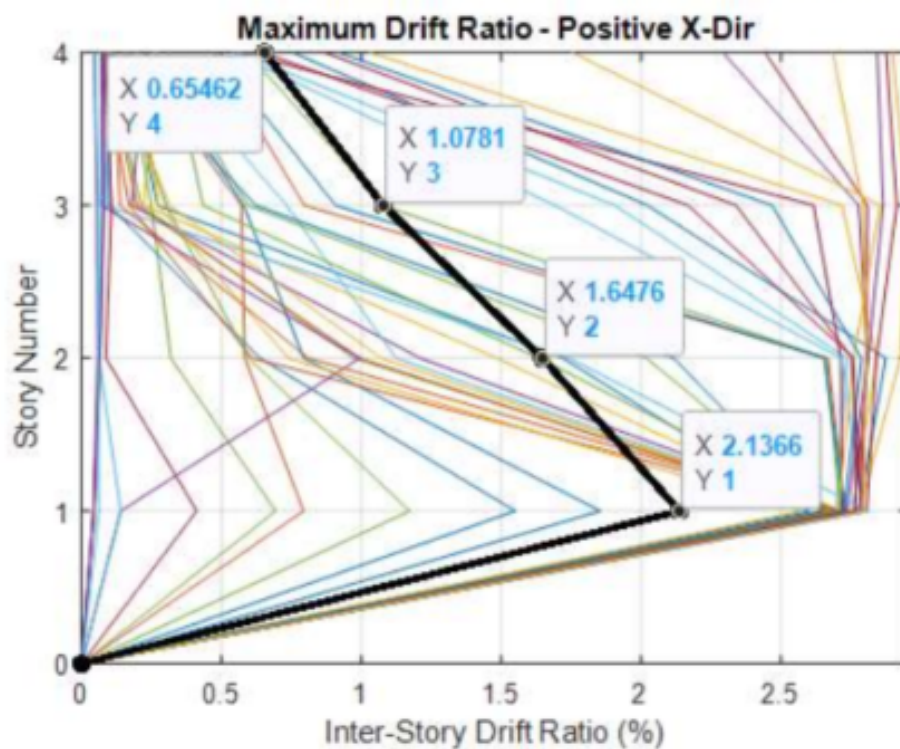


Figure D-1: Story Number versus Drift Ratio - Positive Drift - 0.4 Scaled Initial Trials.

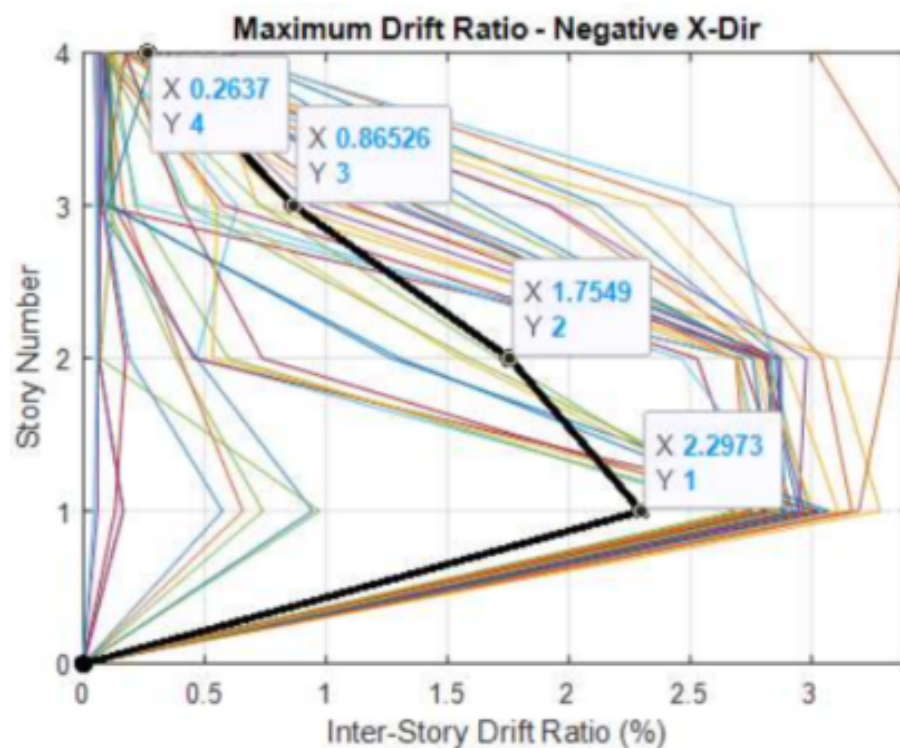


Figure D-2: Story Number versus Drift Ratio - Negative Drift - 0.4 Scaled Initial Trials.

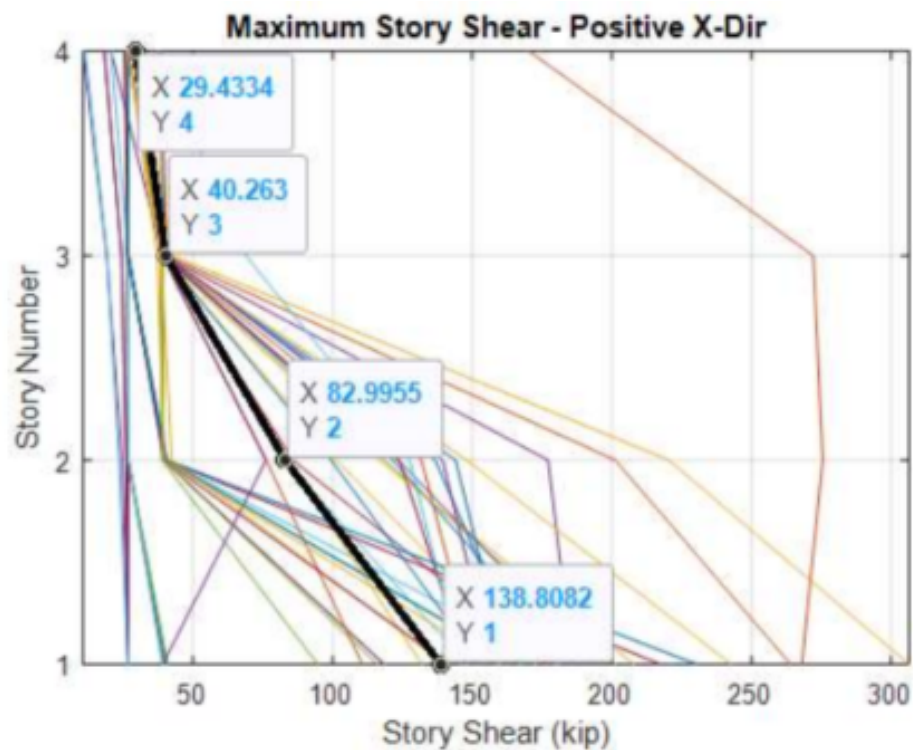


Figure D-3: Story Number versus Maximum Shear - Positive Shear - 0.4 Scaled Initial Trials.

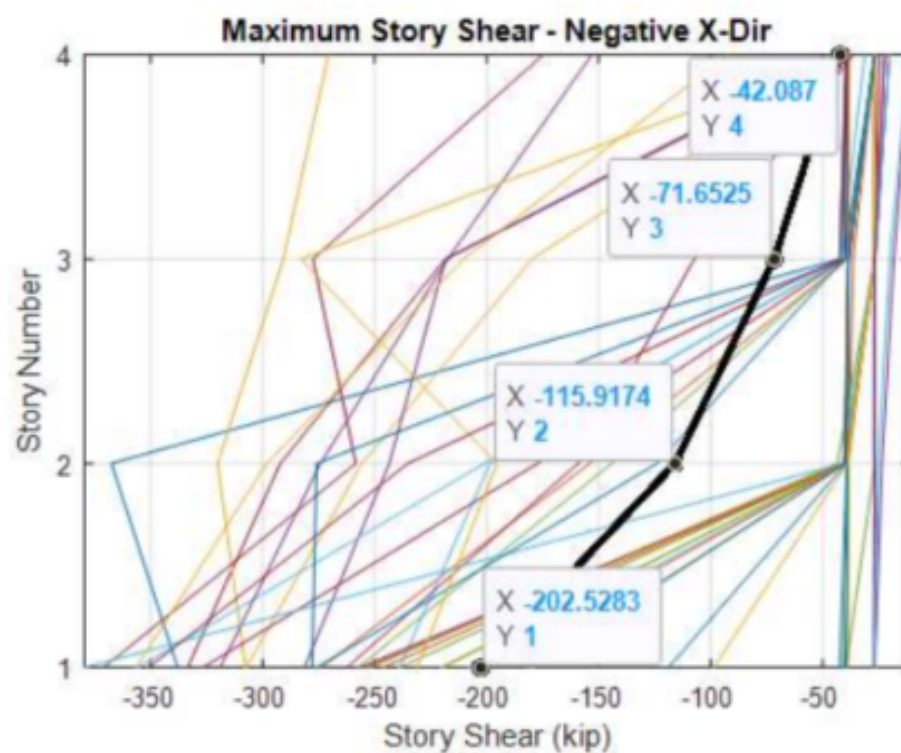


Figure D-4: Story Number versus Maximum Shear - Negative Shear - 0.4 Scaled Initial Trials.

APPENDIX E
4-STORY, 4-BAY UPDATED FINAL TRIAL

Story Displacement & Story Shear Forces - w/ Friction Damper - SLE

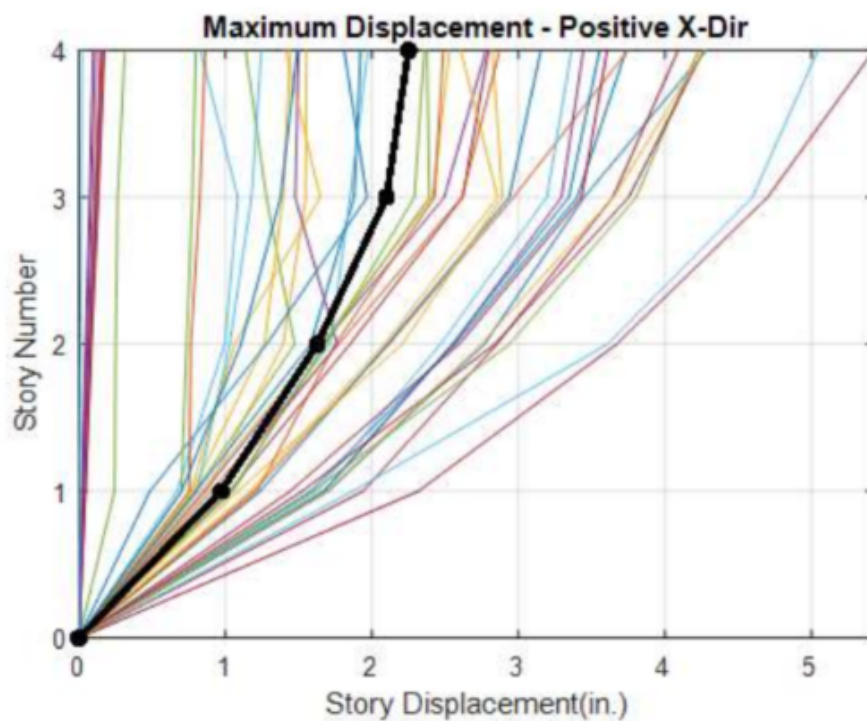


Figure E-1: Story Number versus Displacement - Positive Displacement - SLE Trials.

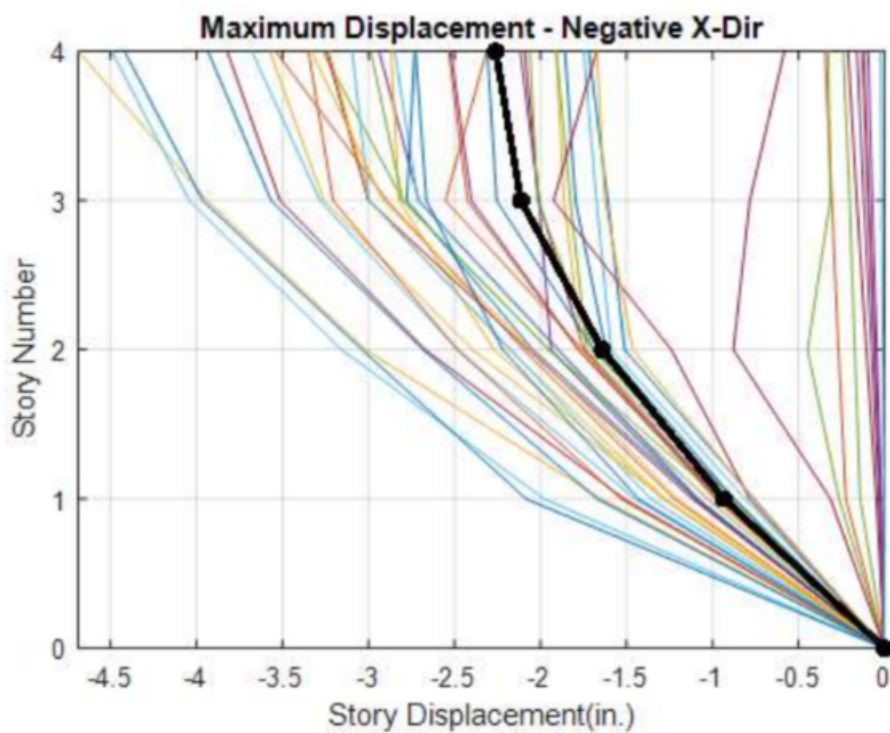


Figure E-2: Story Number versus Displacement - Negative Displacement - SLE Trials.

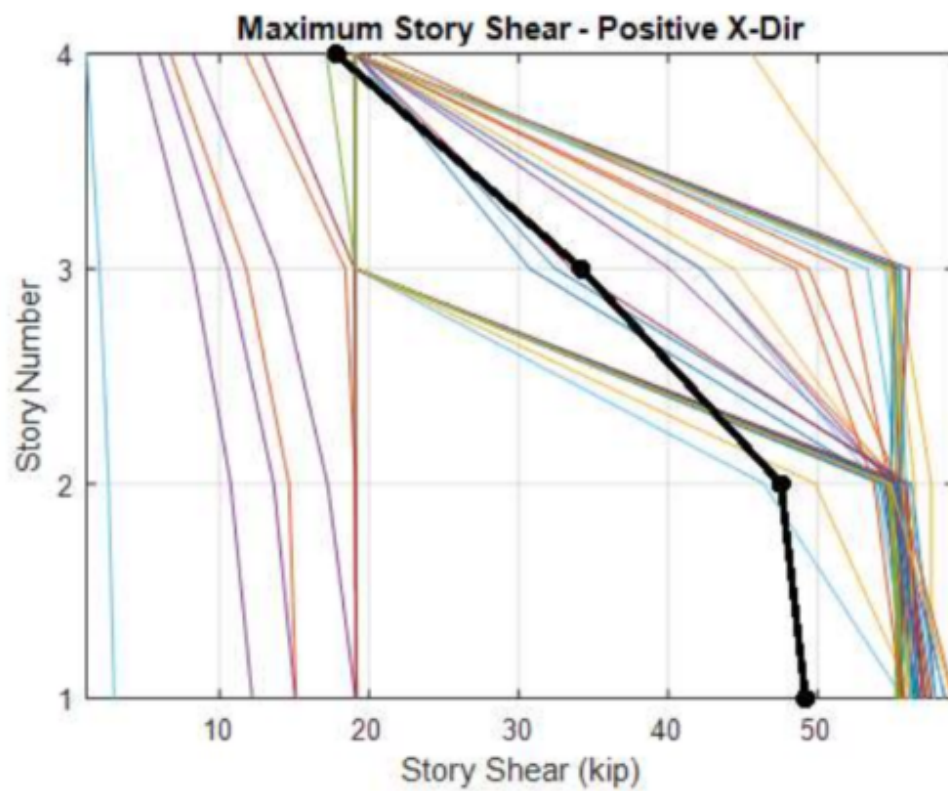


Figure E-3: Story Number versus Shear - Positive Shear - SLE Trials.

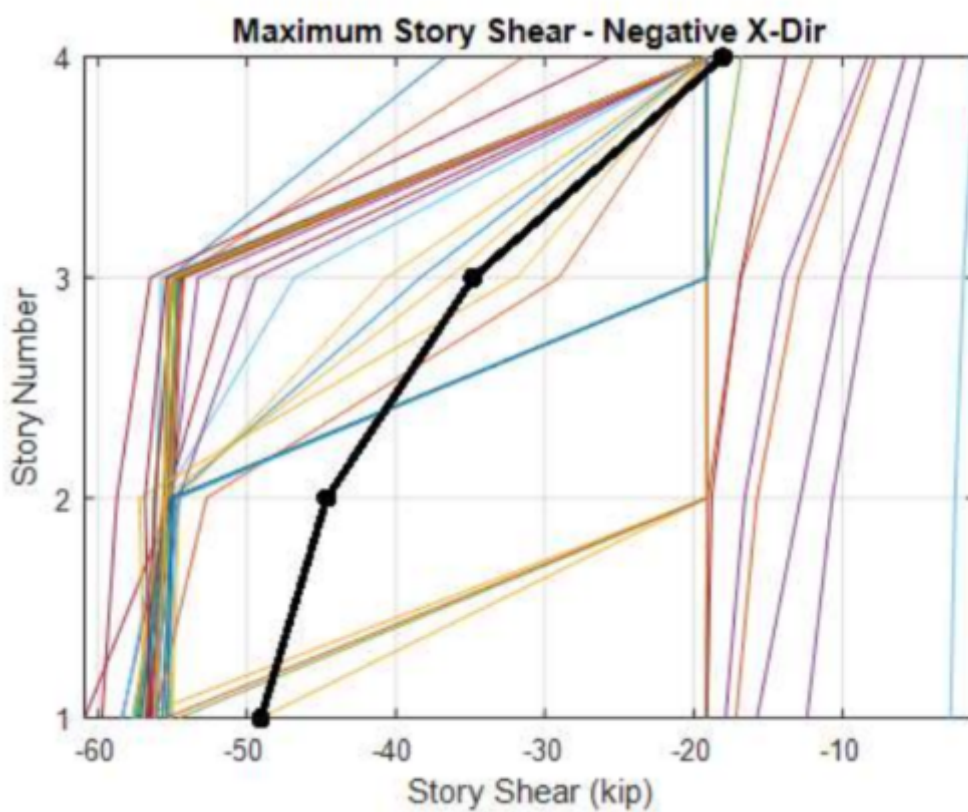


Figure E-4: Story Number versus Shear - Negative Shear - SLE Trials.

Inter-Story Drift Ratios & Story Shear Forces - w/ Friction Damper - SLE

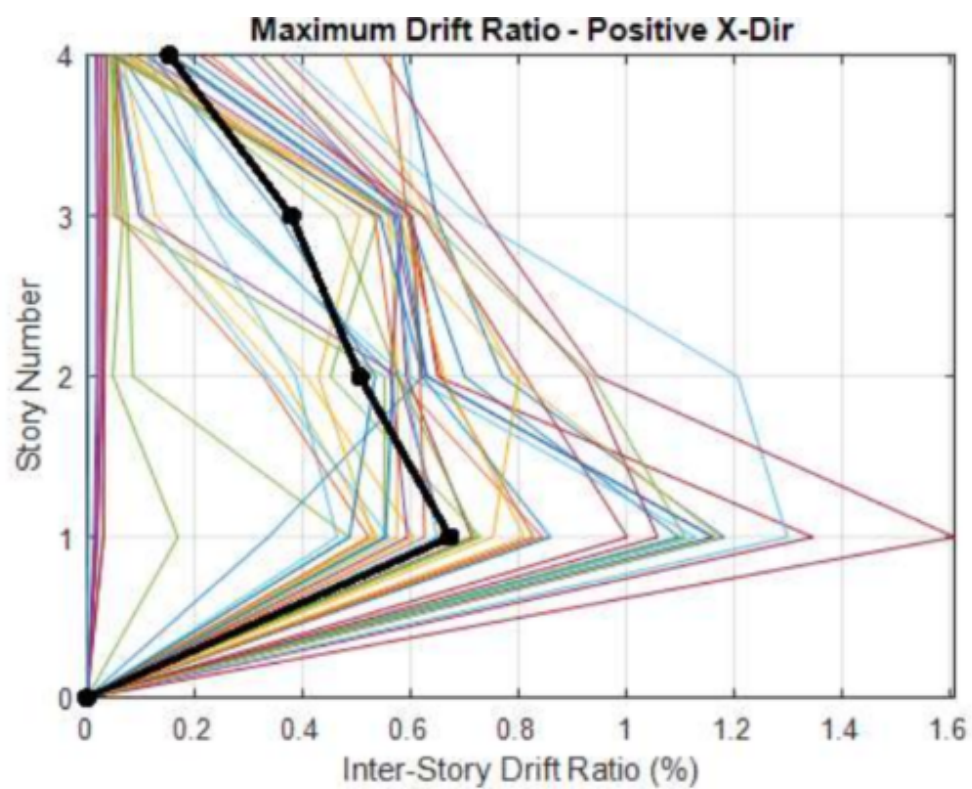


Figure E-5: Story Number versus Drift - Positive Drift - SLE Trials.

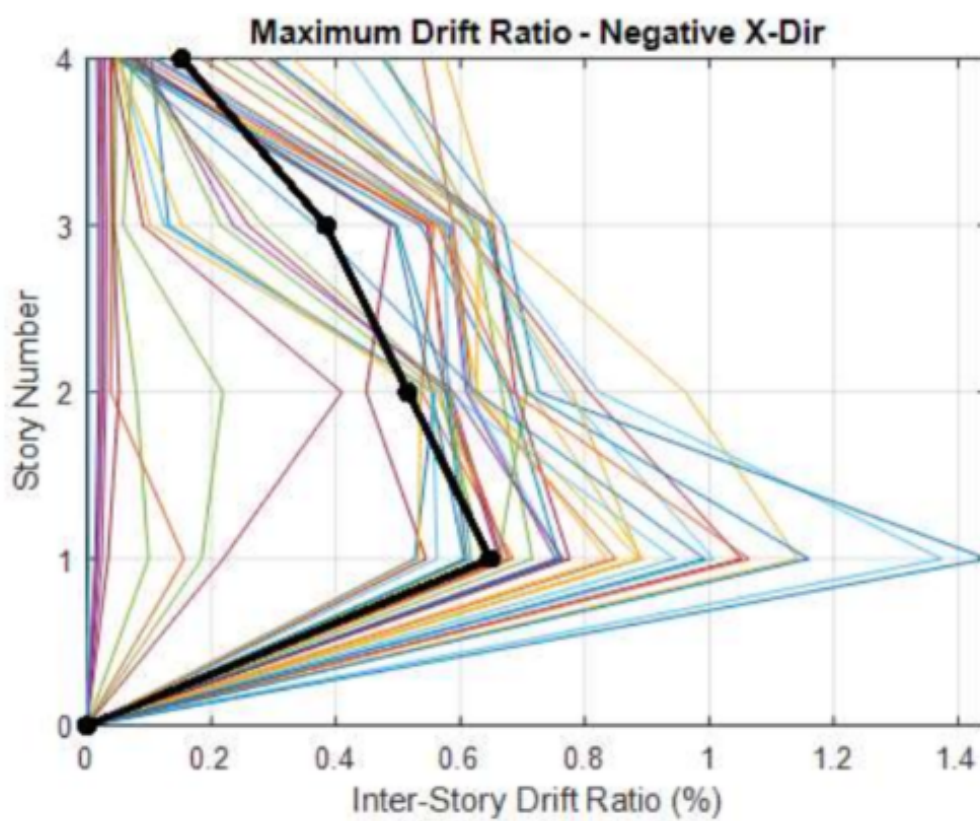


Figure E-6: Story Number versus Drift - Negative Drift - SLE Trials.

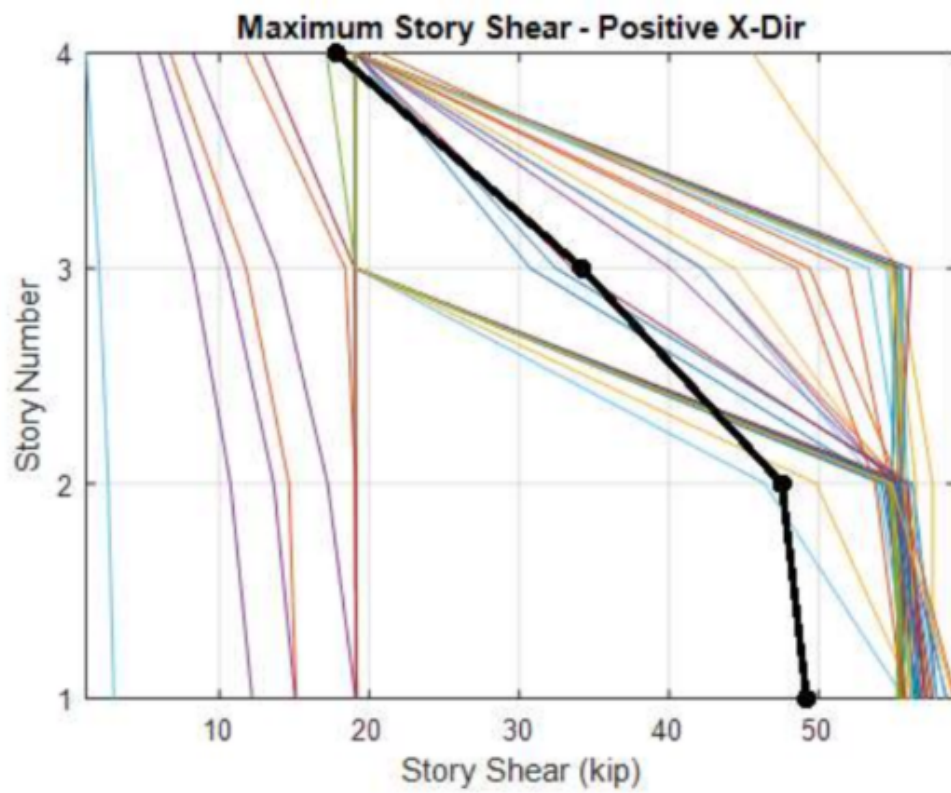


Figure E-7: Story Number versus Shear - Positive Shear - SLE Trials.

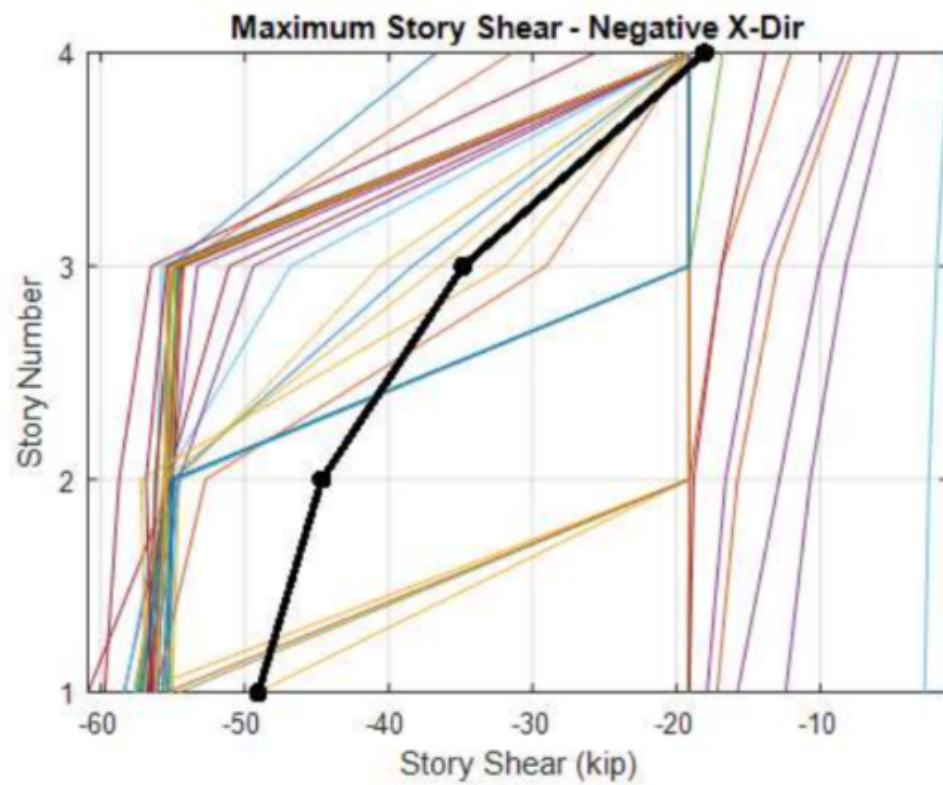


Figure E-8: Story Number versus Shear - Negative Shear - SLE Trials.

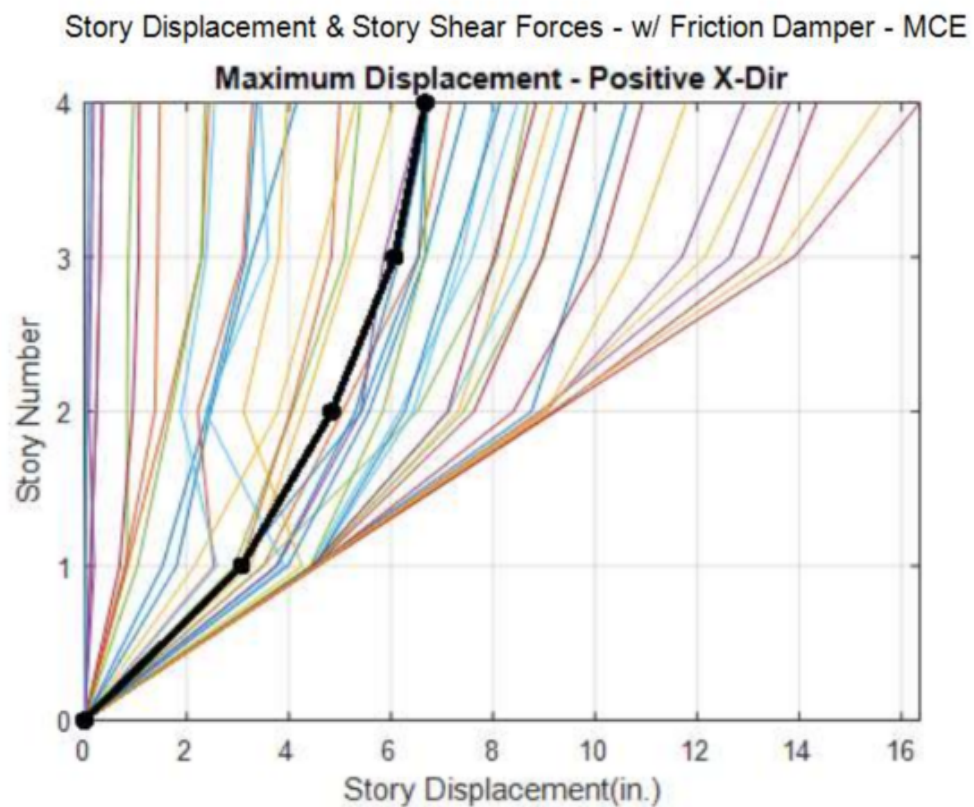


Figure E-9: Story Number versus Displacement - Positive Displacement - MCE Trials.

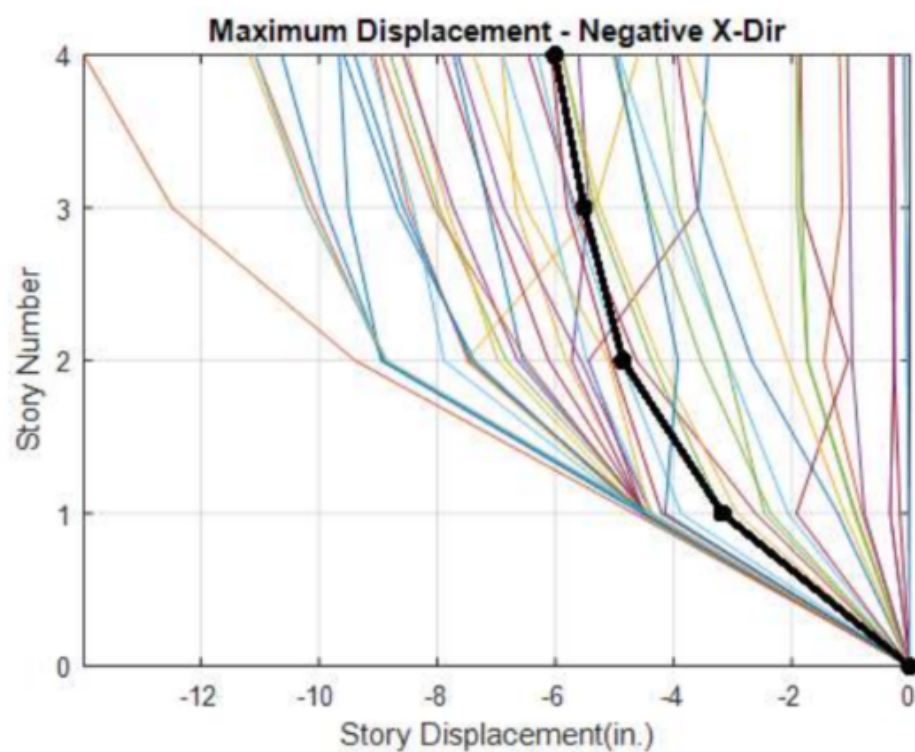


Figure E-10: Story Number versus Displacement - Negative Displacement - MCE Trials.

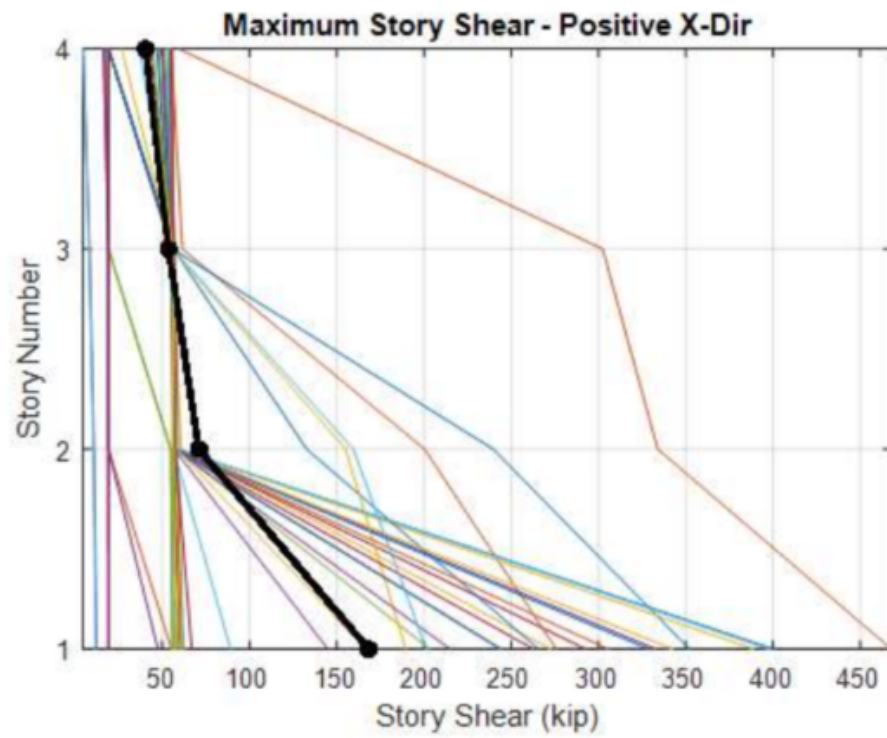


Figure E-11: Story Number versus Shear - Positive Shear - MCE Trials.

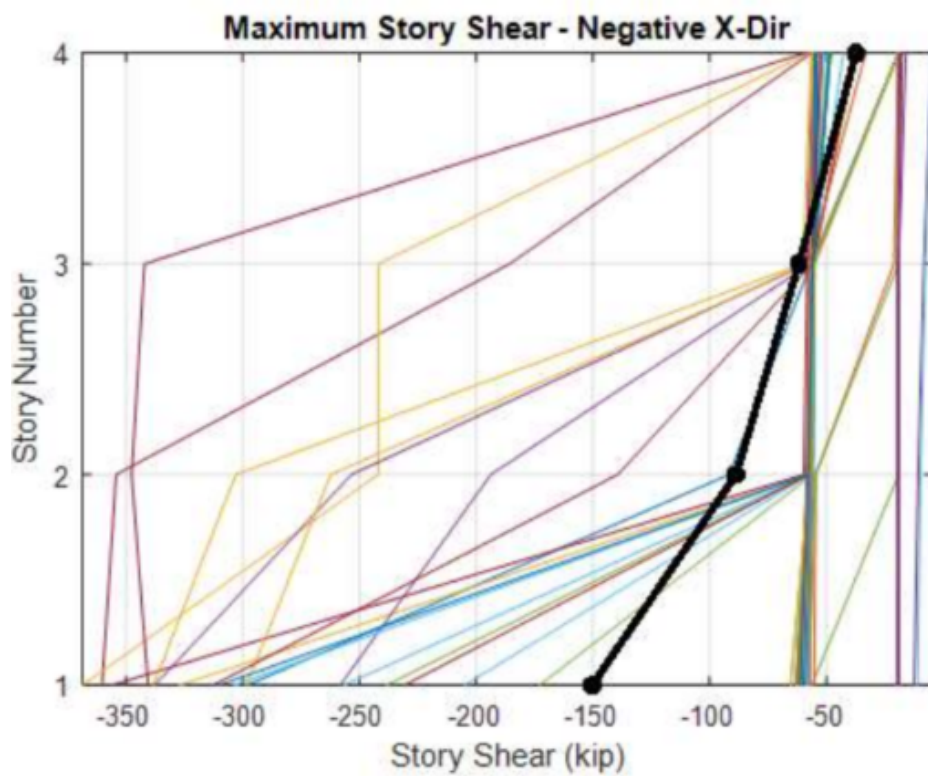


Figure E-12: Story Number versus Shear - Negative Shear - MCE Trials.

Inter-Story Drift Ratios & Story Shear Forces - w/ Friction Damper - MCE

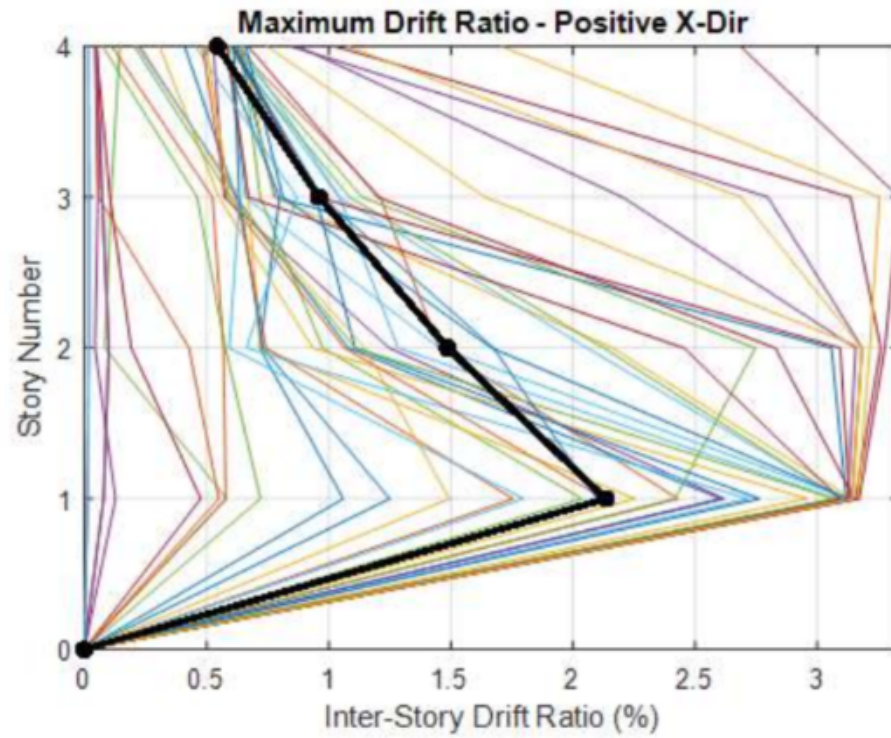


Figure E-13: Story Number versus Drift - Positive Drift - MCE Trials.

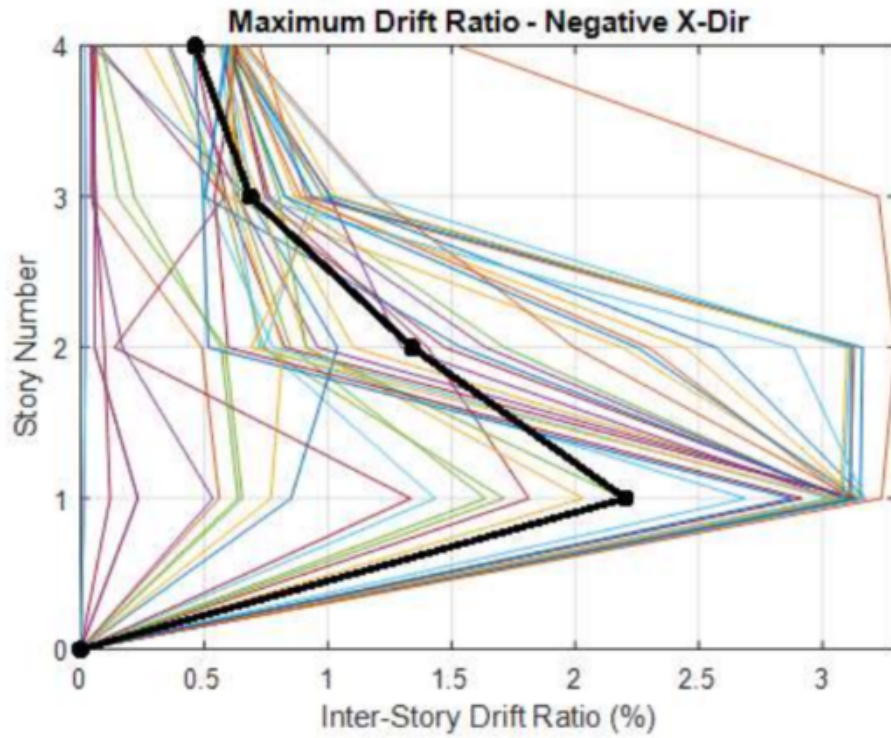


Figure E-14: Story Number versus Drift - Negative Drift - MCE Trials.

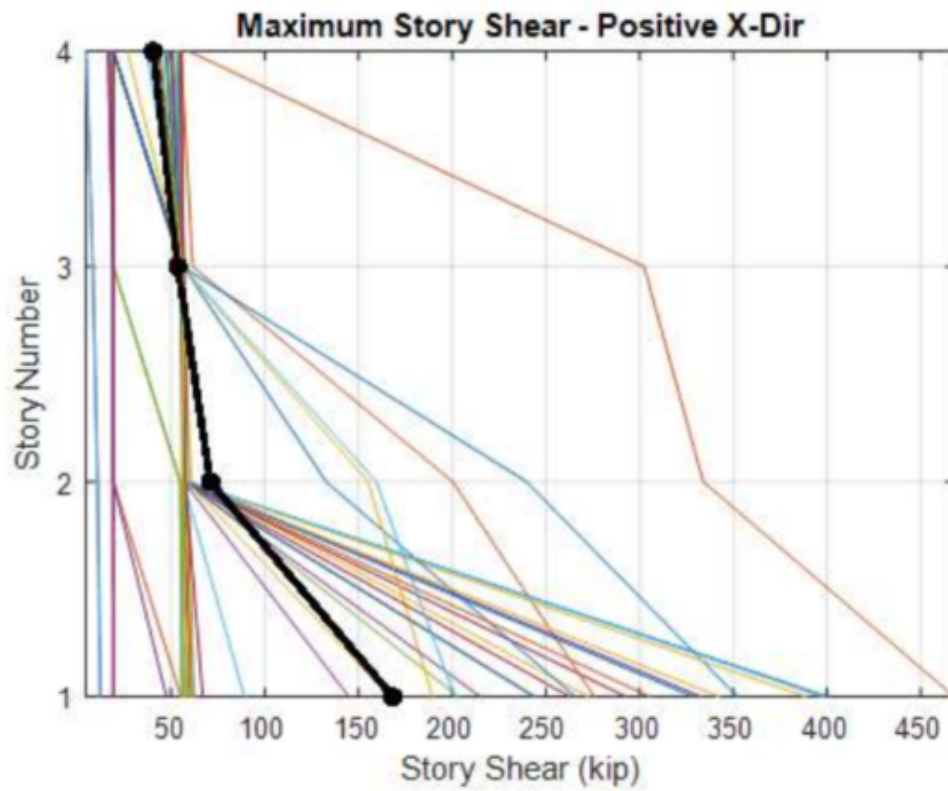


Figure E-15: Story Number versus Shear - Positive Shear - MCE Trials.

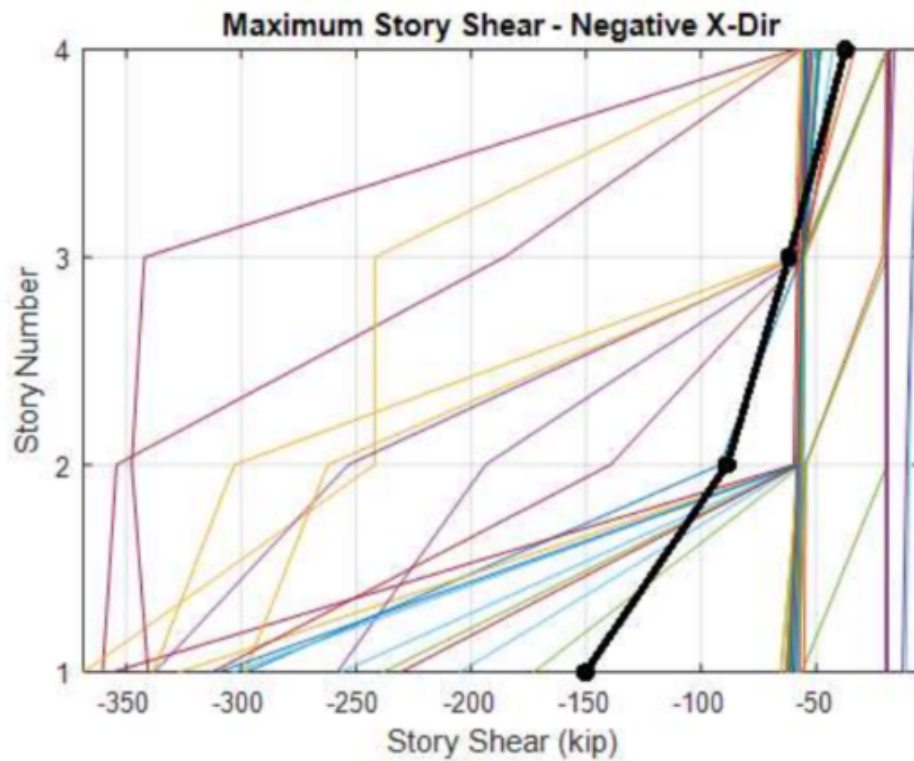


Figure E-16: Story Number versus Shear - Negative Shear - MCE Trials.

APPENDIX F
4-STORY, 4-BAY ELASTIC TRIALS (NO
FRICTION DAMPER APPLIED)

Story Displacement & Story Shear Forces - w/o Friction Damper (Elastic) - SLE

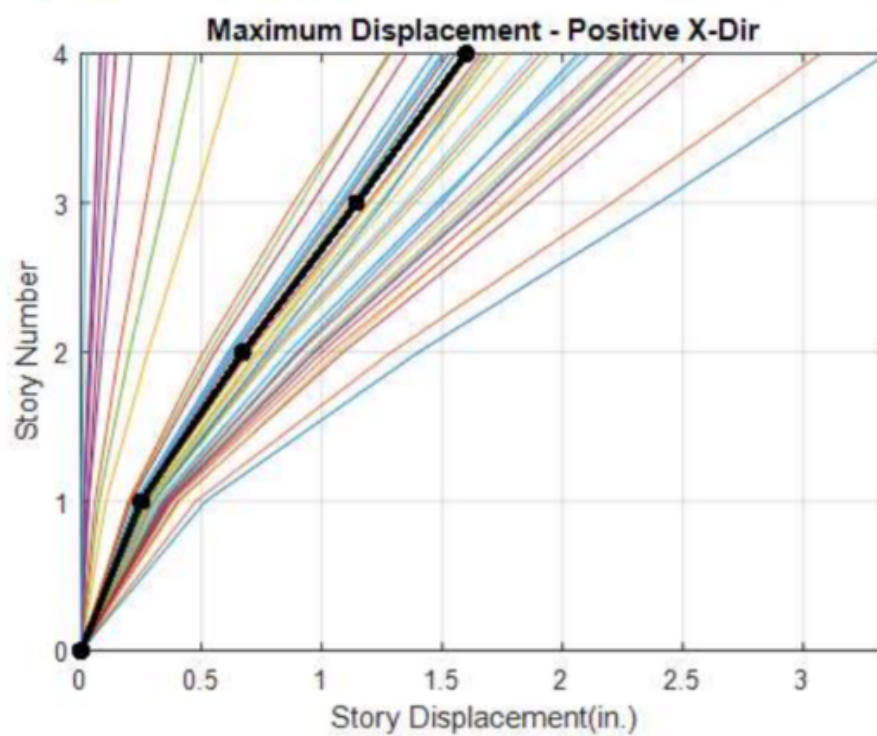


Figure F-1: Story Number versus Displacement - Positive Displacement - SLE Elastic Trials.

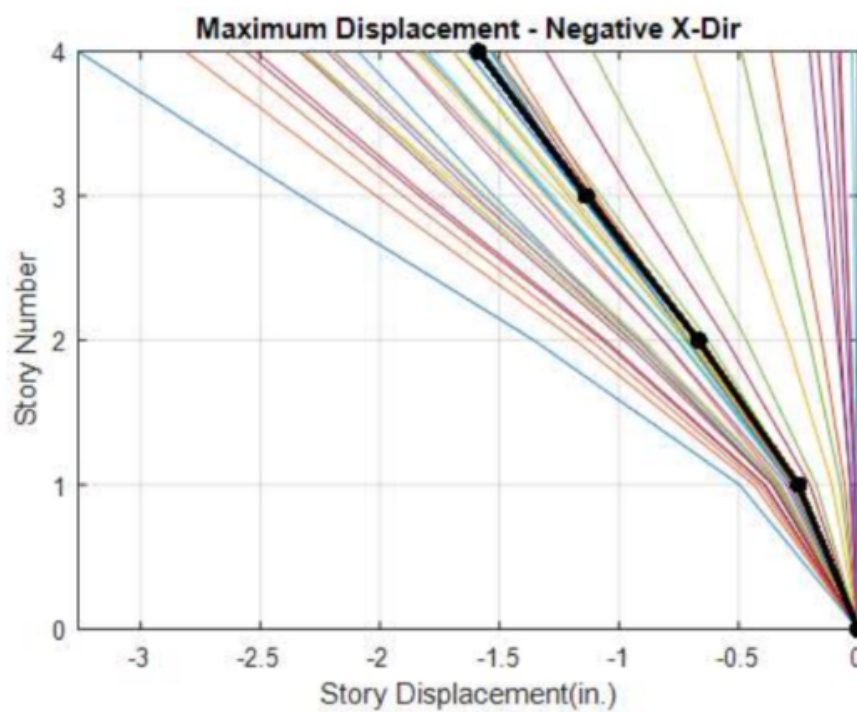


Figure F-2: Story Number versus Displacement - Negative Displacement - SLE Elastic Trials.

Inter-Story Drift Ratios & Story Shear Forces - w/o Friction Damper (Elastic) - SLE

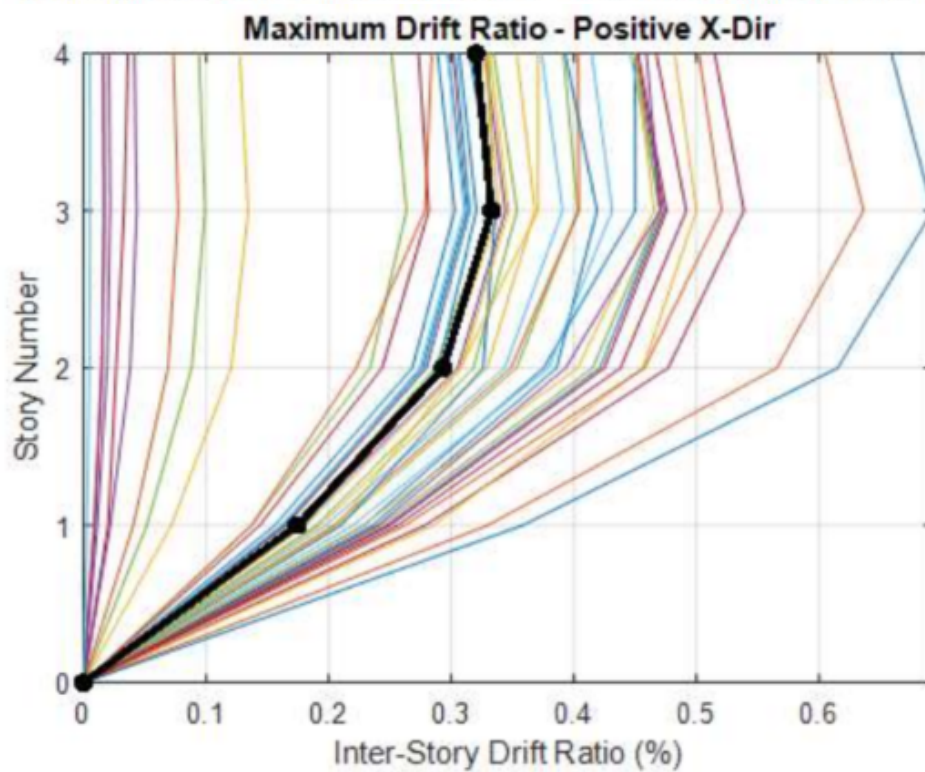


Figure F-3: Story Number versus Drift - Positive Drift - SLE Elastic Trials.

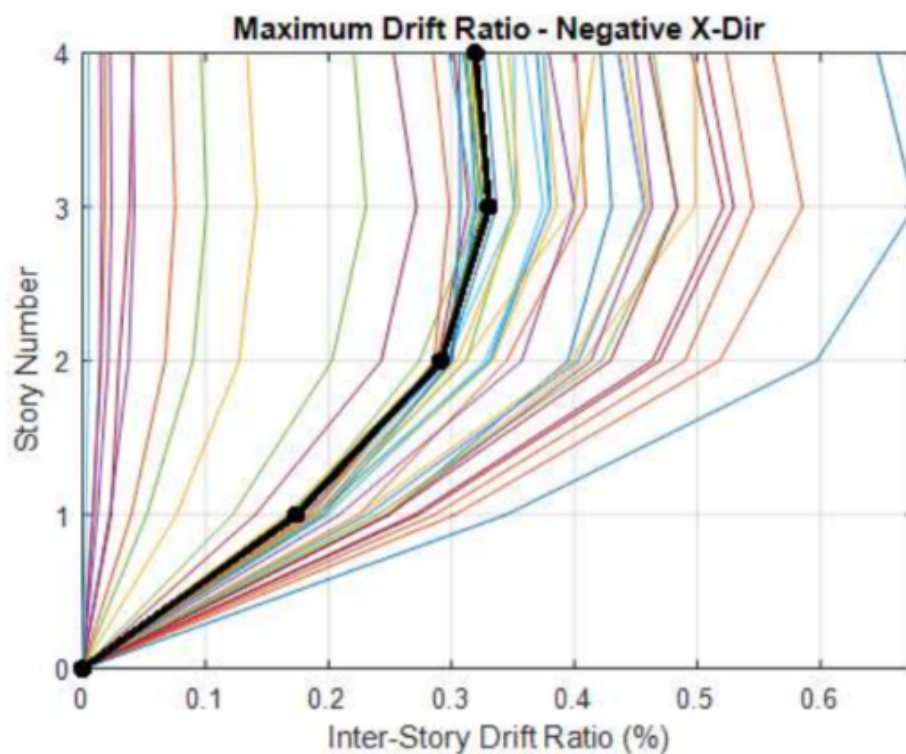


Figure F-4: Story Number versus Drift - Negative Drift - SLE Elastic Trials.

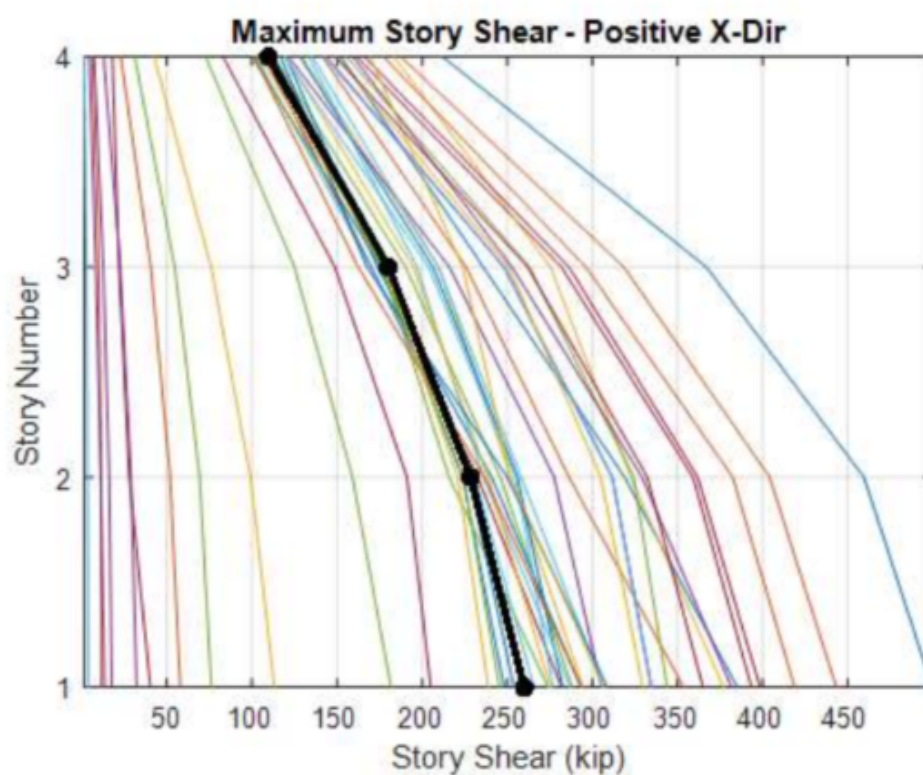


Figure F-5: Story Number versus Shear - Positive Shear - SLE Elastic Trials.

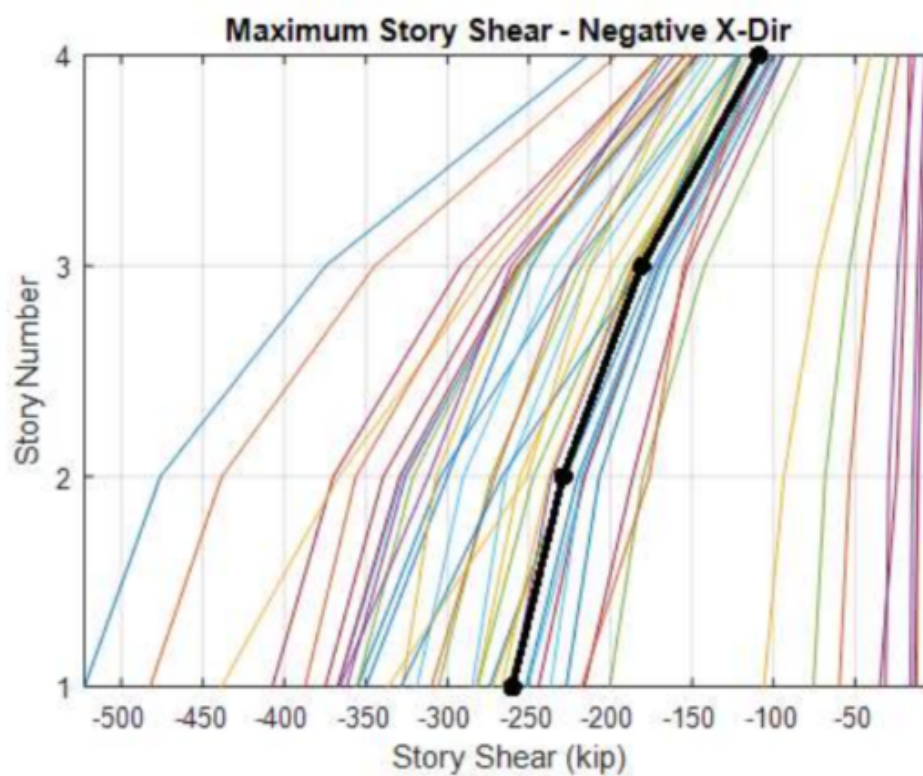


Figure F-6: Story Number versus Shear - Negative Shear - SLE Elastic Trials.

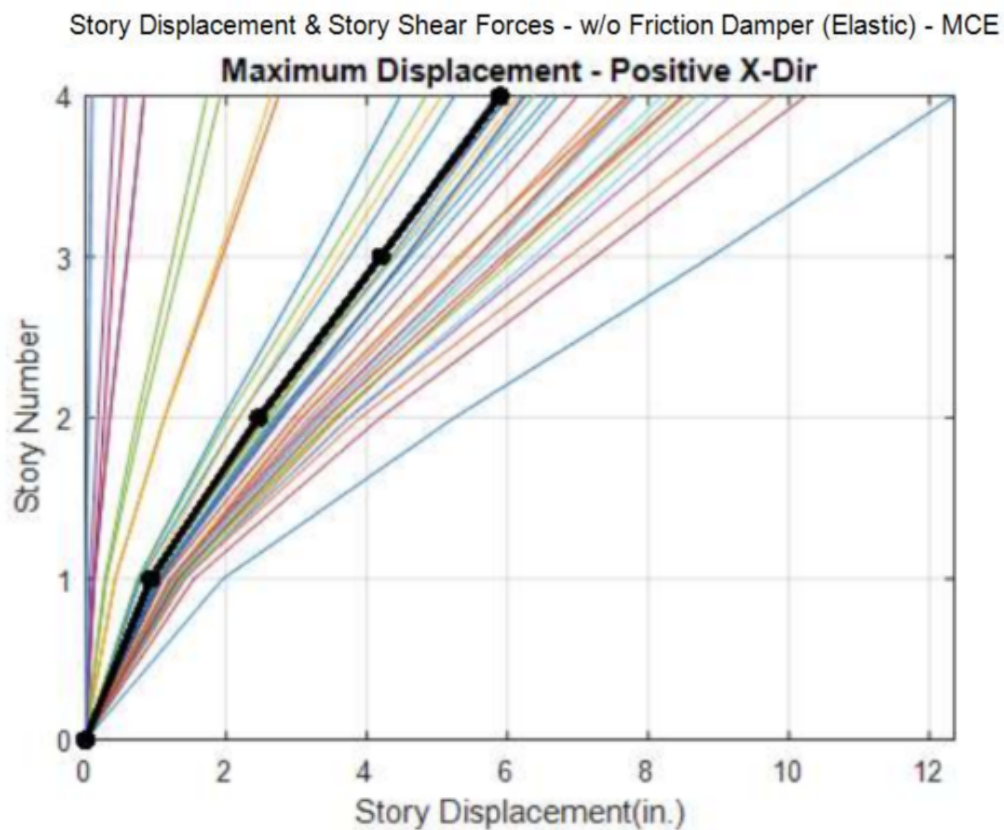


Figure F-7: Story Number versus Displacement - Positive Displacement - MCE Elastic Trials.

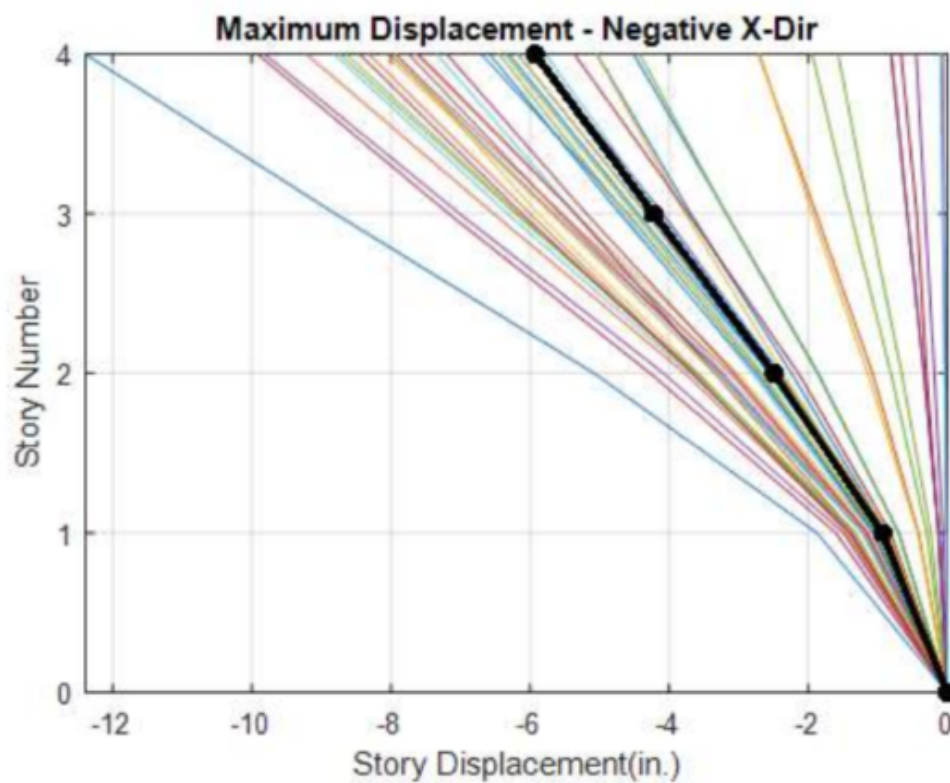


Figure F-8: Story Number versus Displacement - Negative Displacement - MCE Elastic Trials.

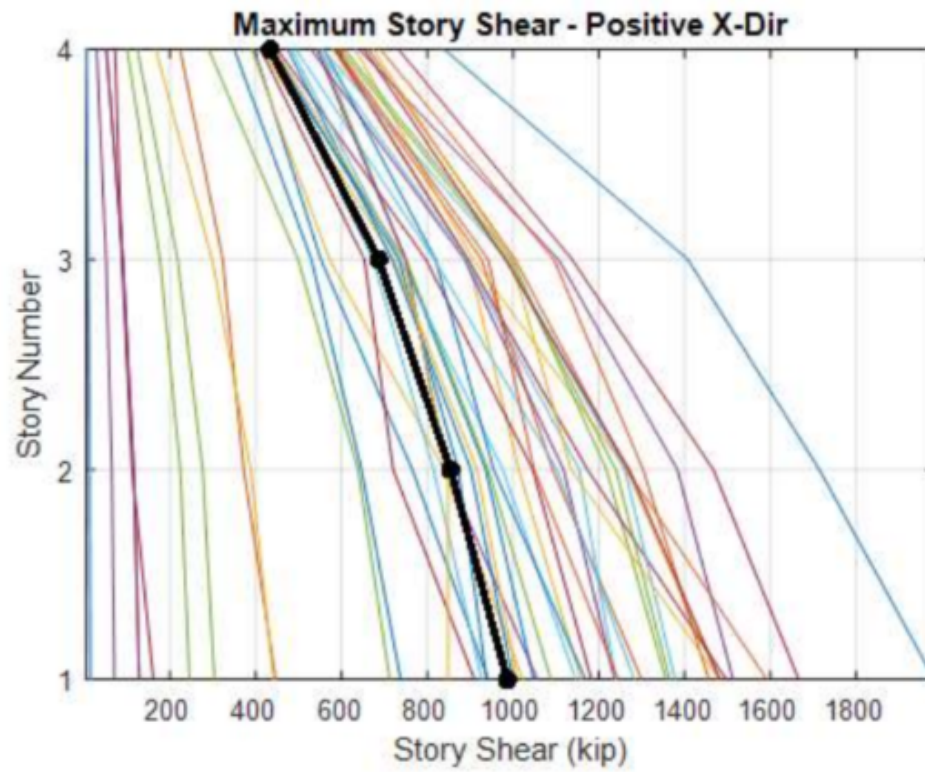


Figure F-9: Story Number versus Shear - Positive Shear - MCE Elastic Trials.

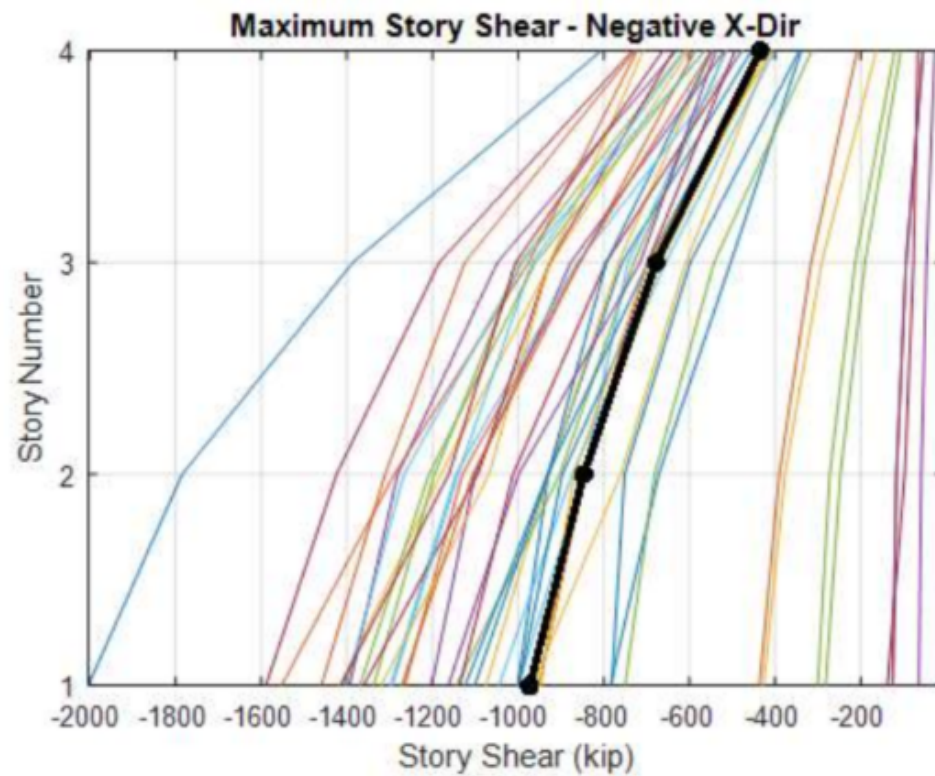


Figure F-10: Story Number versus Shear - Negative Shear - MCE Elastic Trials.

Inter-Story Drift Ratios & Story Shear Forces - w/o Friction Damper (Elastic) - MCE

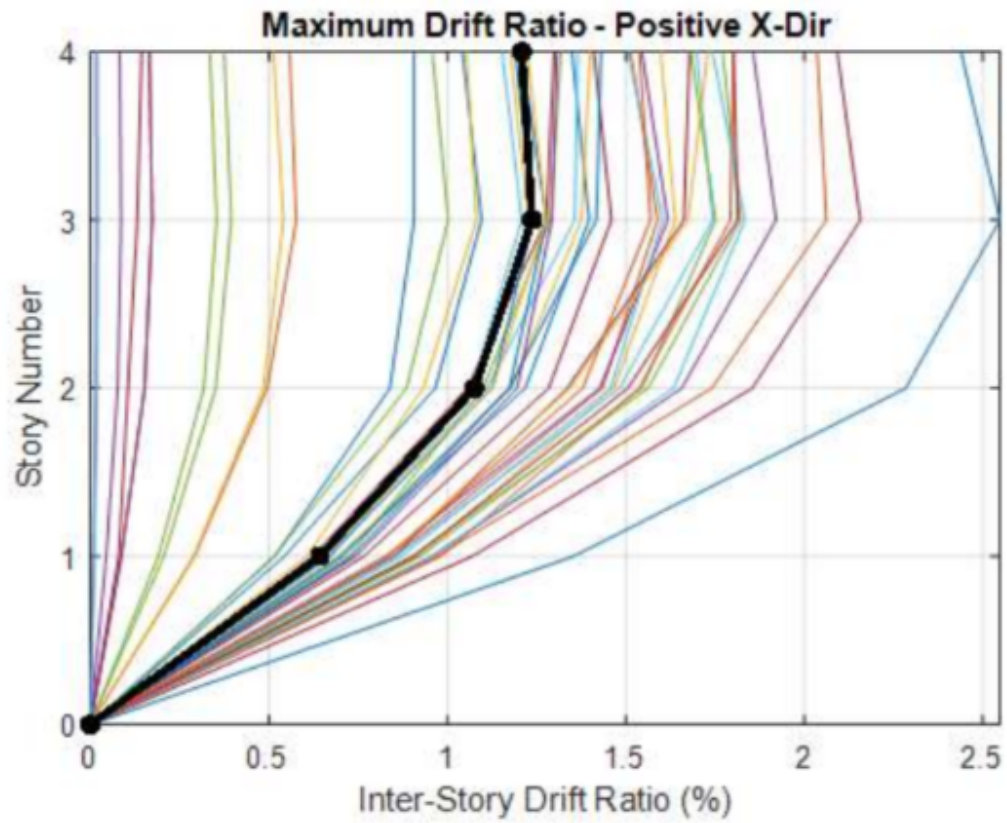


Figure F-11: Story Number versus Drift - Positive Drift - MCE Elastic Trials.

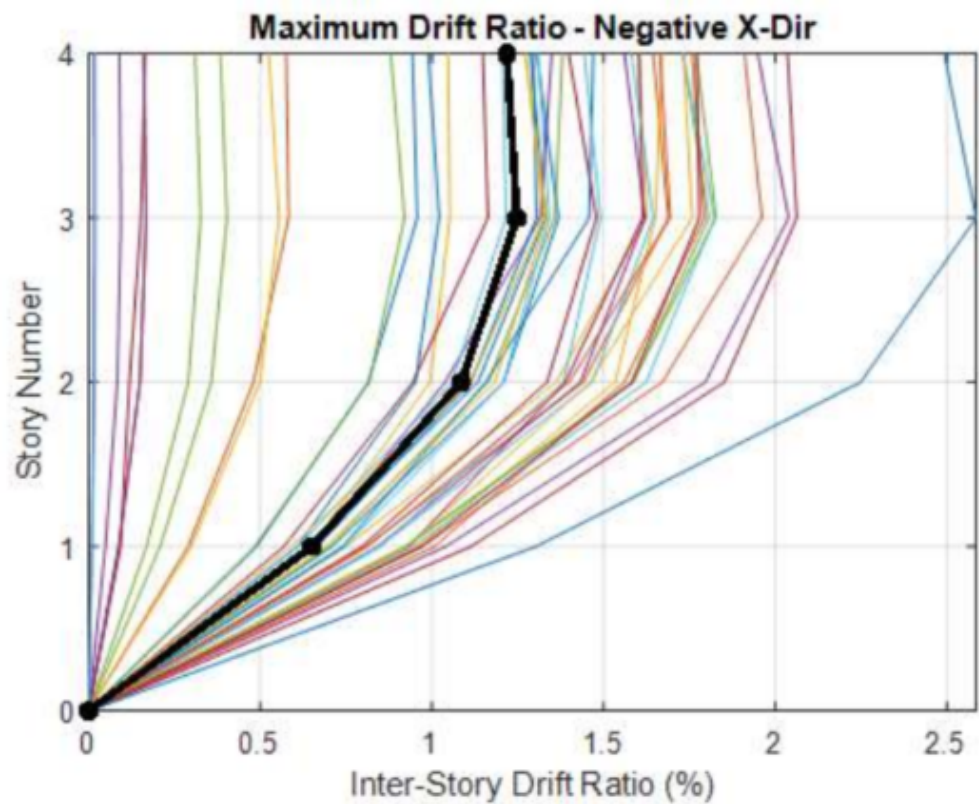


Figure F-12: Story Number versus Drift - Negative Drift - MCE Elastic Trials.

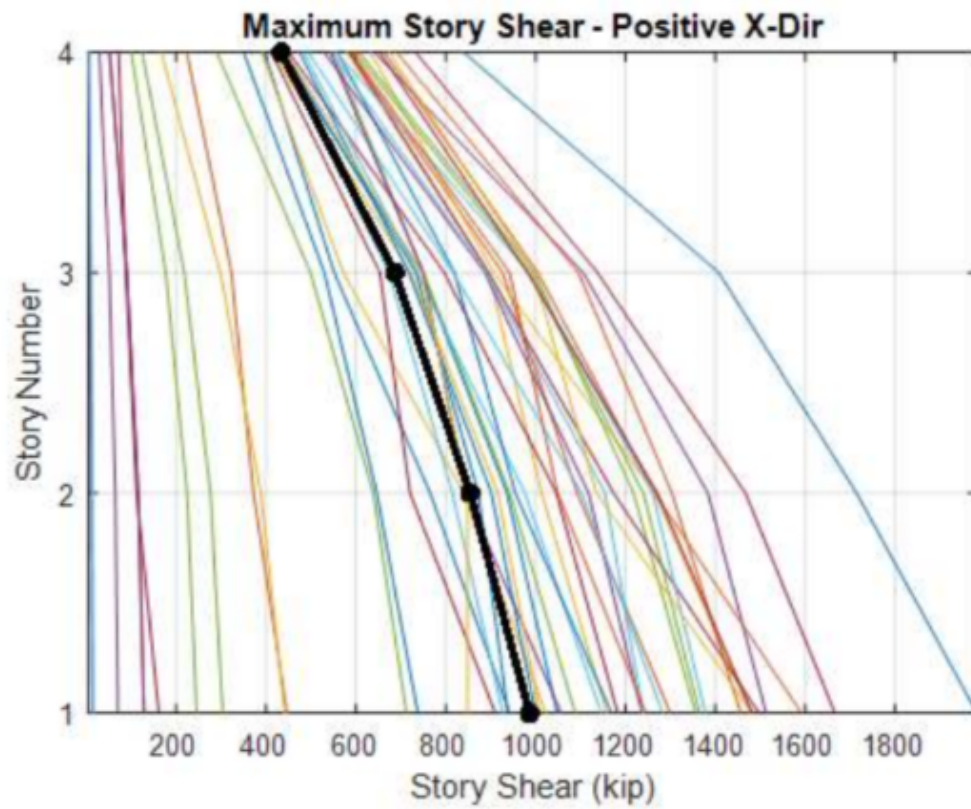


Figure F-13: Story Number versus Shear - Positive Shear - MCE Elastic Trials.

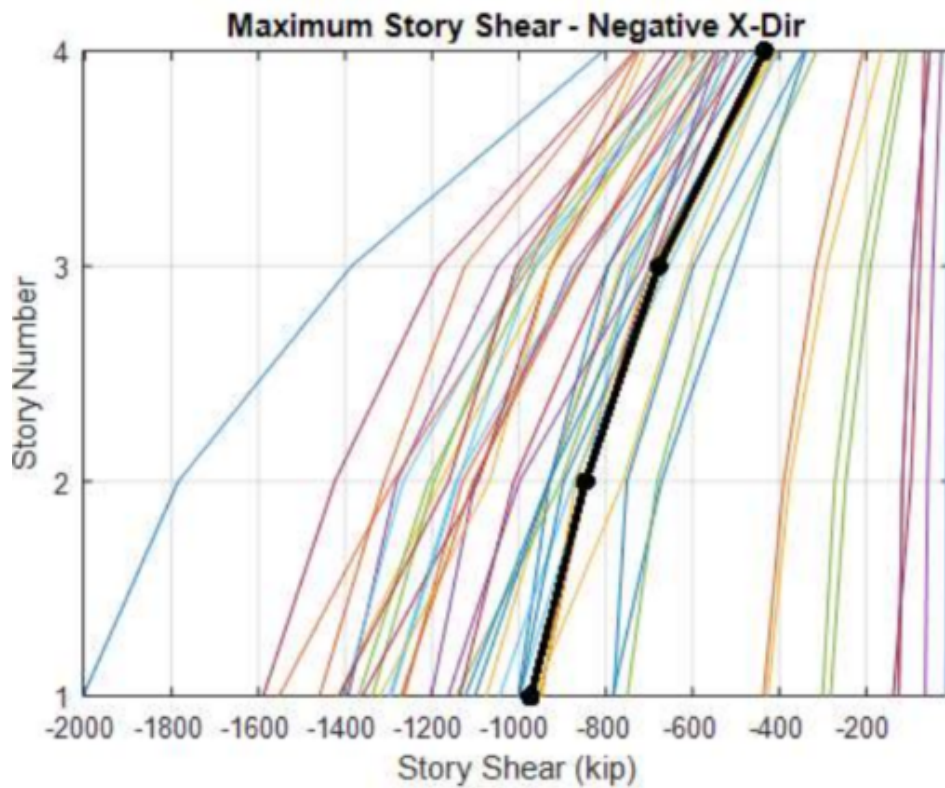


Figure F-14: Story Number versus Shear - Negative Shear - MCE Elastic Trials.